Muon Magnetic Anomaly

— A precision probe for SM and BSM Physics

Zhiqing Zhang
IJCLab, CNRS / Univ. Paris-Saclay

Outline

- ➢ Brief historical introduction to electron and muon magnetic anomalies
- ➢ Precision measurements and SM predictions
- ➢ Hadronic contributions to muon magnetic anomaly and running α
- ➢ Direct contribution of BEPC(II) / BES(III)
- ➢ Lessons learnt
- ➢ Summary and prospects

Based whenever possible on materials in my personal publications in close collaboration with Davier (D), Eidelman (E), Hoecker (H), Malaescu (M), Yuan (Y) et al.

Magnetic Moment

The magnetic dipole moment of a particle can be observed from its motion in a magnetic field

Intrinsic magnetic moment discovered in Stern-Gerlach experiment, 1922:

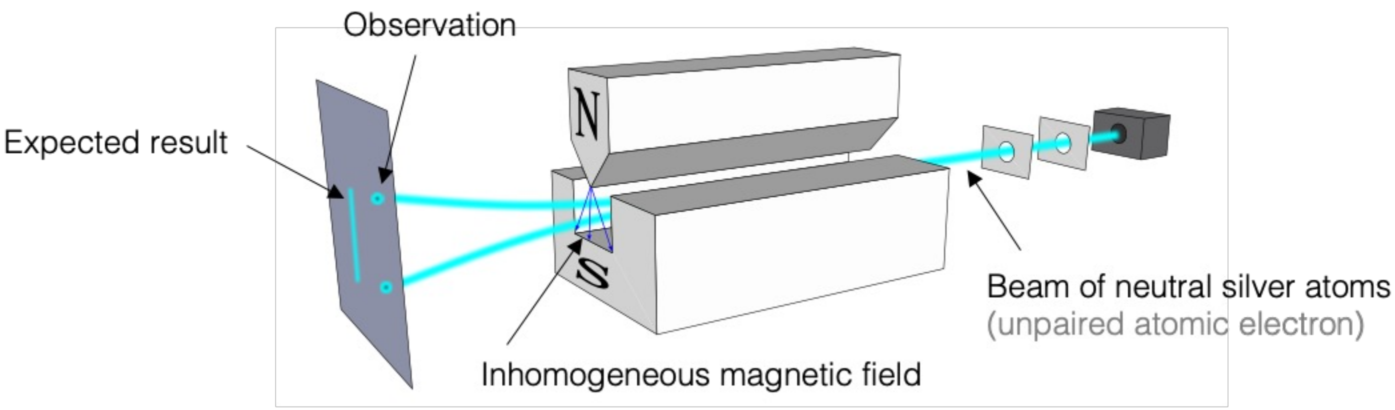

➔ Atoms have intrinsic and quantised angular momentum

(Anomalous) Magnetic Moment of a Charged Lepton

For a lepton with charge q_ℓ and mass m_ℓ, its magnetic moment is connected to its spin by a g_ℓ factor:

$$\vec{\mu}_\ell = g_\ell \left(\frac{q_\ell}{2m_\ell}\right) \vec{S}_\ell$$

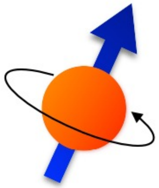

Dirac predicted $g_e = 2$ for electron in 1928 [Proc. Roy. Soc. Lond. A 118, 351 (1928)]
It was confirmed to 0.1% by Kinsler & Houston in 1934 through studying the Zeeman effect in neon [Phys. Rev. 46, 533 (1934)]

(Anomalous) Magnetic Moment of a Charged Lepton

For a lepton with charge q_ℓ and mass m_ℓ, its magnetic moment is connected to its spin by a g_ℓ factor:

$$\vec{\mu}_\ell = g_\ell \left(\frac{q_\ell}{2m_\ell}\right) \vec{S}_\ell$$

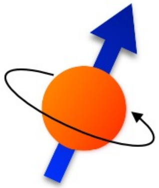

Dirac predicted $g_e = 2$ for electron in 1928 [Proc. Roy. Soc. Lond. A 118, 351 (1928)]
It was confirmed to 0.1% by Kinsler & Houston in 1934 through studying the Zeeman effect in neon [Phys. Rev. 46, 533 (1934)]

A deviation from $g_e = 2$ was established by Nafe, Nels & Rabi only in 1947 by comparing the hyperfine structure of hydrogen and deuterium spectra [Phys. Rev. 71, 914 (1947)]

A first precision measurement of $g_e = 2.00344(12)$ (wrong: 2.00232…!) was made by Kusch & Foley in 1947 using Rabi's atomic beam magnetic resonance technique [Phys. Rev. 72, 1256 (1947)]

The anomalous magnetic moment a_ℓ was introduced to quantify the deviation from 2:

$$a_\ell = \frac{g_\ell - 2}{2} \sim 0.001$$

The a_e Measurements

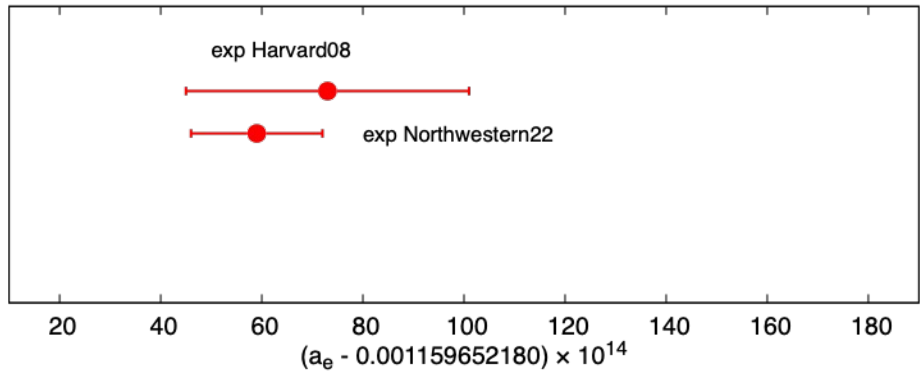

$a_e = 1\ 159\ 652\ 180.59(13) \times 10^{-12}$ [Phys. Rev. Lett. 130 (2023) 071801]

112 ppt precision

using a one-electron quantum cyclotron in a cylindrical Penning trap cavity*, a technique invented by Dehmelt in 70's who was awarded with a Nobel Prize in Physics in 1989

This is the most precisely measured quantity in particle physics

Do we have a prediction with a comparable precision to compare with?

* In which a single electron suspended in a magnetic field and cooled to its lowest quantum states (more on slide 56)

ppt = one part per trillion (10^{-12})

The a_e Prediction

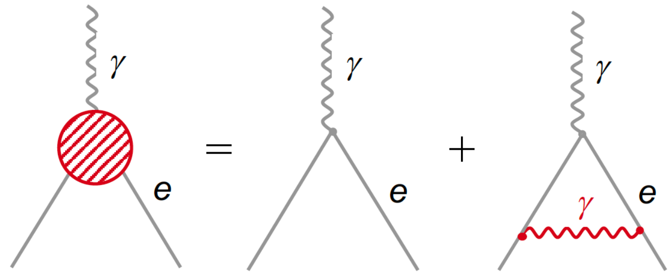

$+$ 2-loop $+$ 3-loop $+$ 4-loop $+$ 5-loop $+ \ldots$

$$a_e\,(\text{QED}) = 0 + \frac{\alpha}{2\pi} + A_2\left(\frac{\alpha}{\pi}\right)^2 + A_3\left(\frac{\alpha}{\pi}\right)^3 + A_4\left(\frac{\alpha}{\pi}\right)^4 + A_5\left(\frac{\alpha}{\pi}\right)^5 + \cdots$$

(Dirac: $g_e = 2$)
(1928)

(Schwinger)
(1947)

A_2, A_3 known analytically
A_2-A_4: cross-checked by different groups using different methods
A_5: previous difference between two groups better understood and now in good agreement

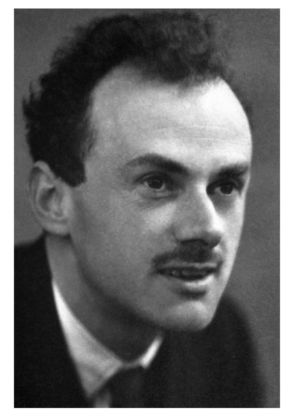

Paul Dirac
Nobel prize 1933

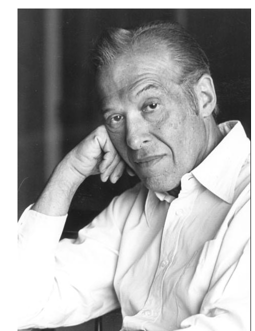

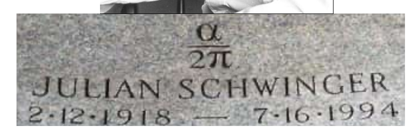

Nobel prize 1965

The a_e Prediction

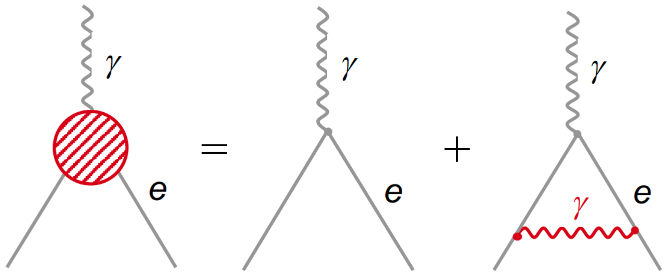

$+$ 2-loop $+$ 3-loop $+$ 4-loop $+$ 5-loop $+ \ldots$

$$a_e\,(\mathrm{QED}) \;=\; 0 \;+\; \frac{\alpha}{2\pi} \;+\; A_2\left(\frac{\alpha}{\pi}\right)^2 + A_3\left(\frac{\alpha}{\pi}\right)^3 + A_4\left(\frac{\alpha}{\pi}\right)^4 + A_5\left(\frac{\alpha}{\pi}\right)^5 + \cdots$$

a_e (QED) depends on the α value to use
a_e (hadron, LO) = (1.861−1.920) × 10^{-12} data-driven evaluations
a_e (hadron, NLO) = −0.2263(35) × 10^{-12}
The sum of other hadronic and EW contribution < 0.1 × 10^{-12}

Relative fractions:
QED: 99.9999998%
Hadron: 1.7 × 10^{-9}
EW: 2.6 × 10^{-11}

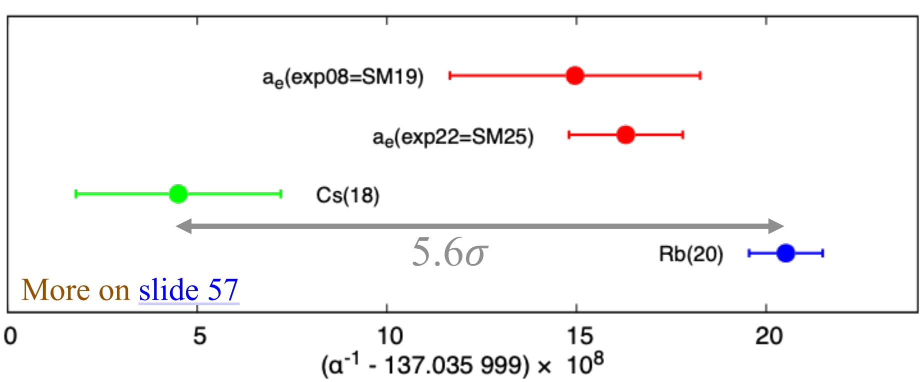

More on slide 57

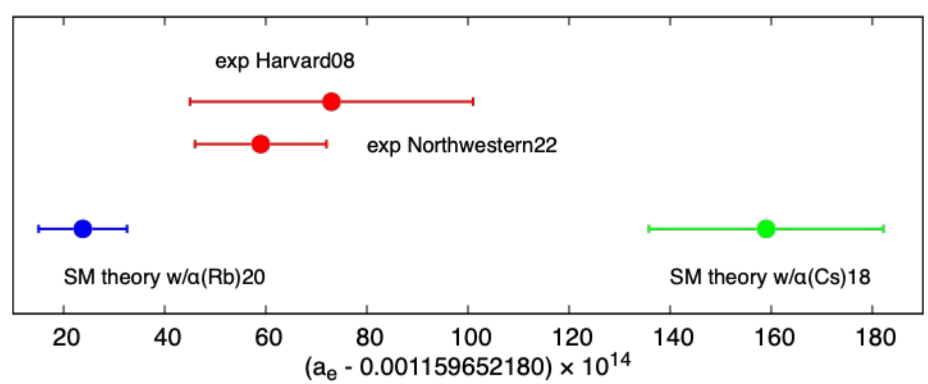

Summary on a_e and α

The a_e measurement has an extraordinary precision

$$a_e^{\rm exp}(\text{NW22}) = 1\,159\,652\,180.59(13) \times 10^{-12} \quad [0.11\ \text{ppb}]$$

The SM a_e prediction is currently limited by the different α values to use

$$a_e^{\rm SM}\big[\alpha(\text{Cs})\big] = 1\,159\,652\,181.59(23)(0)(3) \times 10^{-12} \qquad [0.20\ \text{ppb}]\,,$$

$$a_e^{\rm SM}\big[\alpha(\text{Rb})\big] = 1\,159\,652\,180.238(82)(4)(30) \times 10^{-12} \qquad [0.075\ \text{ppb}]\,,$$

The comparison gives

$$a_e^{\rm exp}(\text{NW22}) - a_e^{\rm SM}\big[\alpha(\text{Cs})\big] = -1.00(26) \times 10^{-12}$$

$$a_e^{\rm exp}(\text{NW22}) - a_e^{\rm SM}\big[\alpha(\text{Rb})\big] = +0.35(16) \times 10^{-12}$$

corresponding to -3.8σ and $+2.2\sigma$, respectively

ppb = one part per billion (10^{-9})

Why Are We Interested in a_μ?

Contrary to the electron, the muon is unstable (2.2μs, boosted to 64.4μs at 3.09 GeV)

so it is more difficult to measure (and predict), nevertheless

a_μ receives sizeable contributions from all three sectors of the SM

and due to its heavier mass, its sensitivity to new physics is $\sim (m_\mu / m_e)^2 \sim$ 43 000 larger

Overview of a Muon *g* - 2 Experiment

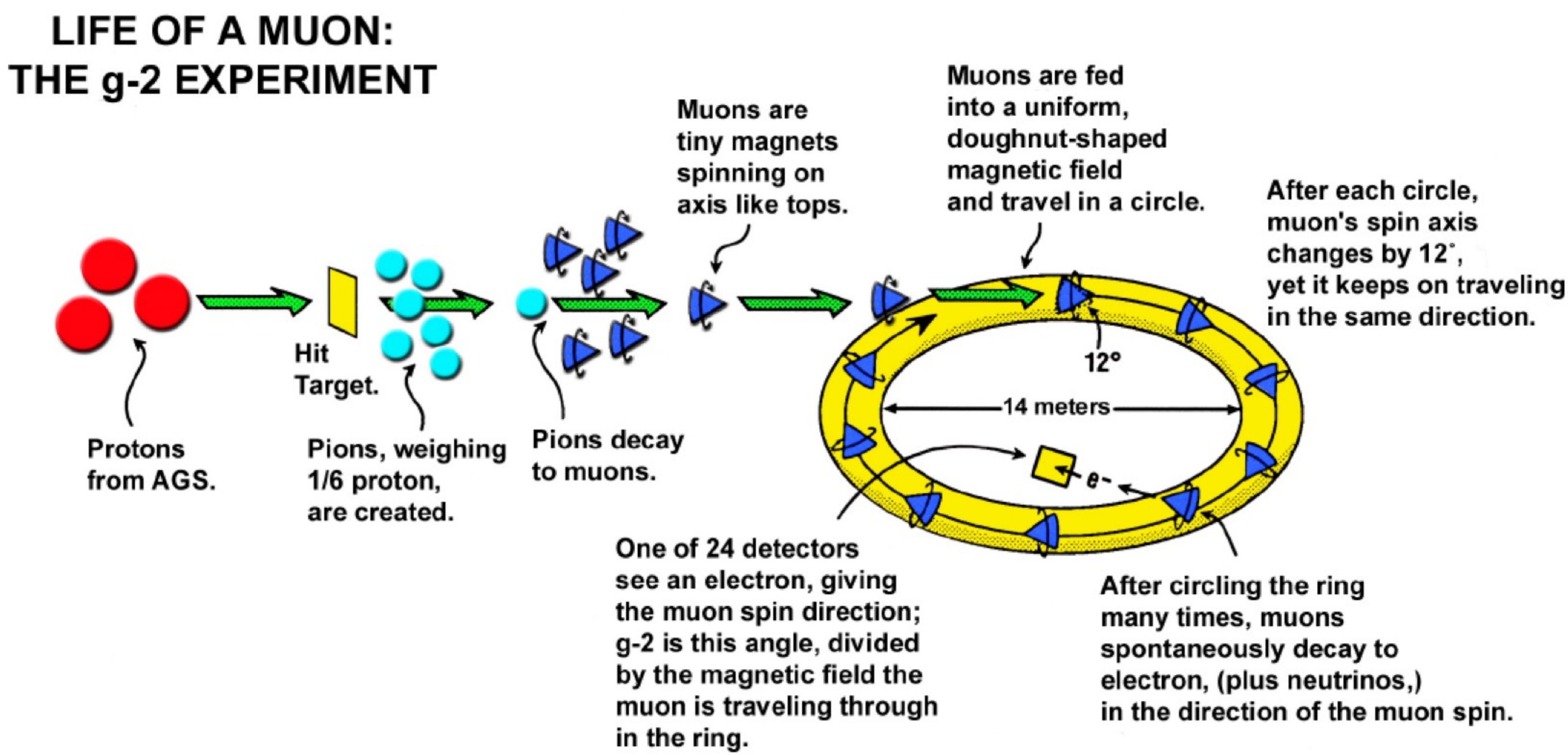

The key elements:

1. Parity violation in pion decay: polarised muons
2. Parity violation in muon decay: positron emitted in the direction of muon spin

The a_μ Measurement Concept

Measure "anomalous" frequency difference between spin precession and cyclotron frequencies:

$$\vec{\omega}_a \equiv \vec{\omega}_s - \vec{\omega}_c = \frac{e}{m_\mu c}\left[a_\mu \vec{B} - \cancelto{0}{\left(a_\mu - \frac{1}{\gamma^2 - 1}\right)} \vec{\beta} \times \vec{E}\right]$$

One defines a magic γ value of 29.3 (i.e. p_μ=3.09 GeV) to remove the 2nd term

The magnetic filed B is determined from $\omega_p = 2\mu_p B$

Thus $$a_\mu = \frac{\omega_a}{\omega_p}\left[\frac{\mu_p}{\mu_e}\frac{m_\mu}{m_e}\frac{g_e}{2}\right]$$

The 1st term is measured in a doubly blinded way

The 2nd term is known from literatures with high precision ± 25 ppb → 22 ppb

(2021) (2025)

FNAL 2021 Run 1 Result

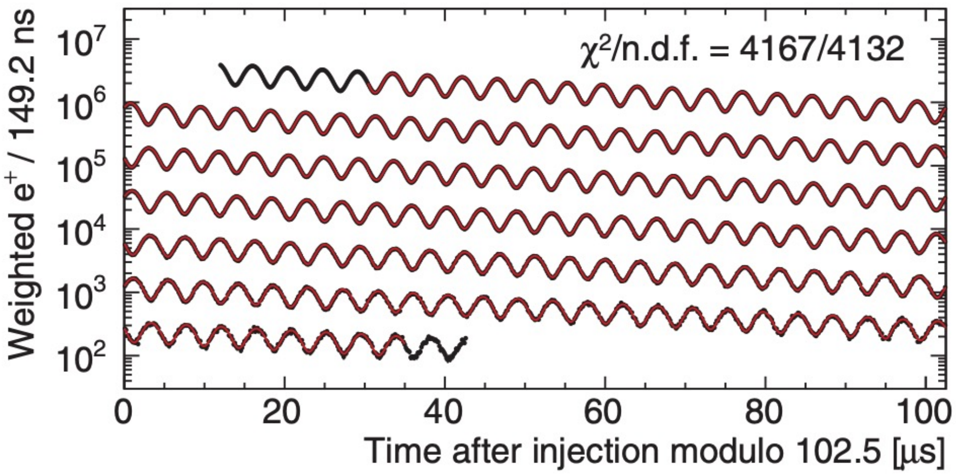

Positron rate measured in the calorimeters is fitted with

$$N(t) = N_0 e^{-t/\gamma\tau}[1 - A \cdot \cos(\omega_a t + \phi)]$$

to determine ω_a with a stat and syst error of 0.43, 0.56 ppm

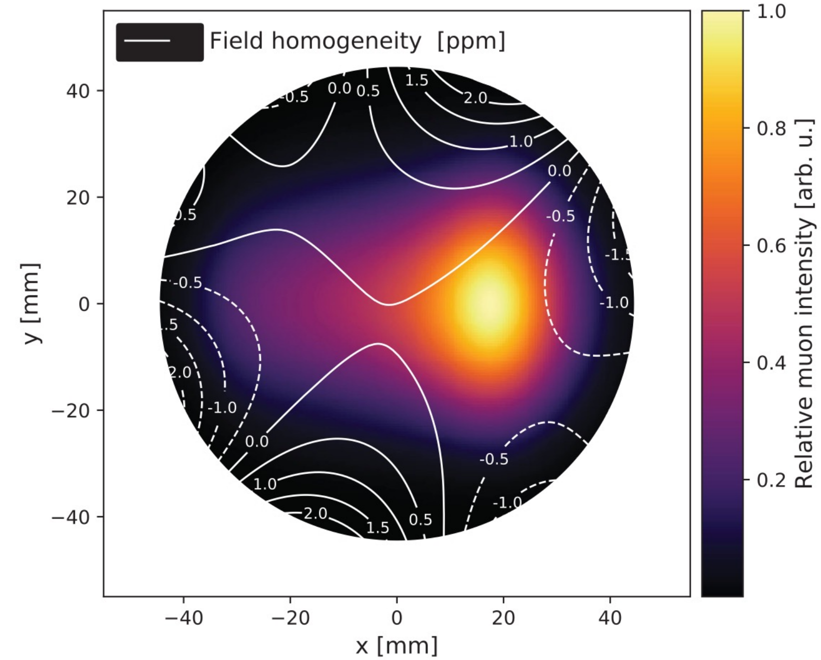

The magnetic field is measured with a syst error of 0.56 ppm

$$a_\mu(\text{FNAL}) = 116\,592\,040(54) \times 10^{-11} \quad (0.46 \text{ ppm})$$

The total uncertainty of 0.46 ppm is dominated by statistical one of 0.43 ppm at Run 1

ppm = one part per million (10^{-6})

Final FNAL Results

- ➢ Statistics significantly increased over time
- ➢ Yet the final measurement is still statistically limited (98 ppb)
- ➢ The experiment did a good job in improving data quality, systematic uncertainty control over time
- ➢ The final precision of 127 ppb exceeds the original goal of 140 ppb
- ➢ A factor of 4.2 improvement over BNL E821

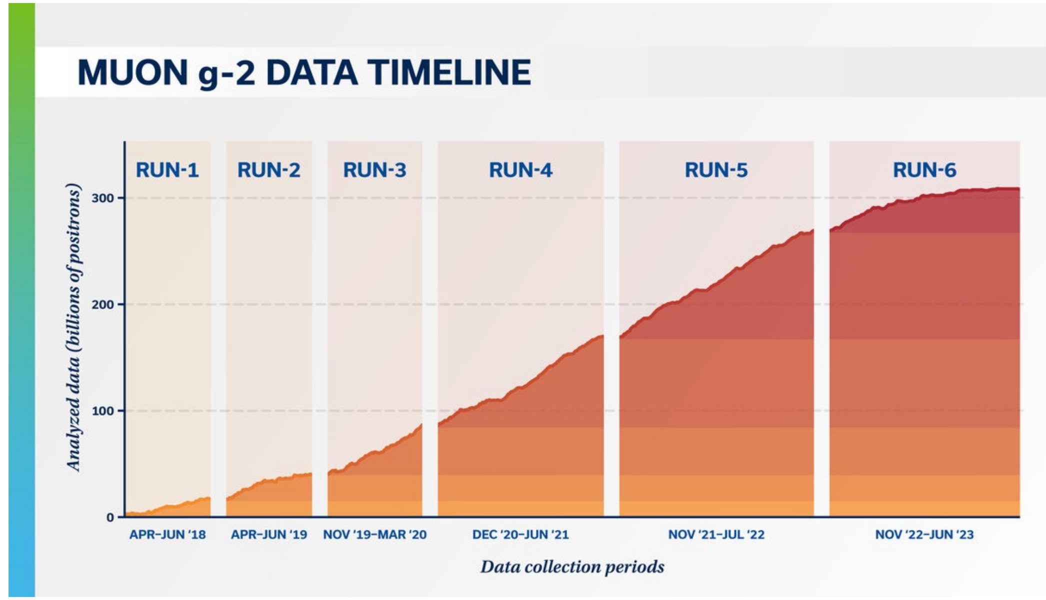

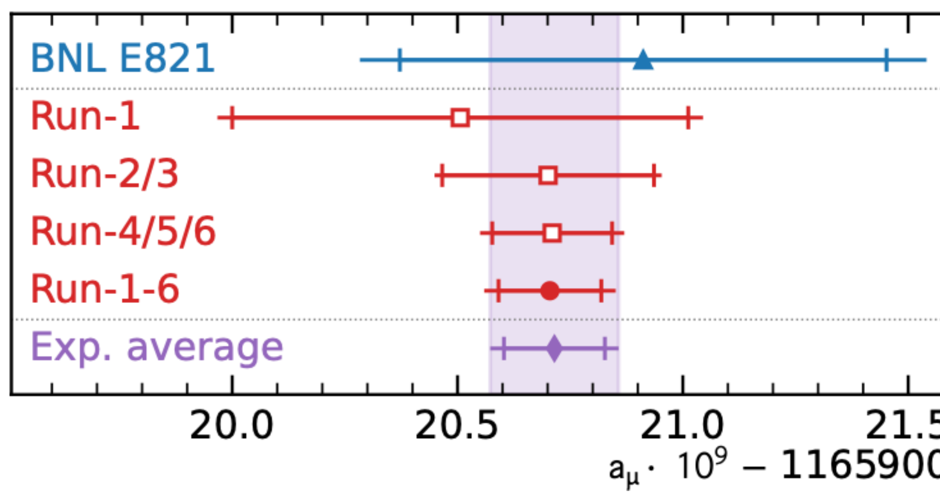

More than 60 years of a_μ measurements

Experiment	Beam	Measurement	$\delta a_\mu/a_\mu$	Required th. terms
Columbia-Nevis (57)	μ^+	g=2.00±0.10		g=2
Columbia-Nevis (59)	μ^+	0.001 13(+16)(−12)	12.4%	α/π
CERN 1 (61)	μ^+	0.001 145(22)	1.9%	α/π
CERN 1 (62)	μ^+	0.001 162(5)	0.43%	$(\alpha/\pi)^2$
CERN 2 (68)	μ^+	0.001 166 16(31)	265 ppm	$(\alpha/\pi)^3$
CERN 3 (75)	$\mu^\pm$	0.001 165 895(27)	23 ppm	$(\alpha/\pi)^3$ + had
CERN 3 (79)	$\mu^\pm$	0.001 165 911(11)	7.3 ppm	$(\alpha/\pi)^3$ + had
BNL E821 (00)	μ^+	0.001 165 919 1(59)	5 ppm	$(\alpha/\pi)^3$ + had
BNL E821 (01)	μ^+	0.001 165 920 2(16)	1.3 ppm	$(\alpha/\pi)^4$ + had + weak
BNL E821 (02)	μ^+	0.001 165 920 3(8)	0.7 ppm	$(\alpha/\pi)^4$ + had + weak + ?
BNL E821 (04)	μ^-	0.001 165 921 4(8)(3)	0.7 ppm	$(\alpha/\pi)^4$ + had + weak + ?
FNAL Run-1 (21)	μ^+	0.001 165 920 40(54)	0.46 ppm	$(\alpha/\pi)^4$ + had + weak + ?
FNAL Run-2/3 (23)	μ^+	0.001 165 920 57(25)	0.21 ppm	$(\alpha/\pi)^4$ + had + weak + ?
FNAL Run-4-6 (25)	μ^+	0.001 165 920 710(162)	139 ppb	$(\alpha/\pi)^4$ + had + weak + ?

More than 60 years of a_μ measurements

David Hertzog, Moriond 2026

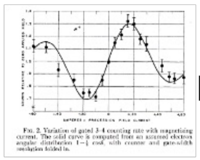

Nevis 1957
(at rest)
g_μ

Parity Violation

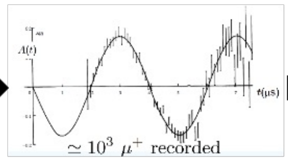

CERN I
1962

In-flight
"g-2" is measured

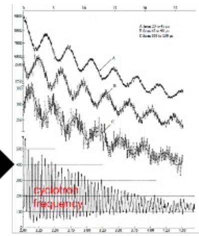

CERN II

1^{st} Storage Ring

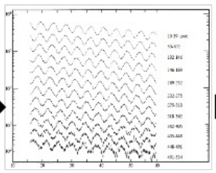

CERN III
1976

Magic Momentum

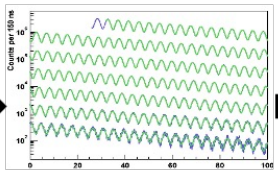

BNL
2003

Muon Injection

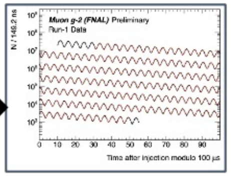

FNAL
2025

Pure Muon Beam and everything else
"gold standard"

34,000 times improvement in precision

Theoretical a_μ Contributions

$$a_\mu^{\rm th} = a_\mu^{\rm SM} + a_\mu^{\rm BSM}$$

$$a_\mu^{\rm SM} = a_\mu^{\rm QED} + a_\mu^{\rm had} + a_\mu^{\rm Weak}$$

$$a_\mu^{\rm BSM}$$

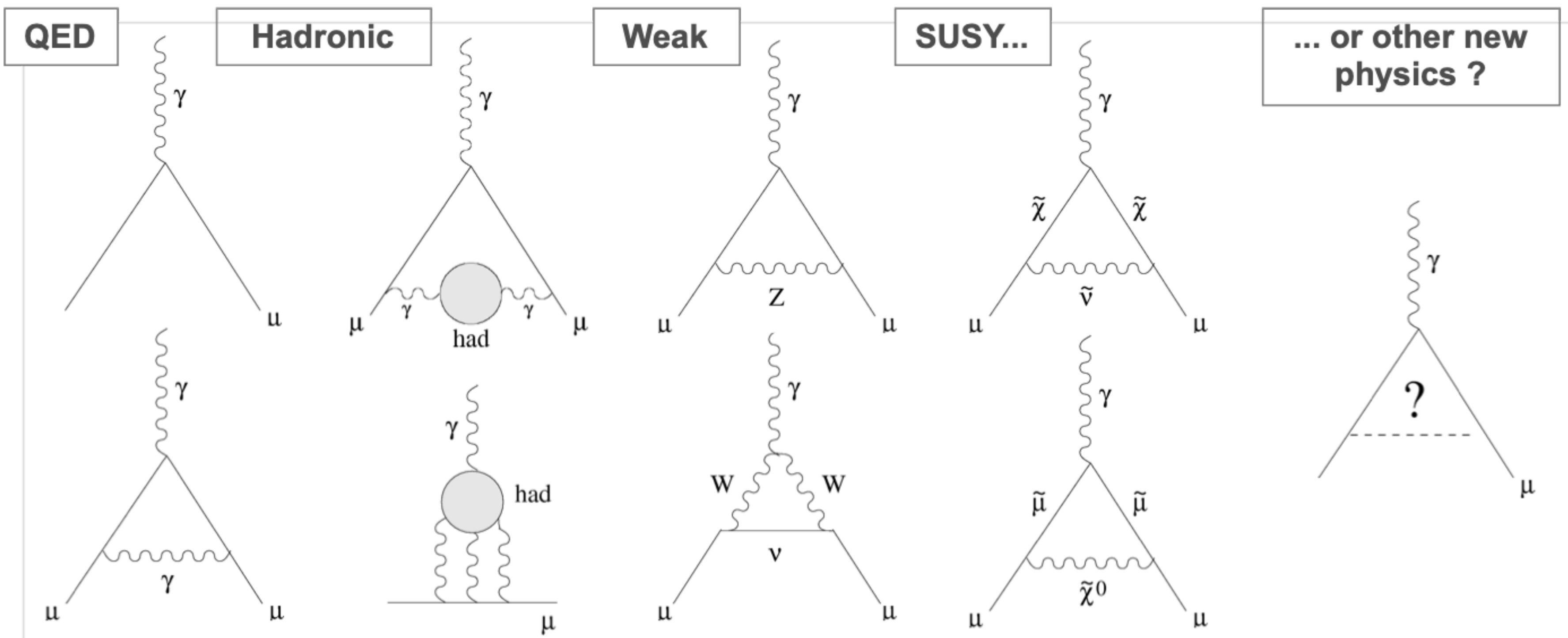

Prediction QED

$$a_\mu^{\mathrm{QED}} = \frac{\alpha}{2\pi} + A_2\left(\frac{\alpha}{\pi}\right)^2 + A_3\left(\frac{\alpha}{\pi}\right)^3 + A_4\left(\frac{\alpha}{\pi}\right)^4 + A_5\left(\frac{\alpha}{\pi}\right)^5$$

			No of Feynman diagrams:
$=$	$116\,140\,793.321\ (23) \times 10^{-11}$	$\mathcal{O}(\alpha)$	1
$+$	$413\,217.626\ (7) \times 10^{-11}$	$\mathcal{O}(\alpha^2)$	7
$+$	$30\,141.902\ (33) \times 10^{-11}$	$\mathcal{O}(\alpha^3)$	72
$+$	$381.004\ (17) \times 10^{-11}$	$\mathcal{O}(\alpha^4)$	891
$+$	$5.078\ (6) \times 10^{-11}$	$\mathcal{O}(\alpha^5)$	12 672
$=$	$116\,584\,718.931\ (104) \times 10^{-11}$		

Based on α^{-1}(Cs)=137.035 999 046(27) [1]

Note: QED contribution for muon is larger than for electron due to mass-dependent terms: m_μ/m_e, m_μ/m_τ vs m_e/m_μ, m_e/m_τ

[1] White Paper (WP) 2020: Phys. Rept. 887 (2020) 1

Prediction Weak

The weak contributions are defined as all SM contributions that are not contained in the pure QED, the HVP, or the HLbL contributions

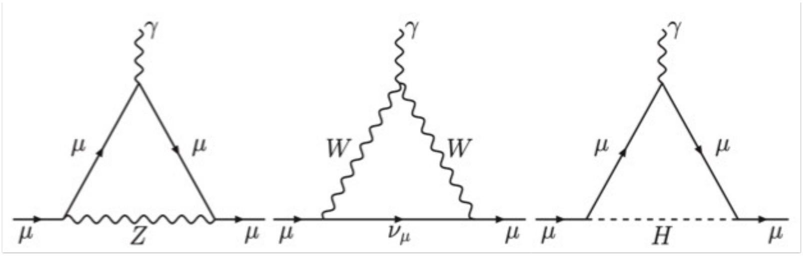

$$a_\mu^{\mathrm{Weak}(1)} = \frac{G_F}{\sqrt{2}}\frac{m_\mu^2}{8\pi^2}\left[\frac{5}{3}+\frac{1}{3}\left(1-4\sin^2_W\right)^2+\mathcal{O}\left(\frac{m_\mu^2}{m_W^2}\right)+\mathcal{O}\left(\frac{m_\mu^2}{m_H^2}\right)\right]$$
$$= 194.79\,(1)\times 10^{-11}$$

$$a_\mu^{\mathrm{Weak}(2)} = a_\mu^{\mathrm{bos}} + a_\mu^{e,\mu,u,c,d,s} + a_\mu^{\tau,t,b} + a_\mu^{H} + a_\mu^{\mathrm{no}\,H}$$
$$= [-19.96\,(1) - 6.91\,(20)(30) - 8.21\,(10) - 1.51\,(1) - 4.64\,(10)]\times 10^{-11}$$

$$a_\mu^{\mathrm{Weak}(\geq 3)} = 0\,(0.20)\times 10^{-11}$$

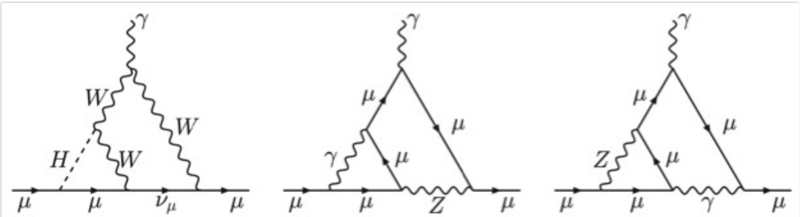

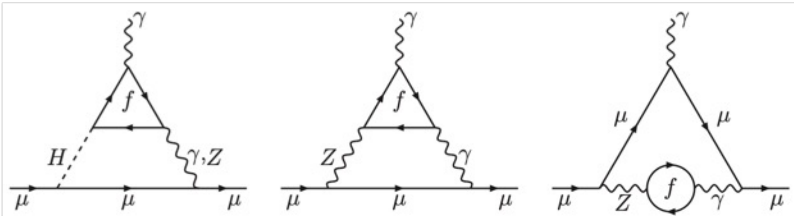

Prediction Hadronic

$$a_\mu^{\text{had}} = a_\mu^{\text{had,LO}} + a_\mu^{\text{had,HO}} + a_\mu^{\text{had,LBL}}$$

Based on analyticity and unitarity, the LO HVP contribution can be calculated using the dispersion relation [1] over $e^+e^- \to$ hadrons cross sections

$$a_\mu^{\text{had,LO}} = \frac{\alpha^2}{3\pi^2}\int_{4m_\pi^2}^{\infty} ds \boxed{\frac{K(s)}{s}} R(s)$$

Born: $\sigma^{(0)}(s) = \sigma(s)\left(\alpha/\alpha(s)\right)^2$

$$12\pi\,\mathrm{Im}\Pi_\gamma(s) = \frac{\sigma^0\,[e^+e^- \to \text{hadrons}\,(\gamma_{FSR})]}{\sigma_{pt}} \equiv R(s)$$

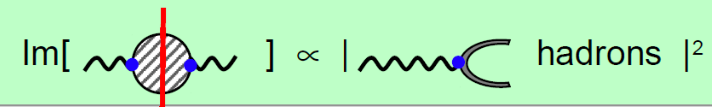

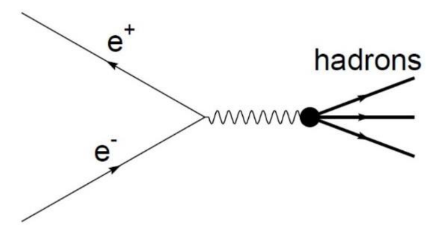

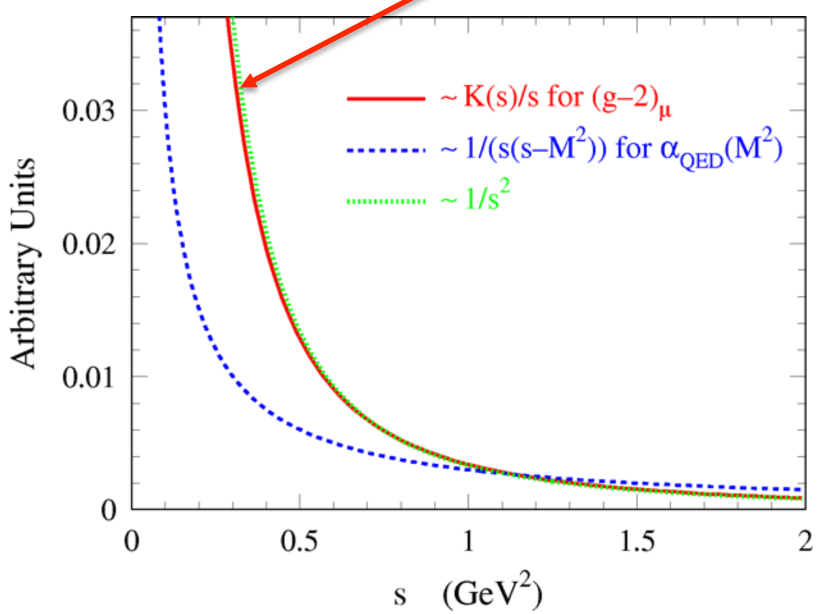

The QED kernel K(s) [2] has such an s dependence that low energy data contribute most:

→ The precision is driven by that of $e^+e^- \to$ hadrons

[1] Bouchiat and Michel, 1961
[2] Brodsky, de Rafael, 1968

R(s) Data

Figures from DHMZ19, EPJC80 (2020) 241

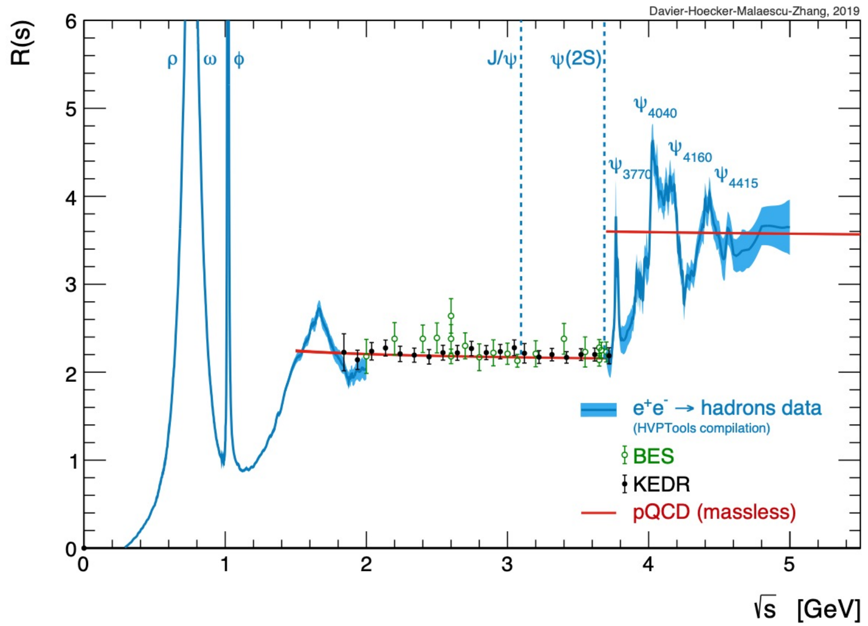

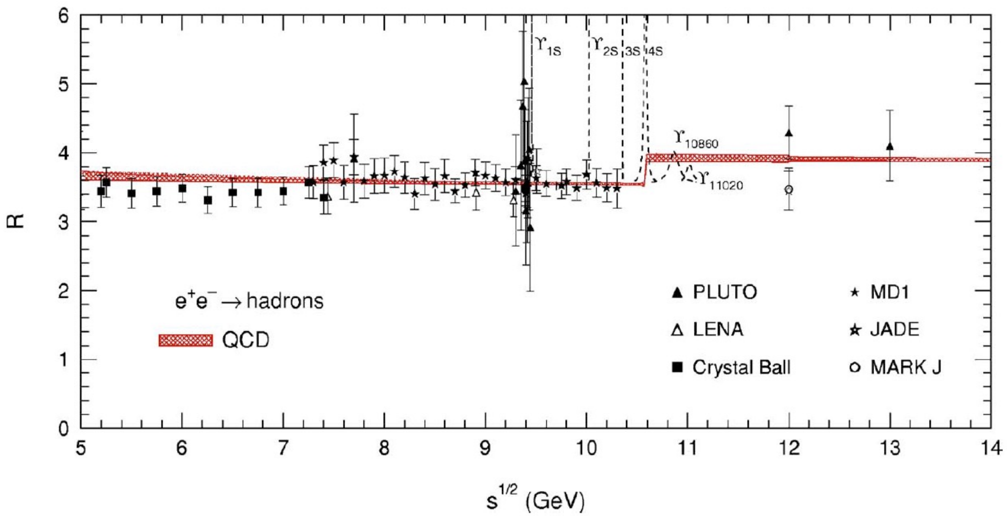

- $[\pi^0\gamma$-1.8 GeV]
  - Over 30 exclusive channels contributes (➔ slide 22)
  - data combination and correlation with one channel and between different channels handled with HVPTools

- [1.8-3.7] GeV
  - good agreement between data and pQCD calculation
    ➛ use 4-loop pQCD
  - J/ψ, ψ(2s): Breit-Wigner integral

- [3.7-5] GeV
  Rich resonance structures, use data

- >5 GeV
  use 4-loop pQCD calculation

Exclusive Channels Below ~1.8 GeV

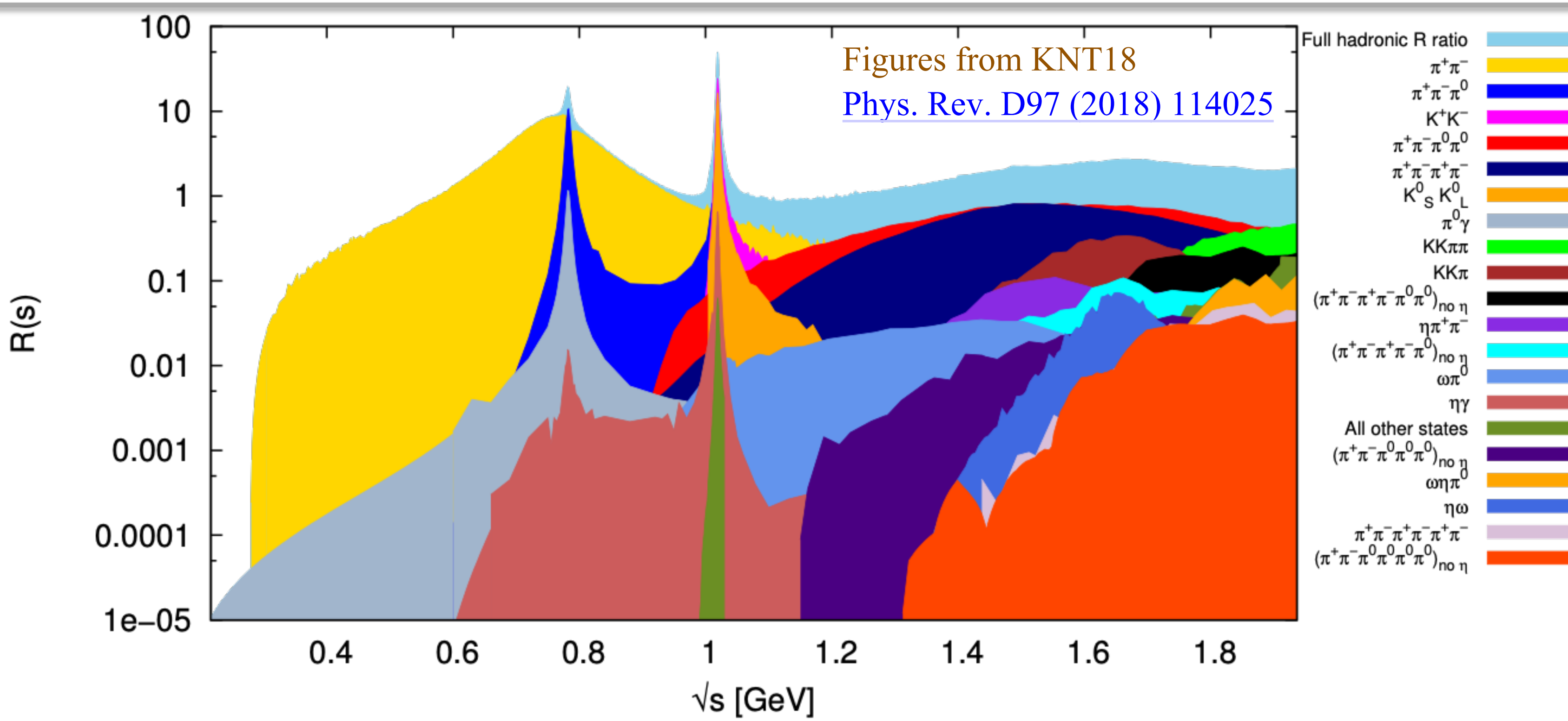

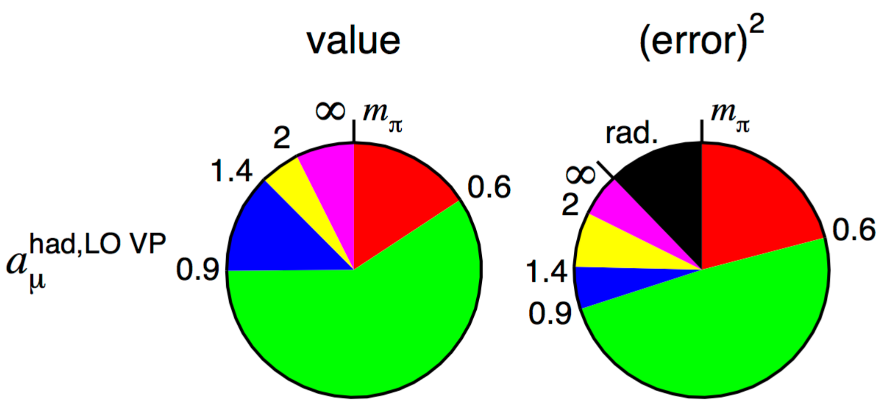

Many exclusive channels contribute

The weight of the kernel function and cross section shape are such that the low energy below ~1.4 GeV has the largest contribution to LO HVP and its error

$e^+e^- \to \pi^+\pi^-$ contributes ~73%

Overall Results

Channel	$a_\mu^{\text{had, LO}}[10^{-10}]$	$\Delta\alpha(m_Z^2)[10^{-4}]$
$\pi^0\gamma$	$4.29 \pm 0.06 \pm 0.04 \pm 0.07$	$0.35 \pm 0.00 \pm 0.00 \pm 0.01$
$\eta\gamma$	$0.65 \pm 0.02 \pm 0.01 \pm 0.01$	$0.08 \pm 0.00 \pm 0.00 \pm 0.00$
$\pi^+\pi^-$	$507.80 \pm 0.83 \pm 3.19 \pm 0.60$	$34.49 \pm 0.06 \pm 0.20 \pm 0.04$
$\pi^+\pi^-\pi^0$	$46.20 \pm 0.40 \pm 1.10 \pm 0.86$	$4.60 \pm 0.04 \pm 0.11 \pm 0.08$
$2\pi^+2\pi^-$	$13.68 \pm 0.03 \pm 0.27 \pm 0.14$	$3.58 \pm 0.01 \pm 0.07 \pm 0.03$
$\pi^+\pi^-2\pi^0$	$18.03 \pm 0.06 \pm 0.48 \pm 0.26$	$4.45 \pm 0.02 \pm 0.12 \pm 0.07$
$2\pi^+2\pi^-\pi^0$ (η excl.)	$0.69 \pm 0.04 \pm 0.06 \pm 0.03$	$0.21 \pm 0.01 \pm 0.02 \pm 0.01$
$\pi^+\pi^-3\pi^0$ (η excl.)	$0.49 \pm 0.03 \pm 0.09 \pm 0.00$	$0.15 \pm 0.01 \pm 0.03 \pm 0.00$
$3\pi^+3\pi^-$	$0.11 \pm 0.00 \pm 0.01 \pm 0.00$	$0.04 \pm 0.00 \pm 0.00 \pm 0.00$
$2\pi^+2\pi^-2\pi^0$ (η excl.)	$0.71 \pm 0.06 \pm 0.07 \pm 0.14$	$0.25 \pm 0.02 \pm 0.02 \pm 0.05$
$\pi^+\pi^-4\pi^0$ (η excl., isospin)	$0.08 \pm 0.01 \pm 0.08 \pm 0.00$	$0.03 \pm 0.00 \pm 0.03 \pm 0.00$
$\eta\pi^+\pi^-$	$1.19 \pm 0.02 \pm 0.04 \pm 0.02$	$0.35 \pm 0.01 \pm 0.01 \pm 0.01$
$\eta\omega$	$0.35 \pm 0.01 \pm 0.02 \pm 0.01$	$0.11 \pm 0.00 \pm 0.01 \pm 0.00$
$\eta\pi^+\pi^-\pi^0$(non-ω,ϕ)	$0.34 \pm 0.03 \pm 0.03 \pm 0.04$	$0.12 \pm 0.01 \pm 0.01 \pm 0.01$
$\eta 2\pi^+2\pi^-$	$0.02 \pm 0.01 \pm 0.00 \pm 0.00$	$0.01 \pm 0.00 \pm 0.00 \pm 0.00$
$\omega\eta\pi^0$	$0.06 \pm 0.01 \pm 0.01 \pm 0.00$	$0.02 \pm 0.00 \pm 0.00 \pm 0.00$
$\omega\pi^0$ ($\omega \to \pi^0\gamma$)	$0.94 \pm 0.01 \pm 0.03 \pm 0.00$	$0.20 \pm 0.00 \pm 0.01 \pm 0.00$
$\omega(\pi\pi)^0$ ($\omega \to \pi^0\gamma$)	$0.07 \pm 0.00 \pm 0.00 \pm 0.00$	$0.02 \pm 0.00 \pm 0.00 \pm 0.00$
ω (non-$3\pi, \pi\gamma, \eta\gamma$)	$0.04 \pm 0.00 \pm 0.00 \pm 0.00$	$0.00 \pm 0.00 \pm 0.00 \pm 0.00$
K^+K^-	$23.08 \pm 0.20 \pm 0.33 \pm 0.21$	$3.35 \pm 0.03 \pm 0.05 \pm 0.03$
K_SK_L	$12.82 \pm 0.06 \pm 0.18 \pm 0.15$	$1.74 \pm 0.01 \pm 0.03 \pm 0.02$
ϕ (non-$K\overline{K}, 3\pi, \pi\gamma, \eta\gamma$)	$0.05 \pm 0.00 \pm 0.00 \pm 0.00$	$0.01 \pm 0.00 \pm 0.00 \pm 0.00$
$K\overline{K}\pi$	$2.45 \pm 0.05 \pm 0.10 \pm 0.06$	$0.78 \pm 0.02 \pm 0.03 \pm 0.02$
$K\overline{K}2\pi$	$0.85 \pm 0.02 \pm 0.05 \pm 0.01$	$0.30 \pm 0.01 \pm 0.02 \pm 0.00$
$K\overline{K}3\pi$ (estimate)	$-0.02 \pm 0.01 \pm 0.01 \pm 0.00$	$-0.01 \pm 0.00 \pm 0.00 \pm 0.00$
$\eta\phi$	$0.33 \pm 0.01 \pm 0.01 \pm 0.00$	$0.11 \pm 0.00 \pm 0.00 \pm 0.00$
$\eta K\overline{K}$ (non-ϕ)	$0.01 \pm 0.01 \pm 0.01 \pm 0.00$	$0.00 \pm 0.00 \pm 0.01 \pm 0.00$
$\omega K\overline{K}$ ($\omega \to \pi^0\gamma$)	$0.01 \pm 0.00 \pm 0.00 \pm 0.00$	$0.00 \pm 0.00 \pm 0.00 \pm 0.00$
$\omega 3\pi$ ($\omega \to \pi^0\gamma$)	$0.06 \pm 0.01 \pm 0.01 \pm 0.01$	$0.02 \pm 0.00 \pm 0.00 \pm 0.00$
7π ($3\pi^+3\pi^-\pi^0$ + estimate)	$0.02 \pm 0.00 \pm 0.01 \pm 0.00$	$0.01 \pm 0.00 \pm 0.00 \pm 0.00$
J/ψ (BW integral)	6.28 ± 0.07	7.09 ± 0.08
$\psi(2S)$ (BW integral)	1.57 ± 0.03	2.50 ± 0.04
R data $[3.7 - 5.0]$ GeV	$7.29 \pm 0.05 \pm 0.30 \pm 0.00$	$15.79 \pm 0.12 \pm 0.66 \pm 0.00$
R_{QCD} $[1.8 - 3.7\ \text{GeV}]_{uds}$	$33.45 \pm 0.28 \pm 0.65_{\text{dual}}$	$24.27 \pm 0.18 \pm 0.28_{\text{dual}}$
R_{QCD} $[5.0 - 9.3\ \text{GeV}]_{udsc}$	6.86 ± 0.04	34.89 ± 0.17
R_{QCD} $[9.3 - 12.0\ \text{GeV}]_{udscb}$	1.21 ± 0.01	15.56 ± 0.04
R_{QCD} $[12.0 - 40.0\ \text{GeV}]_{udscb}$	1.64 ± 0.00	77.94 ± 0.12
R_{QCD} $[> 40.0\ \text{GeV}]_{udscb}$	0.16 ± 0.00	42.70 ± 0.06
R_{QCD} $[> 40.0\ \text{GeV}]_{t}$	0.00 ± 0.00	-0.72 ± 0.01
Sum	$\boxed{693.9 \pm 1.0 \pm 3.4 \pm 1.6 \pm 0.1_{\psi} \pm 0.7_{\text{QCD}}}$	$275.42 \pm 0.15 \pm 0.72 \pm 0.23 \pm 0.09_{\psi} \pm 0.55_{\text{QCD}}$

More than 30 exclusive channels (<1.8 GeV) evaluated

Estimation for missing modes based on isospin constraints becomes negligible (0.016%)

Table taken from DHMZ, EPJC80 (2020) 241

Summary of the SM a_μ Predictions

$$a_\mu^{\rm SM} = a_\mu^{\rm QED} + a_\mu^{\rm had} + a_\mu^{\rm EW} \quad \sim 0.001$$

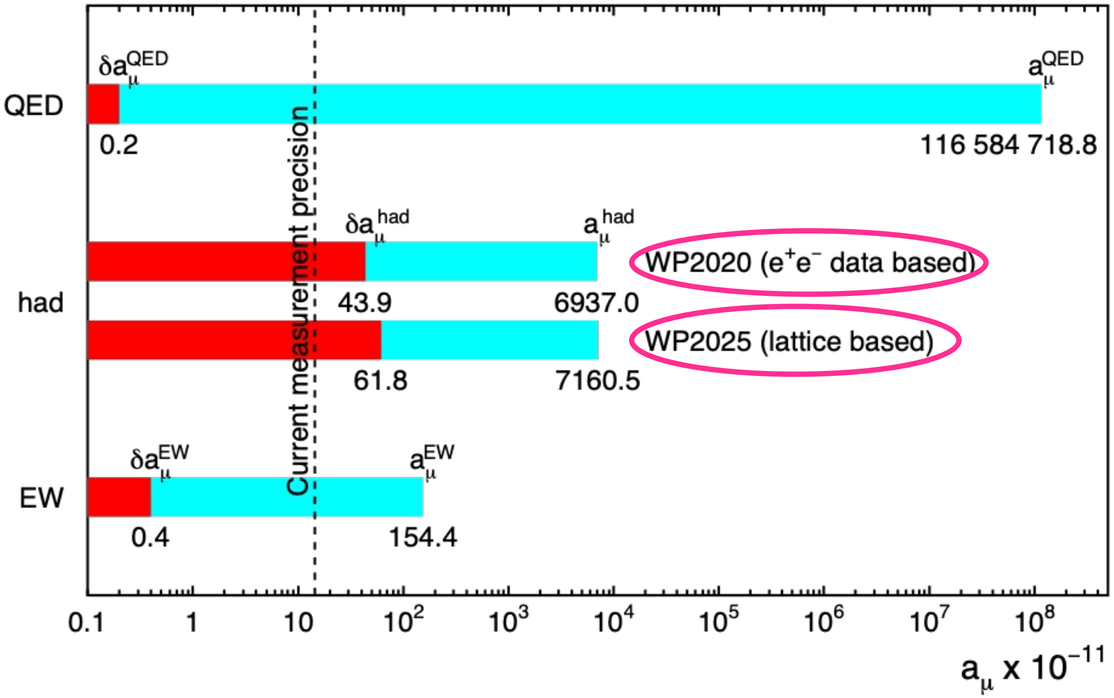

$$a_\mu^{\rm had} = a_\mu^{\rm HVP\ LO} + a_\mu^{\rm HVP\ HO} + a_\mu^{\rm HLbL}$$

had	HVP LO	HVP HO	HLbL
		$a_\mu[10^{-11}]$ (unc)	
WP2020	6931 (40)	−85.9 (0.7)	92 (18)
WP2025	7132 (61)	−87.2 (1.3)	115.5 (9.9)

WP2020: Phys. Rept. 887 (2020) 1
WP2025: arXiv:2505.21476

WP stands for the white paper of the muon g-2 Theory Initiative (TI)

- ➢ QED has by far the largest contribution
- ➢ QED and EW both calculable with high precision within the SM
- ➢ HVP LO, of non-perturbative nature at low energies, has the largest uncertainty ➔ the focus of studies since decades

Comparison & Development over Time

- ➢ Compare the direct a_μ measurements (slide 13) with the SM a_μ predictions ➔ any discrepancy?
- ➢ If yes, hint for new physics? where to improve?
  - ➢ On the a_μ measurements, BNL $\rightarrow$ FNAL
  - ➢ On the a_μ prediction side, the focus is more on the LO HVP
    - ➢ When e^+e^- data precision was still limited, use tau data as an alternative data sample [1] ➔ Isospin corrections?
    - ➢ More precise cross-section data, in particular the two-pion channel
    - ➢ Sophisticated data combination tools (HVPTools [2])
    - ➢ Alternative predictions: lattice QCD

[1] ADH 1998, Eur.Phys.J.C 2 (1998) 123
[2] DHMYZ+ 2010, Eur.Phys.J.C 66 (2010) 1

Comparison Measurement and Prediction: 2003

Figure from DEHZ 2003, EPJC27 (2003) 497

Based on e^+e^- data to hadrons with dominant two-pion samples from CMD, CMD-2, DM1, DM2, OLYA and TOF

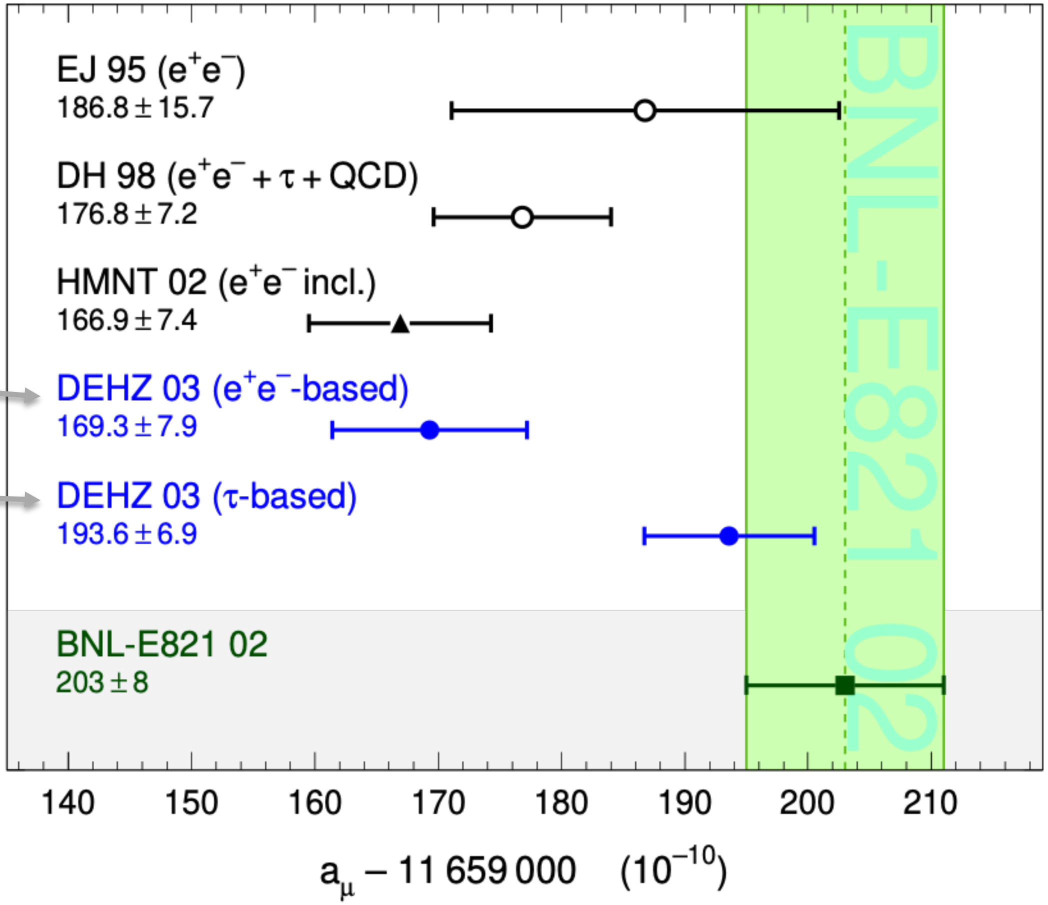

Based on tau data with dominant two-pion samples from ALEPH, CLEO, OPAL

This early discrepancy of ~3σ has motivated further improvements in precision from both the experimental and theoretical sides.

Comparison Measurement and Prediction: 2010

Figures from Ref. [2]

Belle tau two-pion data included
Isospin corrections reevaluated [1]

KLEO 2008 data included [1]

Including BABAR 2009 data
1st application of HVPTools
[1]

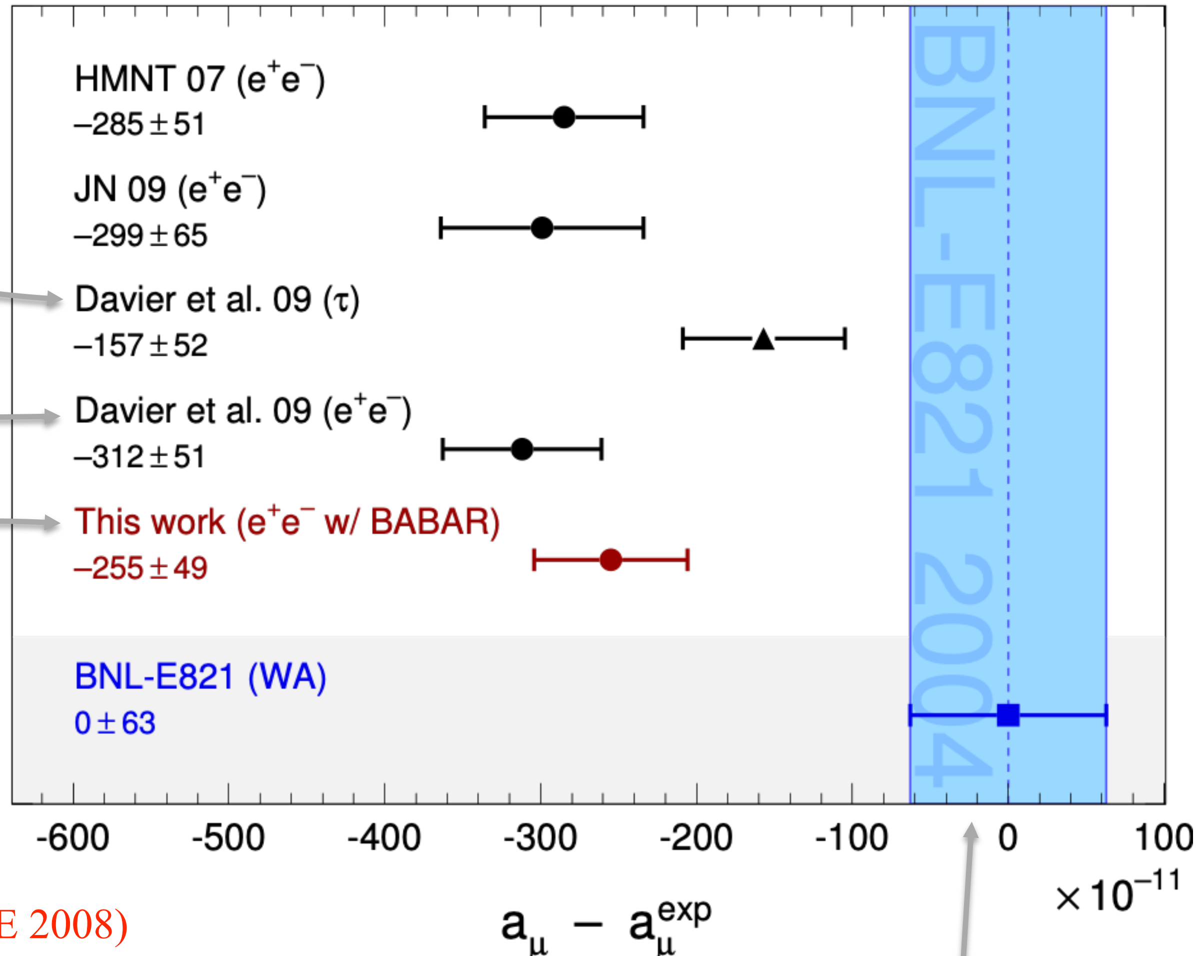

Measurement uncertainty improved from 80 to 63

Discrepancy increased to 3.8σ (KLOE 2008)
or 3.2σ (BABAR 2009)

[1] DHMYZ+ 2010, Eur.Phys.J. C 66 (2010) 127
[2] DHMYZ 2010, Eur. Phys. J. C 66 (2010) 1

Data Combination Using HVPTools [1]

- ❒ Combine experimental spectra with arbitrary spacing/binning
- ❒ Properly propagate uncertainties and correlations
  - ➤ Between measurements (data points/bins) of a given experiment
  - ➤ Between experiments
  - ➤ Between different channels
- ❒ Linear/quadratic splines to interpolate between points/bins of each experiment
  - ➤ For binned measurements: preserve integral inside each bin
- ❒ Fluctuate data points taking into account correlations and redo the splines for each (pseudo)experiment
  - ➤ Each uncertainty fluctuated coherently for all points/bins that it impacts
  - ➤ Eigenvector decomposition for (stat & syst) covariance matrices
- ❒ Resulting combination shown in fine binning
  - ➤ Local error inflation following PDG prescription ($\sqrt{\chi^2/\mathrm{dof}}$) to take better into account data tension

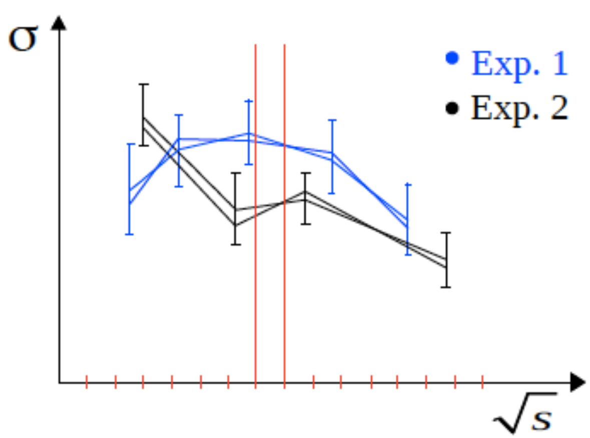

[1] DHMYZ+ 2010, Eur.Phys.J.C 66 (2010) 127

Combination Results of HVPTools

Figures from DHMYZ 2010, EPJC66 (2010) 1

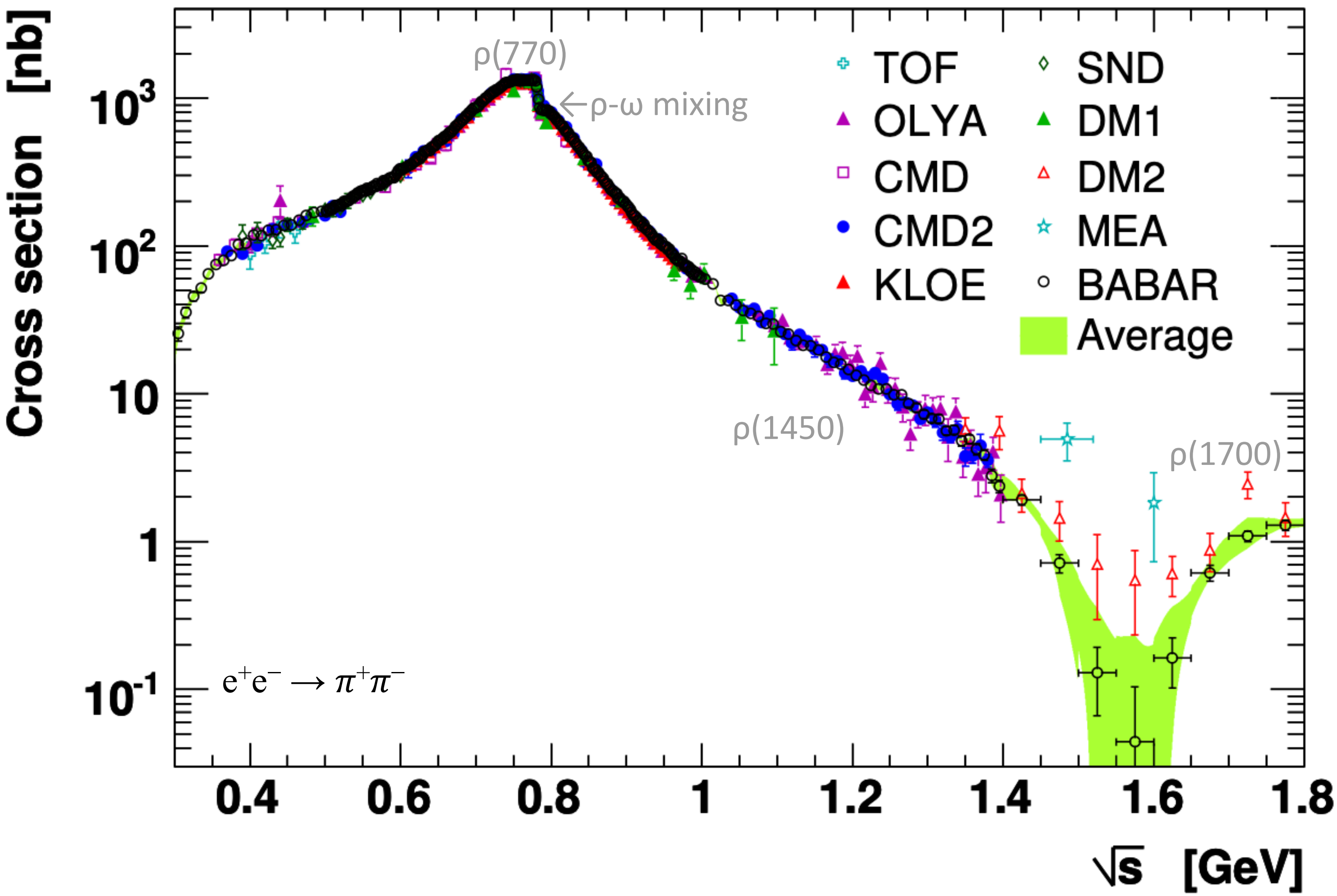

Relative Weights and Tension

Figures from DHMYZ 2010, EPJC66 (2010) 1

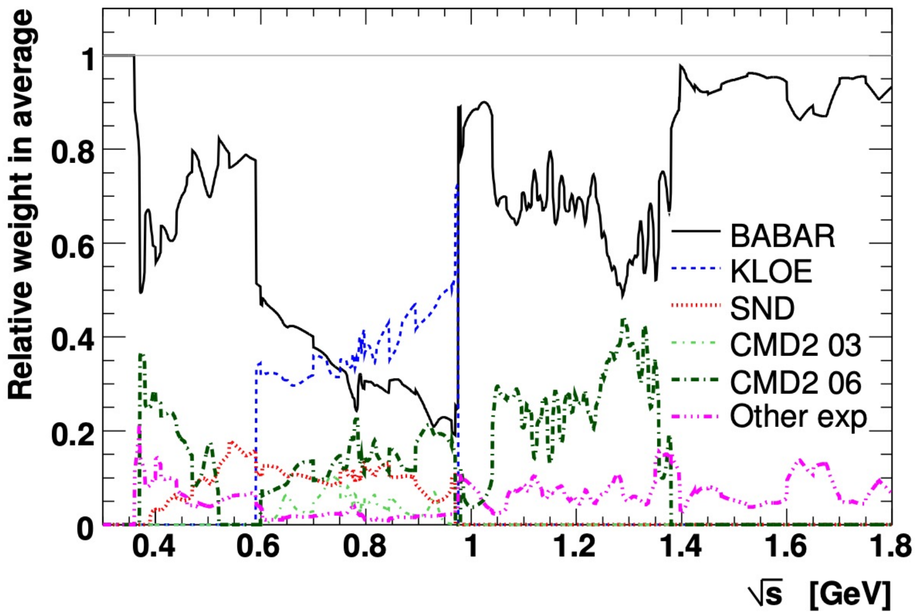

In the energy range of [0.6-0.9] GeV, BABAR and KLOE dominate, elsewhere BABAR has better precision

Inconsistency between measurements reflected by large local scale factor (SF) defined by $\sqrt{\chi^2/\mathrm{dof}}$ a la PDG (~15% increase on δa_μ^{had})

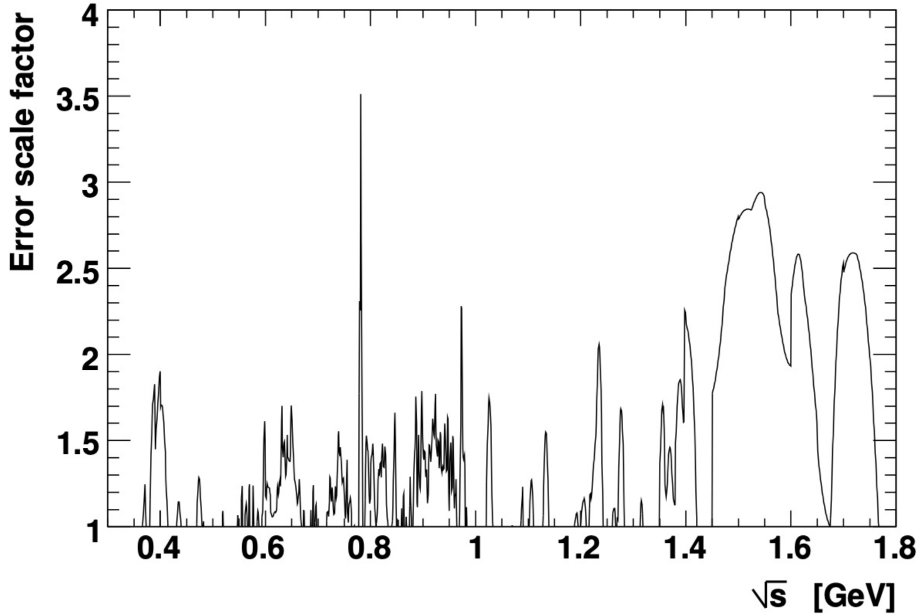

Comparison Measurement and Prediction: 2017

Figures from Ref. [2]

KLOE 2010 data included, plus several BABAR high multiplicity channels [1]

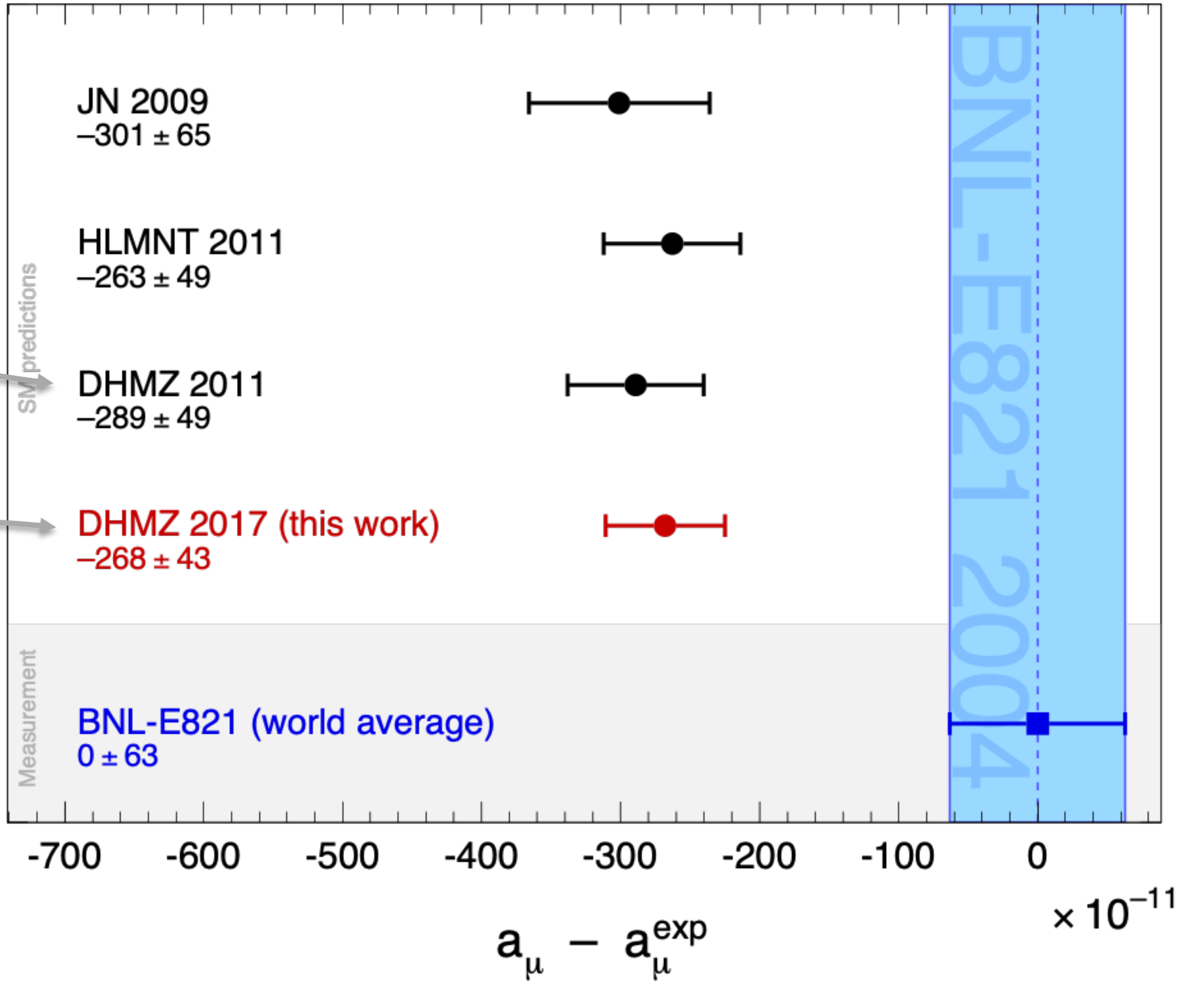

KLOE 2012, BESIII 2015 two-pion data, more BABAR high multiplicity channel included. In total 39 exclusive channels (was 22 in [1]) considered below 1.8 GeV

The discrepancy is around 3.5σ

[1] DHMZ 2011, Eur. Phys. J. C 71 (2011) 1515
[2] DHMYZ 2017, Eur. Phys. J. C77 (2017) 827

Comparison Measurement and Prediction: 2019

Figures from DHMYZ, EPJC80 (2020) 241

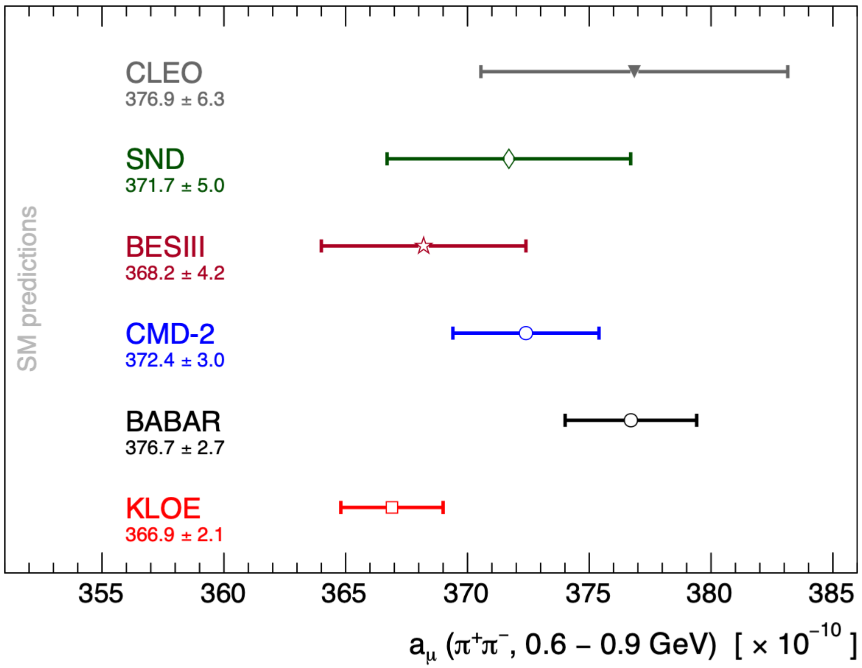

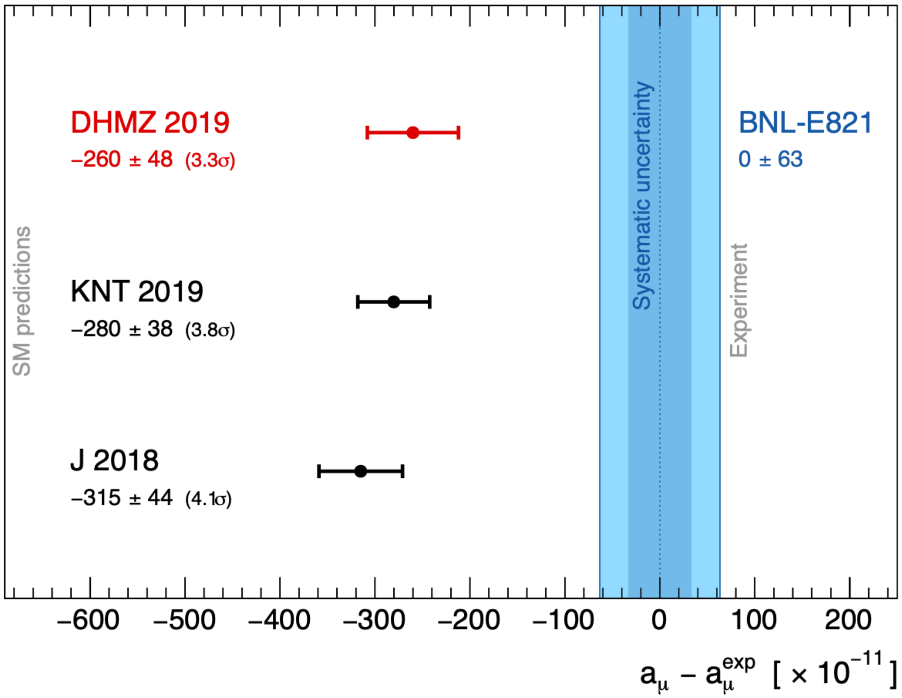

This (DHMZ 2020) was our input to WP2020 (in addition to the tau-data-based evaluation)

We performed a phenomenological fit to supplement less precise data at low energy up to 0.6 GeV (improved the precision by a factor 2, slide 32)

We introduced a scheme to add an uncertainty reflecting the inconsistency BABAR-KLOE input data (slide 33)

Fit Performed to 1 GeV, Results Used to 0.6 GeV

Figures from DHMZ, EPJC80 (2020) 241

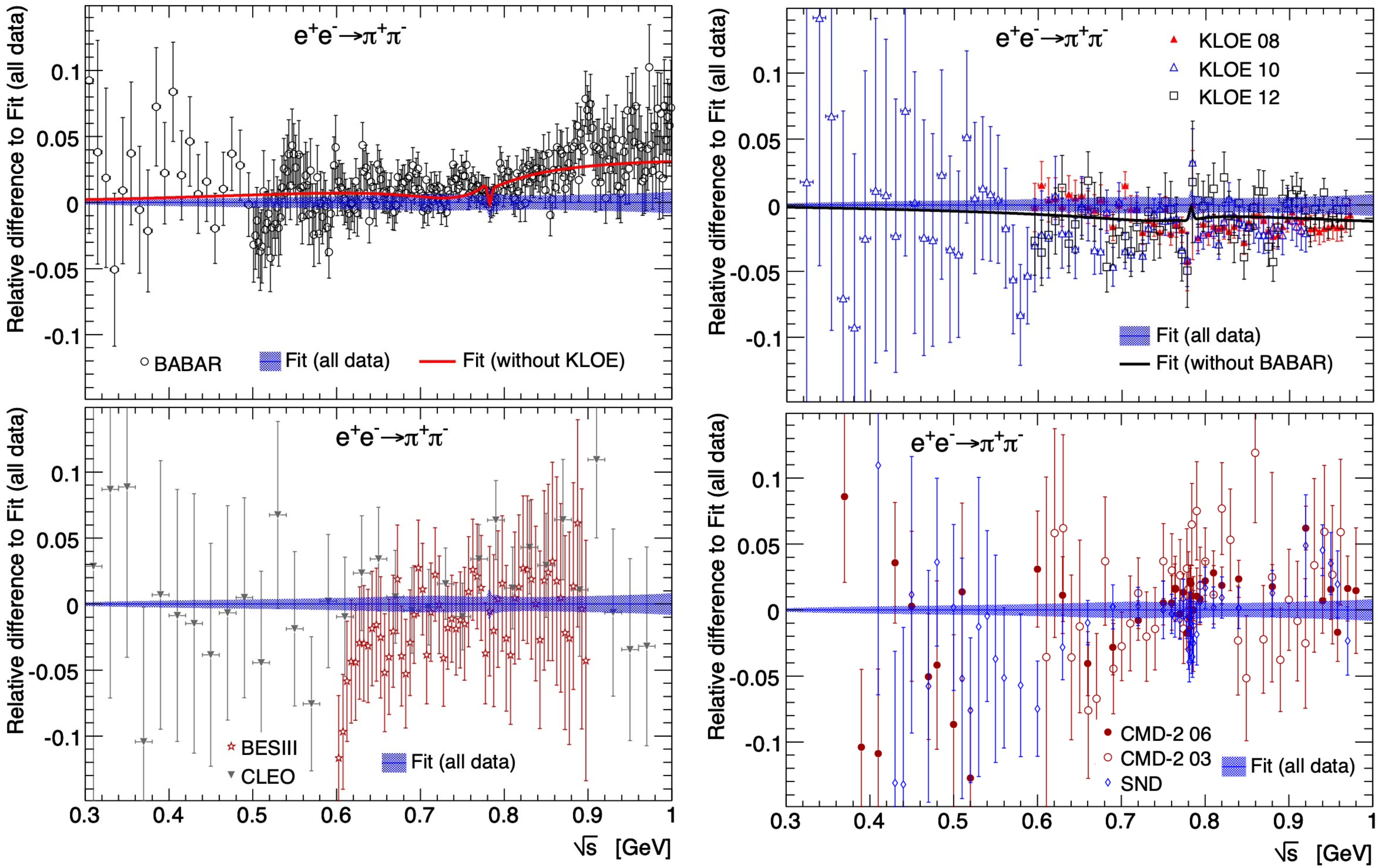

Combined Results Fit [<0.6 GeV] + Data [0.6-1.8 GeV]

Take into account the correlation of 62% (based on pseudo-data samples) of the two regions

$\sqrt{s}$ range [GeV]	a_μ^{had} $[10^{-10}]$ All data	a_μ^{had} $[10^{-10}]$ All but BABAR	a_μ^{had} $[10^{-10}]$ All but KLOE
threshold - 1.8	$506.9 \pm 1.9_{total}$	$505.0 \pm 2.1_{total}$	$510.6 \pm 2.2_{total}$

⇒ The difference "All but BABAR" and "All but KLOE" = 5.6 to be compared with 1.9 uncertainty with "All data"

- ➤ The local error inflation is not sufficient to amplify the uncertainty
- ➤ Global tension (normalisation/shape) not previously accounted for
- ➤ Potential underestimated uncertainty in at least one of the measurements?
- ➤ Other measurements not precise enough and are in agreement with BABAR or KLOE

⇒ Given the fact we do not know which dataset is problematic, we decide to

- ➤ Add half of the discrepancy (2.8) as an additional uncertainty (correcting the local PDG inflation to avoid double counting)
- ➤ Take the mean value "All but BABAR" and "All but KLOE" as our central value

Tension in the 3π (2nd dominant) channel

Most precise $2\pi\pi^0$ measurements:

- SND 2002: [980−1380] MeV
- SND 2003: [660−970] MeV
- CMD-2 2004: [760−810] MeV
- CMD-2 2006: [984−1060] MeV
- BABAR 2021: [620−3500] MeV
- Belle II 2024: [620−3500] MeV
- SND 2026: [560−1100] MeV

The latter two are not yet included in WP2020

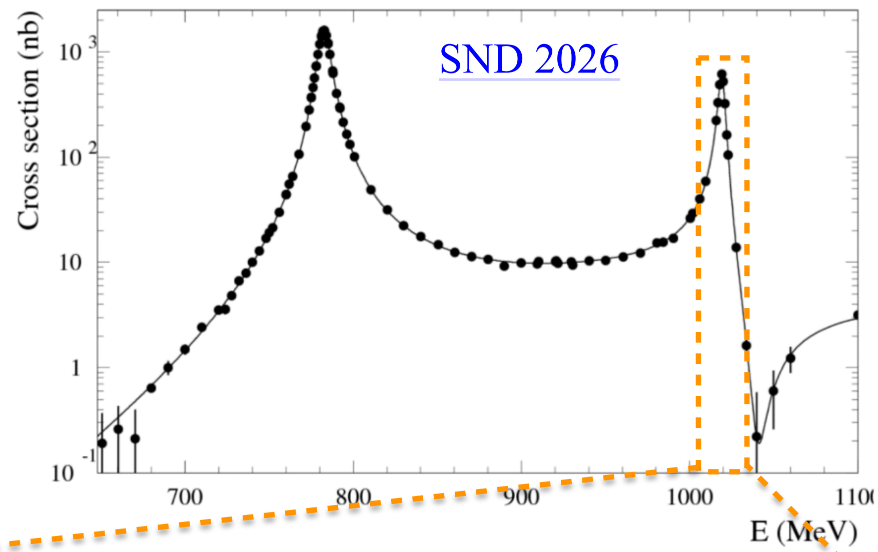

SND 2006 (yellow error band - VMD fit) vs other measurements

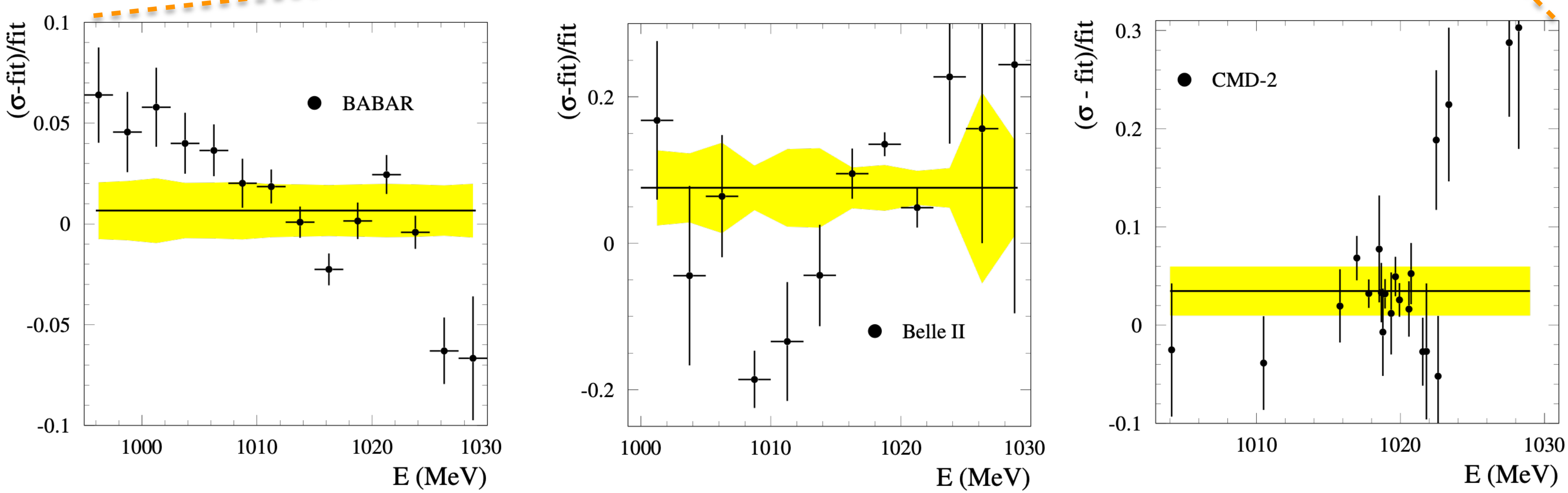

Tension in the 3π (2nd dominant) channel

Figures from Belle II,
[Phys. Rev. D 110 (2024) 112005](https://doi.org/10.1103/PhysRevD.110.112005)

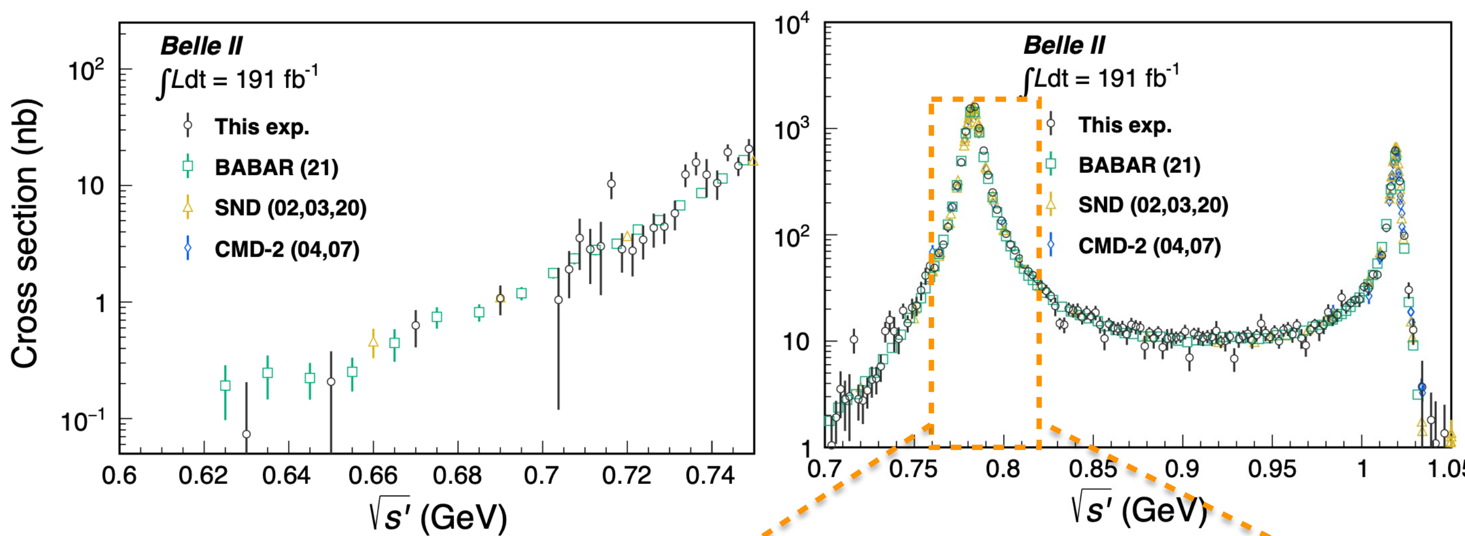

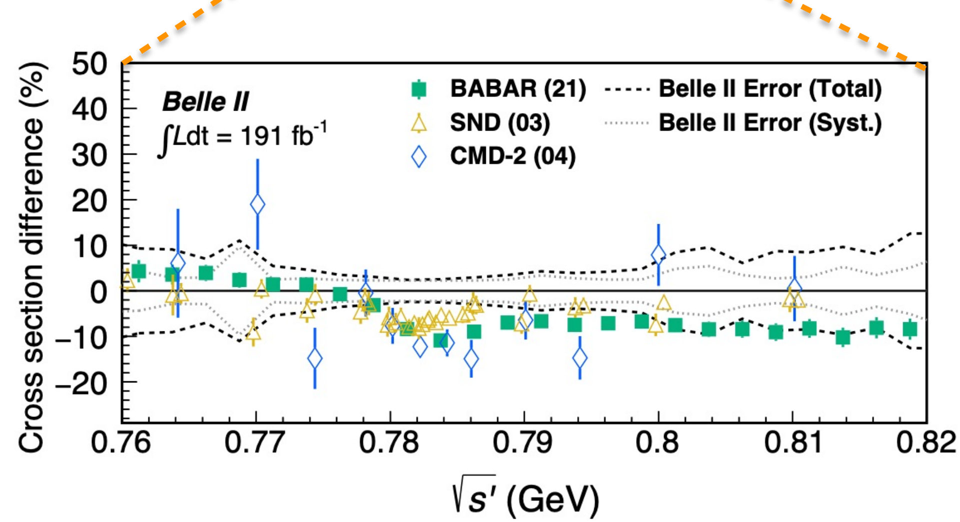

- This channel contributes ~6.7% to LO HVP, 2nd largest channel
- New measurement from Belle II (0.62-3.5 GeV, 191 fb^{-1}) compared with BABAR (0.62-3.5 GeV, 469 fb^{-1}), SND and CMD2
- Some tension beyond the quoted uncertainties

Tension in the KK (3rd dominant) channel

Figures from DHMZ 2020, EPJC80 (2020) 241

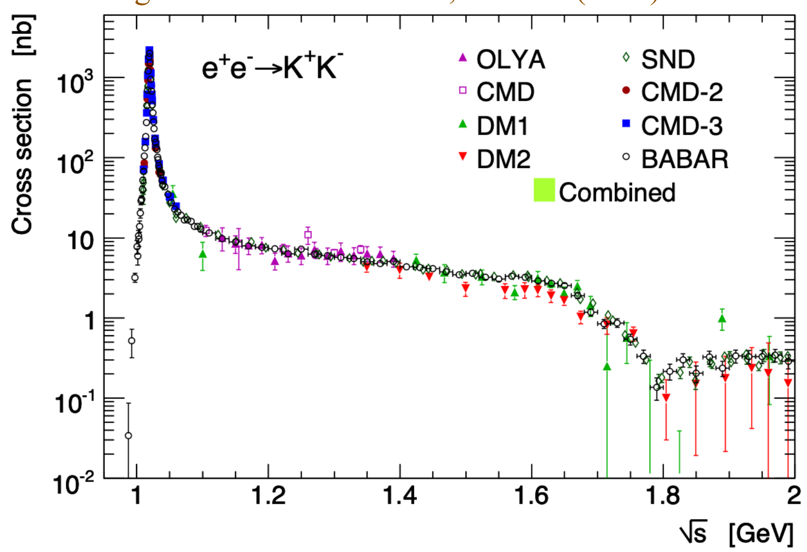

Several measurements with different precisions, CMD-2 and CMD-3 do not agree within the quoted uncertainties!
➜ Large error scaling factors
though this channel only contributes 3.3% to LO HVP and 1.2% to uncertainty-squared.

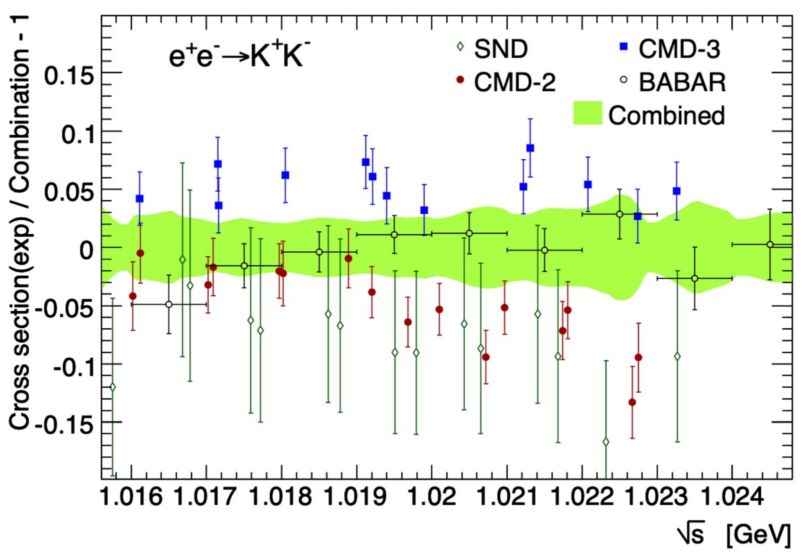

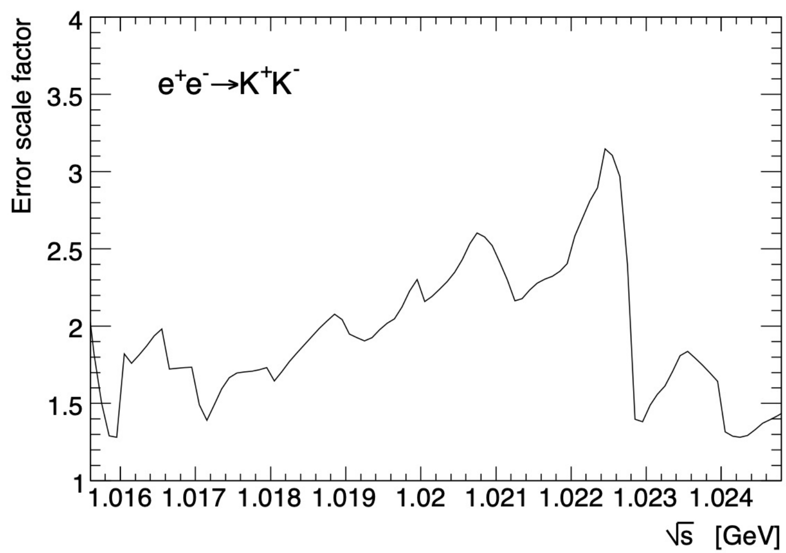

The Situation in 2020 (WP20)

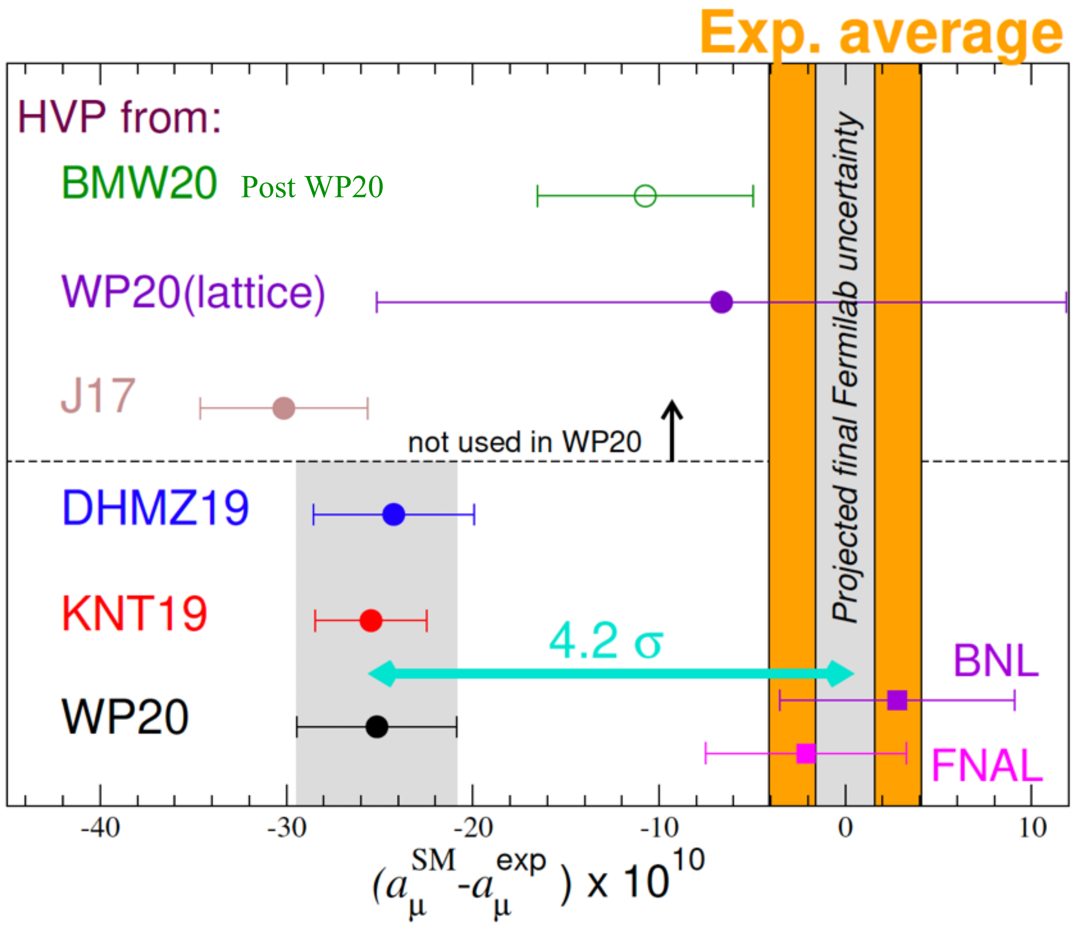

A discrepancy of 4.2σ!

An outcome after several dedicated muon g-2 Theory Initiative workshops since 2017

The Situation in 2025 (WP2025)

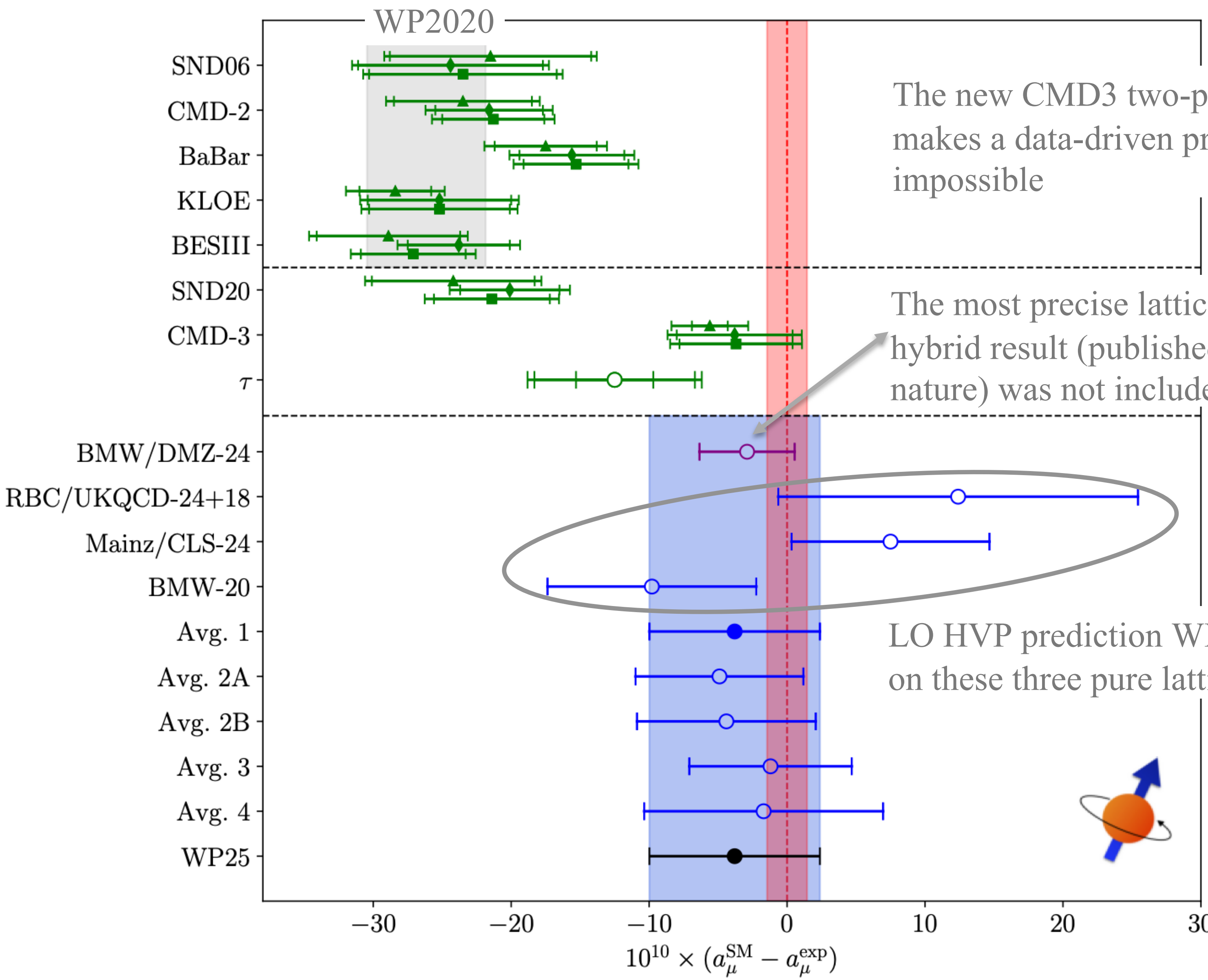

The new CMD3 two-pion data makes a data-driven prediction impossible

The most precise lattice-data hybrid result (published later in nature) was not included!

LO HVP prediction WP25 based on these three pure lattice results

Lattice vs Data-Driven Predictions

$$a_\mu^{\text{HVP, LO}} = \left(\frac{\alpha}{\pi}\right)^2 \int_0^\infty dQ^2 f(Q^2)\hat{\Pi}(Q^2)$$

Space-like lattice calculation

In practice, lattice calculation based on time-momentum representation (TMR) with zero-momentum time correlation $C(x_0)$:

$$a_\mu^{\text{HVP, LO}} = \left(\frac{\alpha}{\pi}\right)^2 \int_0^\infty dx_0\, C(x_0)\tilde{f}(x_0)$$

breaking time integral into Short-Distance (SD), intermediate Window (W) and Long-distance (LD) components:

$$a_\mu^{\text{HVP, LO}} = a_\mu^{\text{SD}} + a_\mu^{\text{W}} + a_\mu^{\text{LD}}$$

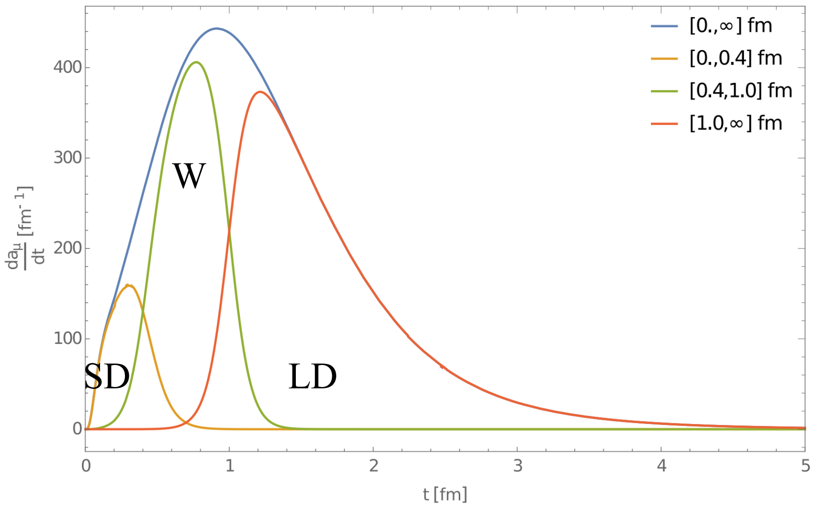

$$a_\mu^{\text{had,LO}} = \frac{\alpha^2}{3\pi^2} \int_{4m_\pi^2}^\infty ds \frac{K(s)}{s} R(s)$$

Time-like data-driven evaluation with inputs from e^+e^- or τ data

No one-to-one correspondance between lattice-time integrals and data-driven time-like regions. Still, LD corresponds to a region where the low energy data have the largest impact

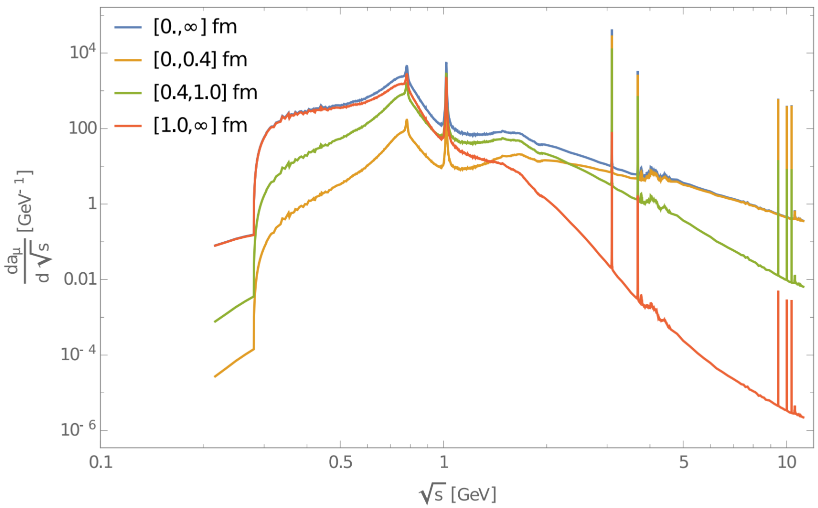

WP2025 Lattice Prediction vs BMW/DMZ-24

$$a_\mu^{\text{HVP, LO}} = a_\mu^{\text{SD}} + a_\mu^{\text{W}} + a_\mu^{\text{LD}}$$

The numerical values of WP2025 [1] for the three items are:

SD [0−0.04] fm: 69.10(26)
W [0.04−1.0] fm: 236.58(43)
LD [1.0−∞] fm: 407.5(6.1)
Total [0−∞] fm: 713.2(6.1)

➔ The LD term has the largest contribution and uncertainty

BMW/DMZ-24 [2] found an optimal splitting of the LD range into two parts:

Lattice-based [1.0−2.8] fm
Data-based [2.8−∞] fm: 27.59(52)

Total [0−∞] fm: 715.1(3.4)

➔ The data-based contribution [2.8−∞] fm represents a few % of the total LO HVP, has however significantly improved the overall uncertainty

[1] WP2025, Phys.Rept. 1143 (2025) 1
[2] BMW/DMZ-24, Nature 653 (2026) 373

HVP Contribution to Running QED $\alpha(s)$

In parallel to the LO HVP evaluations, we regularly evaluate $\Delta\alpha_{\rm had}$ at M_Z

$$\alpha(s) = \frac{\alpha(0)}{1 - \Delta\alpha_{\rm lep}(s) - \Delta\alpha_{\rm had}(s)}$$

$$\Delta\alpha_{\rm had}(s) = -\frac{\alpha(0)}{3\pi}{\rm Re}\int_{4m_\pi^2}^{\infty} ds' \frac{R(s')}{s'(s'-s-i\epsilon)}$$

R(s): the same input as for a_μ LO HVP except that the higher energy part receives relatively larger weights

The current precision for $\Delta\alpha_{\rm had}(s)$ is a limiting factor for stringent SM consistency tests.

$$\Delta\alpha_{\rm lep}(M_Z^2) = 314.979(2) \times 10^{-4}$$
$$\Delta\alpha_{\rm had}^{(5)}(M_Z^2) = 275.7(1.0) \times 10^{-4}$$
$$\Delta\alpha_{\rm had}^{\rm top}(M_Z^2) = -0.72(1) \times 10^{-4}$$

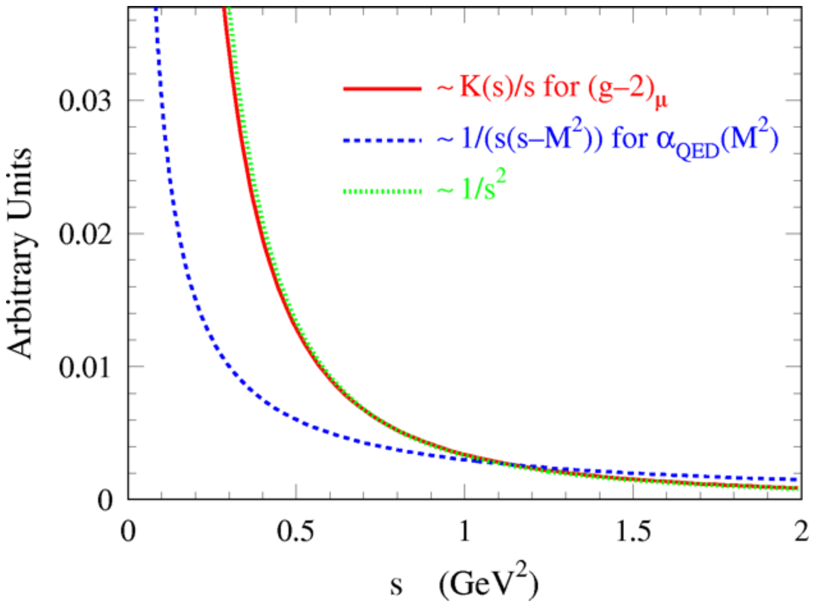

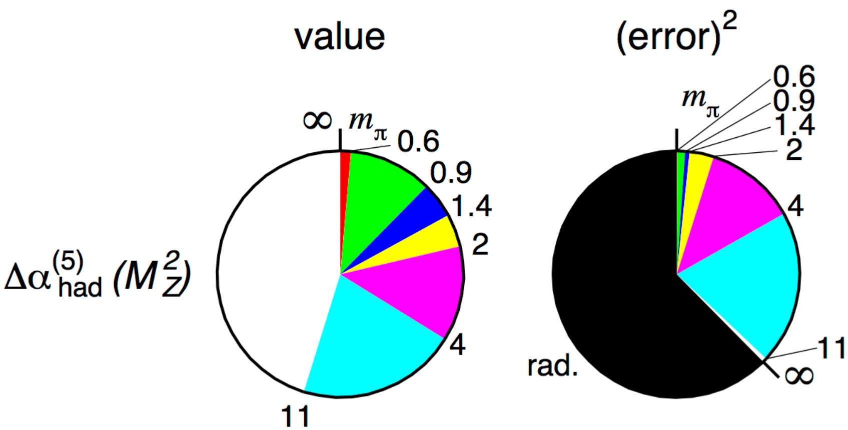

Figures from KNT18 Phys. Rev. D97 (2018) 114025

Impact of the new $\alpha_{had}(s)$ on Higgs Mass

Using our 2011 evaluation increases the most probable Higgs boson mass by +7 GeV from 84 to 91 GeV with un uncertainty of $^{+30}/_{-23}$ GeV

This was in excellent agreement with the discovery of the Higgs boson in 2012 at ~125 GeV

Figure from DHMZ 2011, EPJC71 (2011) 1515

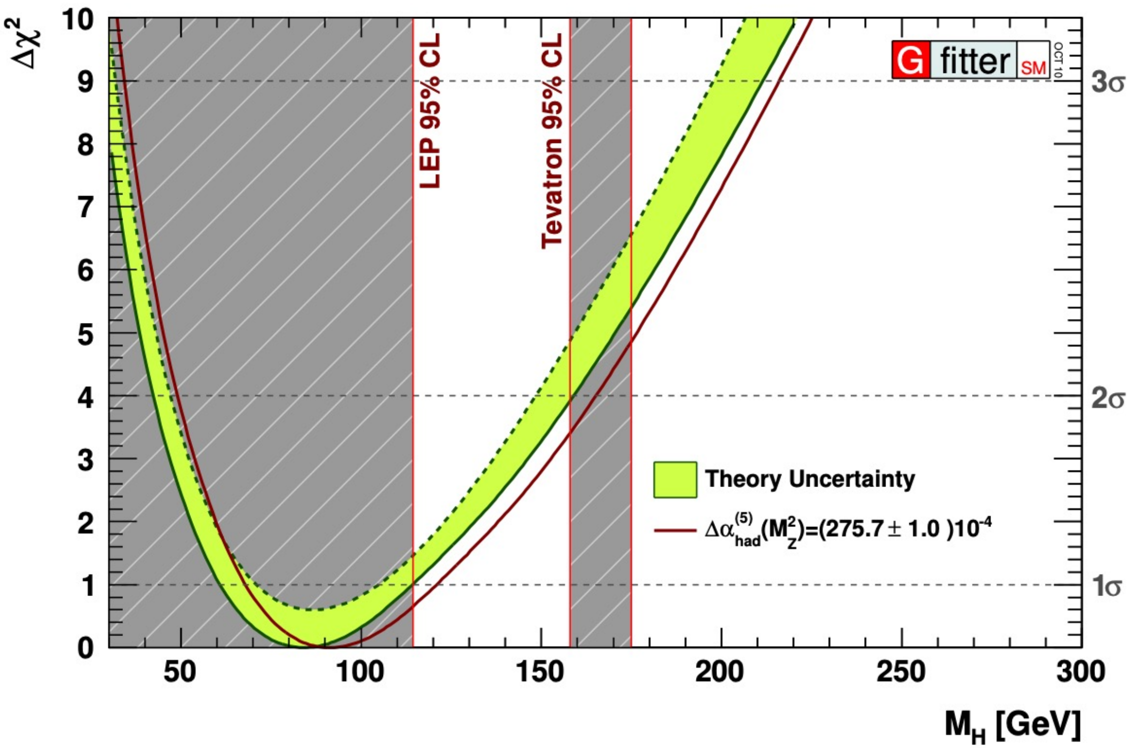

Long History of Data-Driven HVP Evaluation

DHMZ 2015

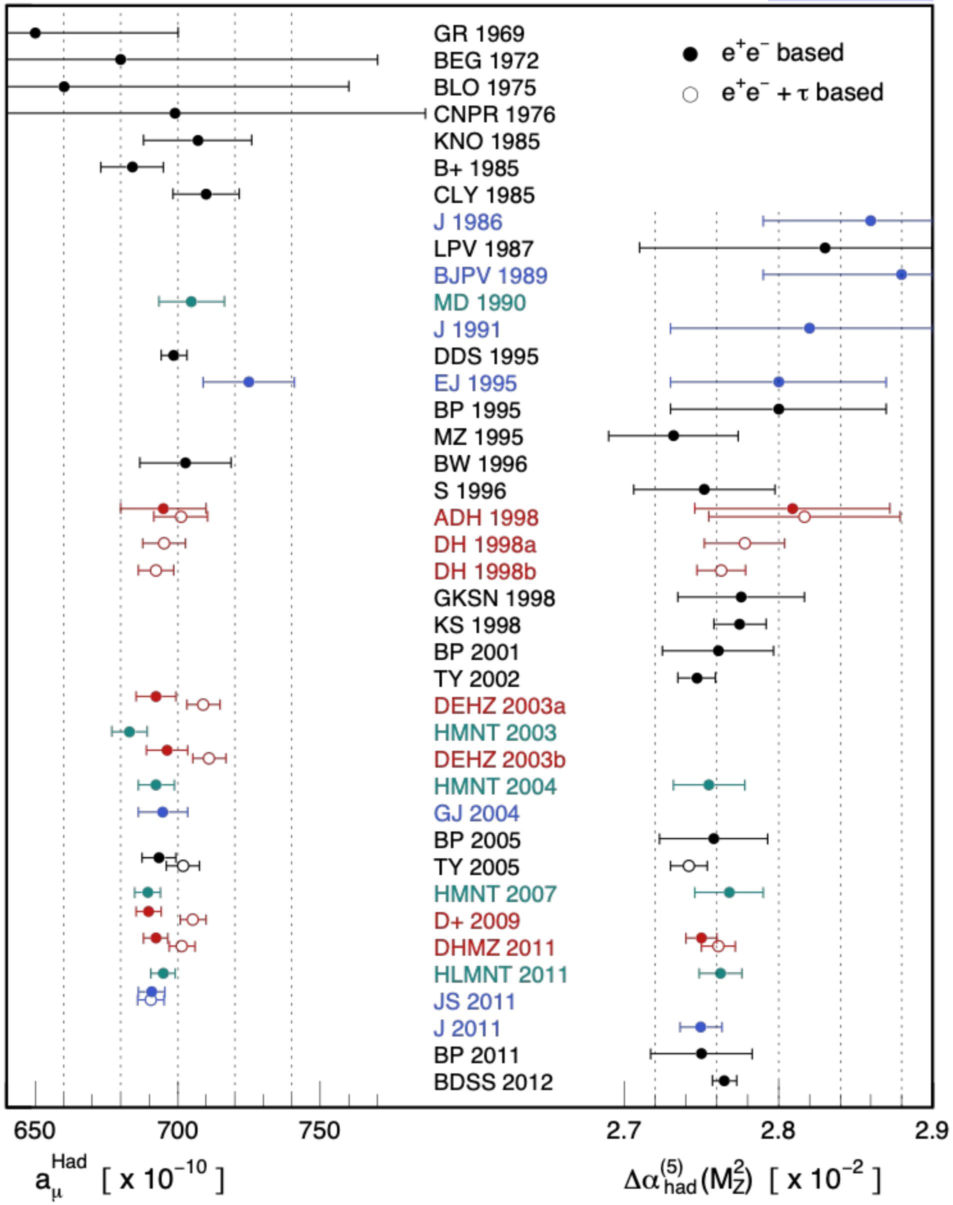

Fig. 3 prepared by Davier, Hoecker, Malaescu, Zhang for "Standard theory essays in the 60th anniversary of CERN"

Our efforts started by Davier with a first publication with Hoecker and Alemany in 1998 (ADH 1998)

Since then ZZ(02), Bogdan(09) and others joined the efforts

In total we have published >10 highly cited articles (link)

Our prediction has been one main reference used for comparing with the direct measurement

The precision of the HVP prediction is data-driven

It depends on
- the precision of e^+e^- annihilation (& tau) data
- state of the art techniques (HVPTools) for data interpolation, combination and error correlation treatment

Direct Contributions by BEPC(II) / BES(III)

- ➢ Contributions to LO HVP:
  - ➢ In the dominant 2π channel [0.6−0.9]GeV
  - ➢ Inclusive measurement [2.0−3.7]GeV allowing to validate the pQCD calculation
  - ➢ Inclusive measurement [3.7−5]GeV, dominant in the combination in this energy region
- ➢ BES(III) has also measurements used in the evaluation of the HLbL contribution

CMD3, Phys. Rev. D 109 (2024) 112002

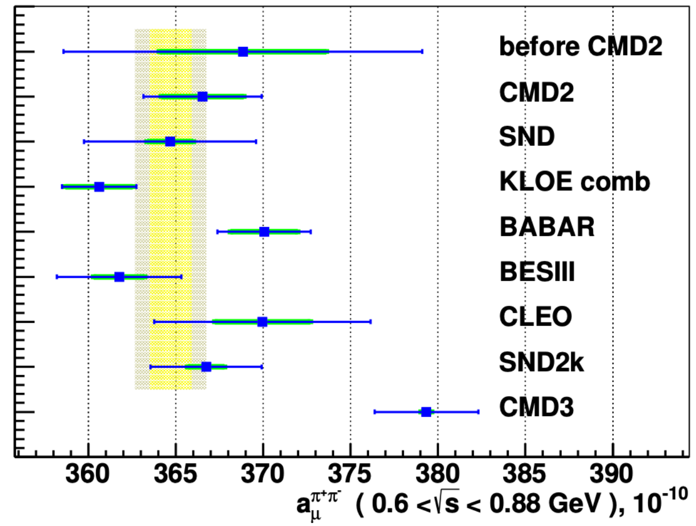

Figures from DHMZ 2017

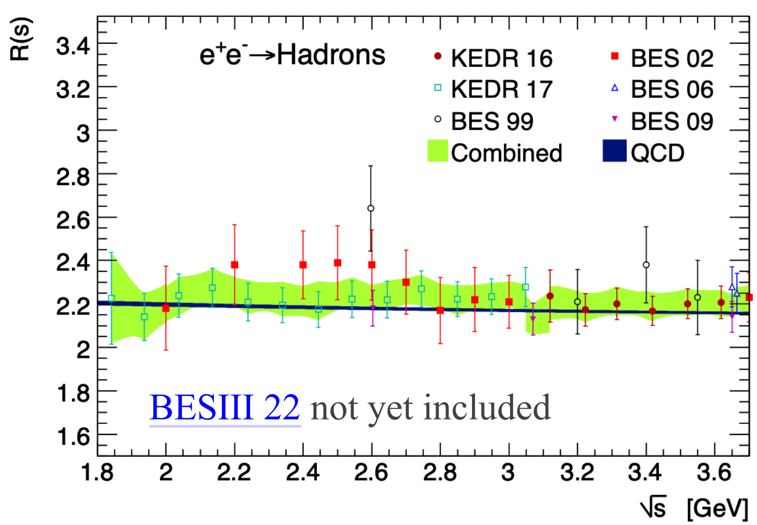

Contributing ~5% of LO HVP

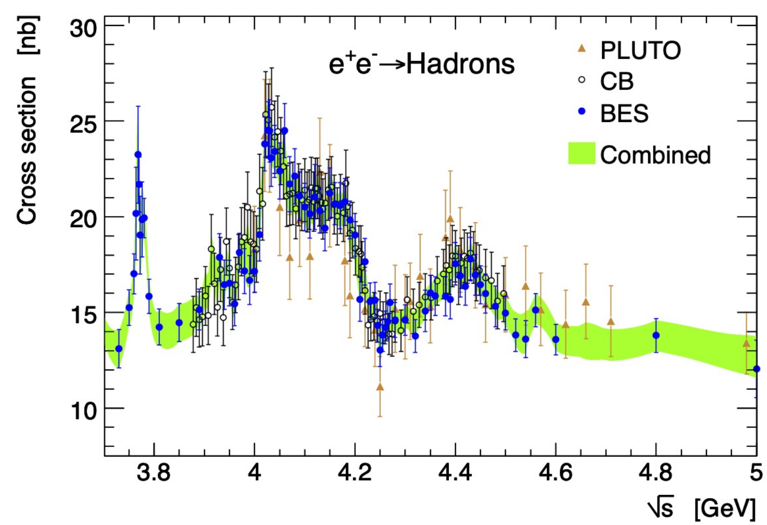

Contributing ~1% of LO HVP

Lessons Learnt

- (Early) $\pi\pi$ cross-section measurements performed without blinding
  - Human bias could not be avoided
  - ➔ Any precision measurement should be rigorously performed in blinded ways

- It is possible that the quoted systematic uncertainties were under-estimated

- Some of the $\pi\pi$ cross-section measurements rely solely/heavily on corrections from the MC simulation
  - A dedicated study by BABAR in 2023 showed some shortcomings of the NLO Phokhara used by most of the ISR measurements

BABAR's Dedicated Higher Order Radiation Study

BABAR 2023

Using the full data samples of BABAR, we performed a unique study of higher order radiation in $\pi\pi\gamma$ & $\mu\mu\gamma$ channels

- ➢ Two NLO fits
  - ➢ Small Angle (SA) fit
  - ➢ Large Angle (LA) fit
- ➢ Three NNLO fits
  - ➢ 2SA fit results
  - ➢ SA+LA fit results
  - ➢ 2LA fit results

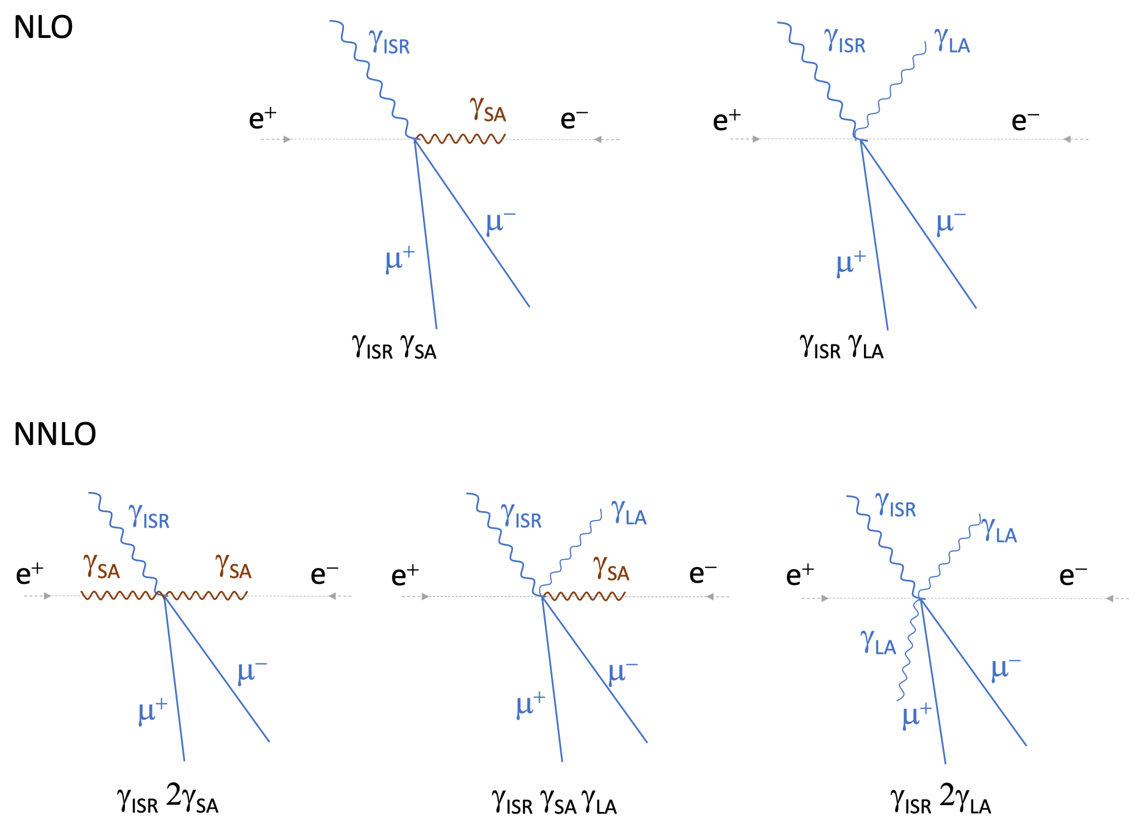

Key results:

- NNLO radiation observed with a fraction ~3.5%
- Phokhara prediction for small angle ISR photons @NLO order is too high by ~25%

Collinear approximation for all SA-related fits

Consequence of BABAR's HO Radiation Study

- ➢ BABAR analysis performed with loose selections, efficiencies obtained with data
  - ➔ The effect of missing NNLO and NLO excess in Phokhara on acceptance (0.03±0.01)% well below the quoted syst. uncertainty
- ➢ Using fast simulations, studied possible NNLO effects e.g. for the KLOE analyses
  - ➔ Efficiency correction relying purely on MC would give larger effects beyond the quoted uncertainty of 0.5%
  - ➔ Real effects can only be accessed by KLOE

Figure from DHMLZ, EPJC84 (2024) 721

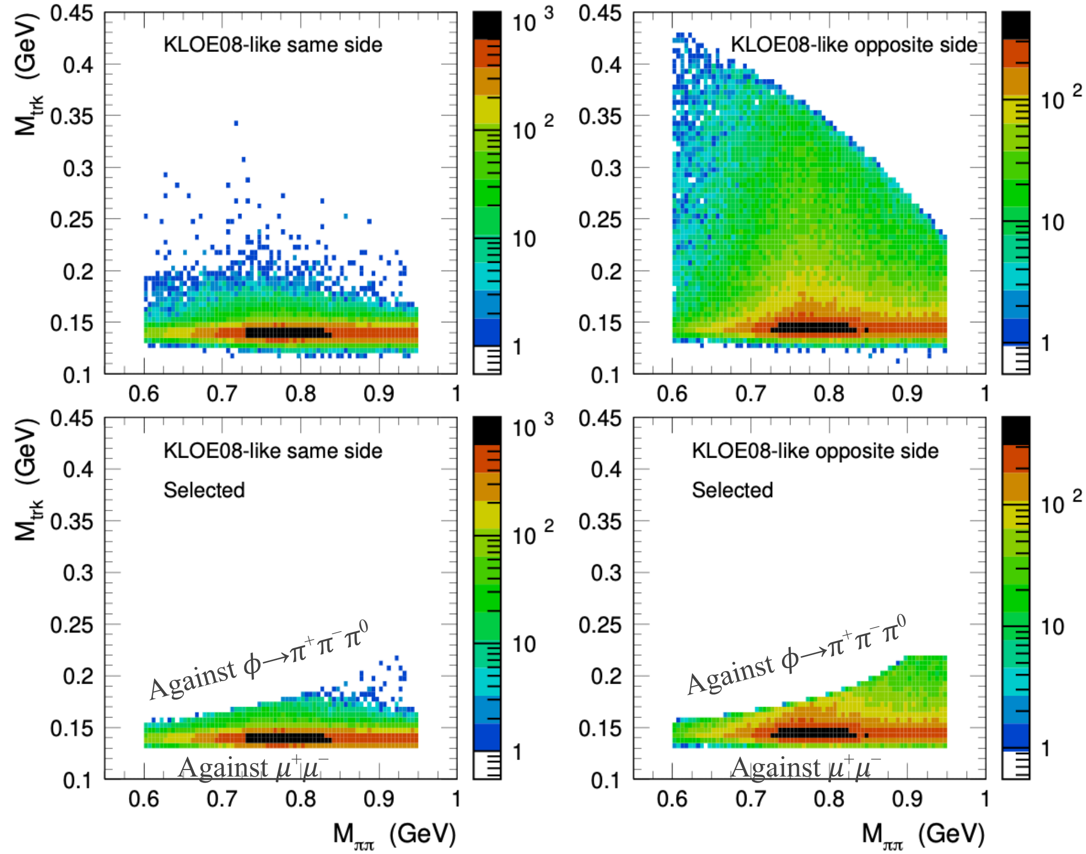

M_{trk}: invariant mass of two charged tracks
Same side: the additional and ISR photons on the same side
Opposite side: otherwise

Prospects

- On the a_μ measurement side, the precision is already good, still
  - An independent a_μ measurement @J-PARC with different systematic uncertainty is being prepared [time-line: begin commissioning 2029] (slide 54)
  - MUonE@CERN, based on measurement of $\Delta_{had}(t)$ in space-like region [time-line: 3 years of data taking after LHC LS3 2030] (slide 55)
  - Coherent Anomalous magNetic momenT ObservatioN with muon (CANTON)-μ proposal in China [Ce Zhang et al. 2512.11486]

- SM a_μ predictions and precision $\pi\pi$ cross-section measurements
  - Lattice: more calculations & uncertainty reduction expected
  - Input cross-section data for LO HVP data-driven evaluations:
    - BABAR ISR 2π [0.3−1.4] GeV new method (slide 49) and results imminent
    - From BESIII
      - ISR 2π [0.3−1.0] GeV (tagged); > 1 GeV (untagged)
      - ISR KK [1.0−3.3] GeV (tagged and untagged)
      - ISR $2\pi\pi^0$ [0.7−2.0] GeV
      - ISR R measurement [0.3−2.0] GeV
      - R measurement [1.8−5.0] GeV
    - CMD-3
    - KLOE
    - SND 2026 (slide 50)

Measurements aiming for a syst precision <0.5% very challenging. The new BABAR analysis took us over 6 years!

New Method used by BABAR

New analysis

- Full data sample (460 fb^{-1})
- Exploit different angular distributions to separate $\pi\pi/\mu\mu$ final states
- Track $p_T > 0.1$ GeV/c
- Signal MC: Phokhara

2009 analysis

- Partial data sample (232 fb^{-1})
- Use particle identification to separate $\pi\pi/\mu\mu$ final states ➔ dominant error source
- Track p > 1 GeV/c
- Signal MC: AfkQED

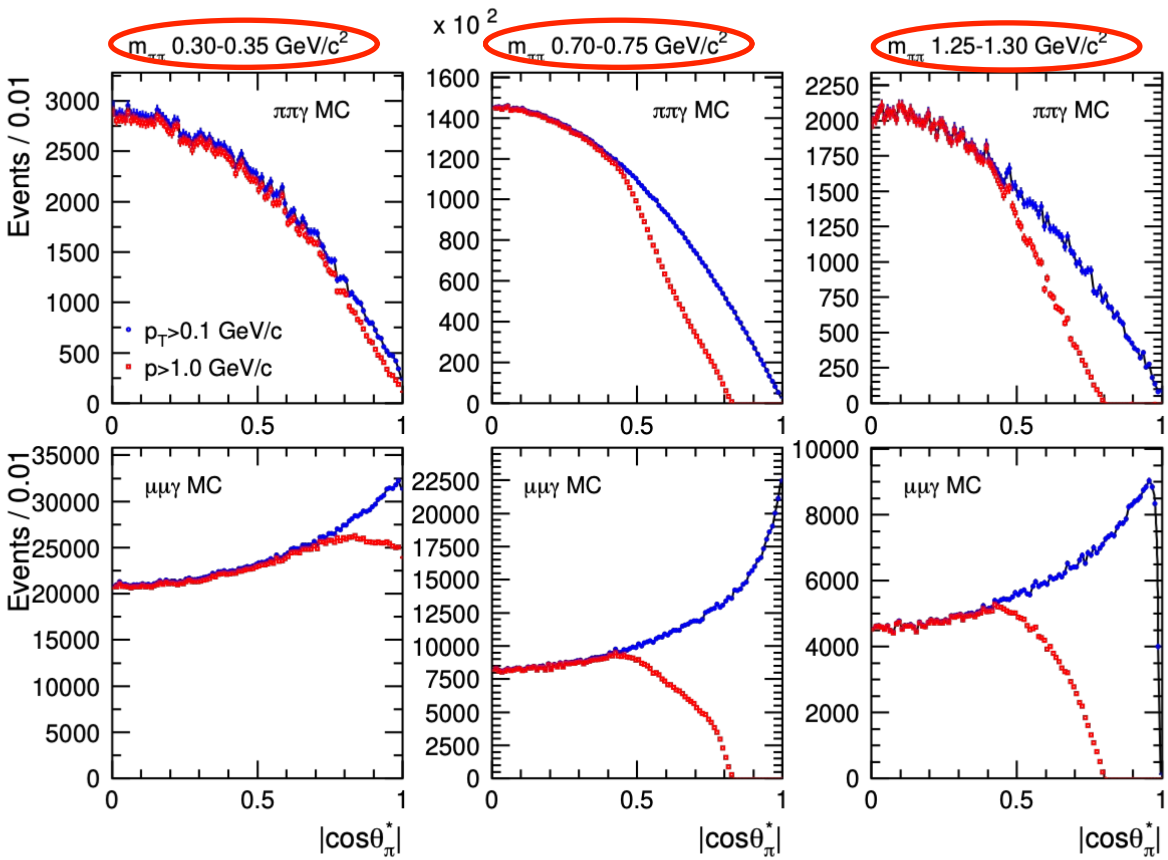

➔ New analysis improved with ×2 larger data sample lower p(T) selection, and a different $\pi\pi/\mu\mu$ separation method

➔ Different systematic uncertainties

➔ Articles for PRL and PRD submission imminent

Back

New SND Results Reported at ICHEP2026

SND, JHEP 2021 (2021) 113

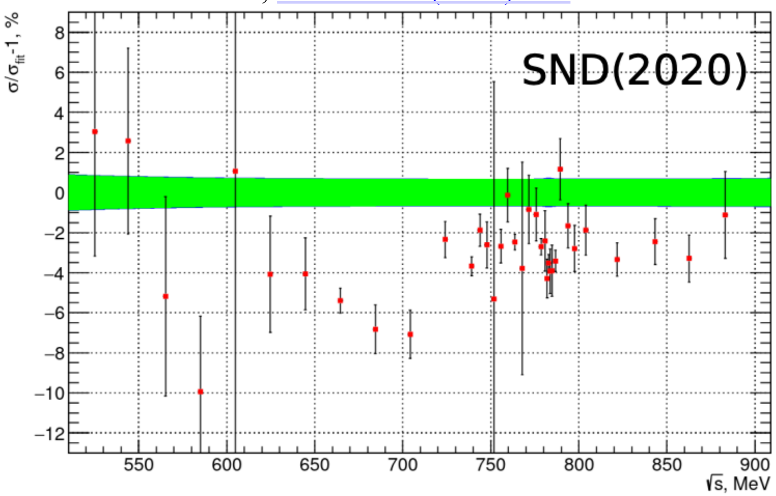

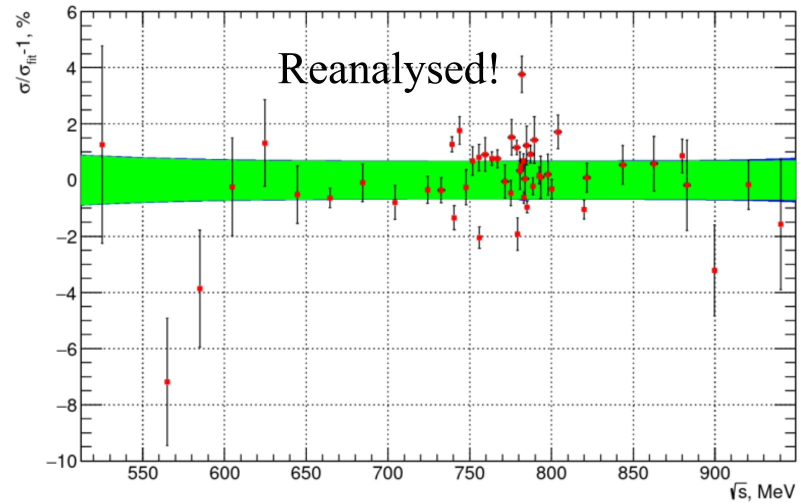

SND reported a new $e^+e^- \to \pi^+\pi^-$ measurement @ICHEP 2026, corresponding to the green error band

They also reanalysed the data used in SND 2020 publication and found reconstruction issues of pion track loss.

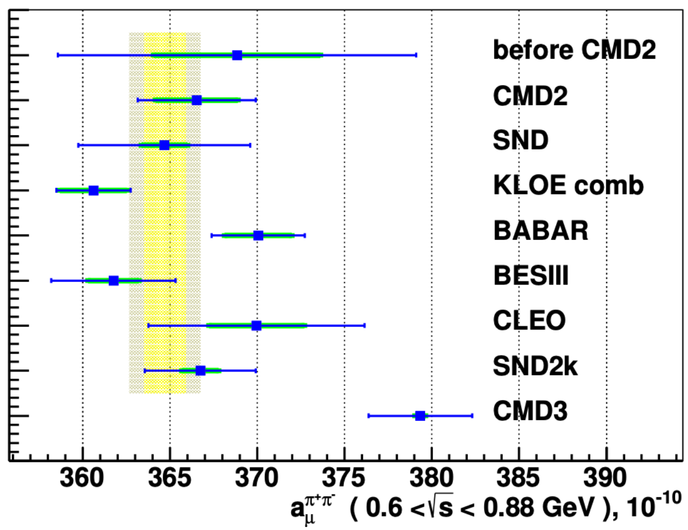

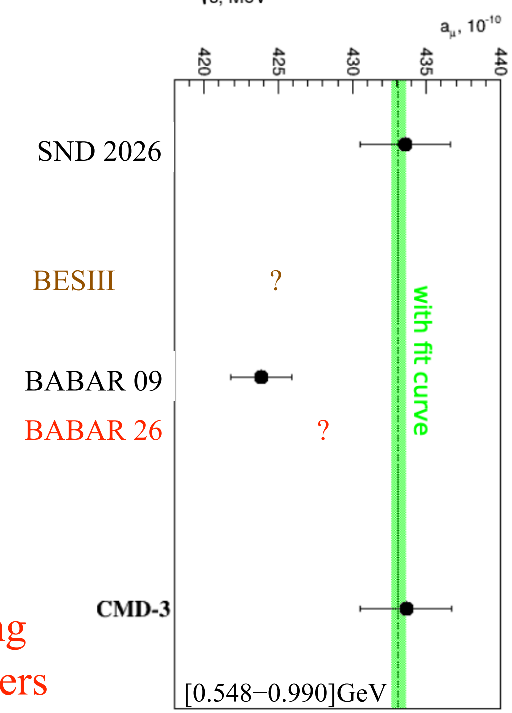

➔ New SND agrees perfectly with CMD-3, in the direction of resolving the data/SM discrepancy; looking forward to confirmation from others

Back

Summary

- Two LO HVP SM a_μ predictions currently in disagreement
- The data-driven prediction used to be the only a_μ prediction (WP2020) having comparable precision as the direct a_μ measurement but disagrees $> 4\sigma$
  - Input cross-section data have however large discrepancies, in particular between CMD-3 and KLOE
  - Such discrepancies have prevented us for providing a meaningful prediction for WP2025
- The lattice QCD-based a_μ calculation has much improved its precision over the last years
  - It becomes the only a_μ prediction (WP2025) in better agreement with the direct a_μ measurement
- Understanding the disagreement between the two a_μ predictions is the most urgent task in the community
- It seems that (some of) previous $e^+e^- \to \pi^+\pi^-$ measurements are problematic and the uncertainties are underestimated

Additional Slides

List of publications

1. ADH 1998, Eur.Phys.J.C 2 (1998) 123 [383 citations*]
2. DH 1998, Phys.Lett.B 419 (1998) 419 [228 citations]
3. DH 1998, Phys.Lett.B 435 (1998) 427 [300 citations]
4. DEHZ 2003, Eur.Phys.J.C 27 (2003) 497 [430 citations]
5. DEHZ 2003, Eur.Phys.J.C 31 (2003) 503 [441 citations]
6. DHMZ+ 2010, Eur.Phys.J.C 66 (2010) 127 [219 citations]
7. DHMYZ 2010, Eur.Phys.J.C 66 (2010) 1 [234 citations]
8. DHMZ 2011, Eur.Phys.J.C 71 (2011) 1515 [1012 citations]
9. DHMZ 2017, Eur.Phys.J.C 77 (2017) 827 [744 citations]
10. DHMZ 2020, Eur.Phys.J.C 80 (2020) 241 [804 citations]
11. Theory initiative WP 2020, Phys.Rept. 887 (2020) 1 [1872 citations]
12. Theory initiative WP2025, Phys.Rept. 1143 (2025) 1 [342 citations]
13. BMW/DMZ 2024, Nature 653 (2026) 373 [187 citations]

* Status of August, 2026

→Total number of citations: >7000

BNL/FNAL vs J-PARC

Experimental Approaches

Spin precession vector with respect to cyclotron motion in EM field

$$\vec{\omega} = -\frac{e}{m}\left[a_\mu \vec{B} - \left(a_\mu - \frac{1}{\gamma^2 - 1}\right)\frac{\vec{\beta}\times\vec{E}}{c} + \frac{\eta}{2}\left(\vec{\beta}\times\vec{B} + \frac{\vec{E}}{c}\right)\right]$$

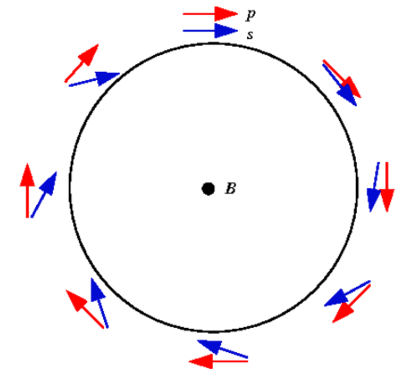

Spin precession in cyclotron motion

BNL/FNAL approach

$$a_\mu - \frac{1}{\gamma^2 - 1} = 0$$

$$\vec{\omega} = -\frac{e}{m}\left[a_\mu \vec{B} + \frac{\eta}{2}\left(\vec{\beta}\times\vec{B} + \frac{\vec{E}}{c}\right)\right]$$

Magic momentum of 3.094 GeV/c is used.

J-PARC approach

$$\vec{E} = 0$$

$$\vec{\omega} = -\frac{e}{m}\left[a_\mu \vec{B} + \frac{\eta}{2}(\vec{\beta}\times\vec{B})\right]$$

Reaccelerated thermal muon beam is a key of this method.

Back

MUonE

MUonE: Muons ON Electron elastic scattering

Use intense muon beam of 160 GeV at CERN scattering off atomic electrons of a light target to measure the shape of differential cross section in order to obtain a measurement of the effective electromagnetic coupling in the space-like region at low momentum transfer

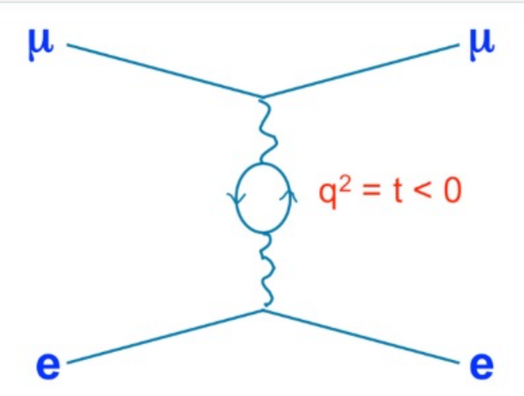

Figures from MUonE 2017

$$a_\mu^{\mathrm{LO,HVP}} = \frac{\alpha}{\pi}\int_0^1 dx(1-x)\Delta\alpha_{\mathrm{had}}[t(x)] \quad \text{with} \quad t(x) = \frac{x^2 m_\mu^2}{x-1} < 0$$

$$\alpha(t) = \frac{\alpha(0)}{1-\Delta\alpha(t)}$$

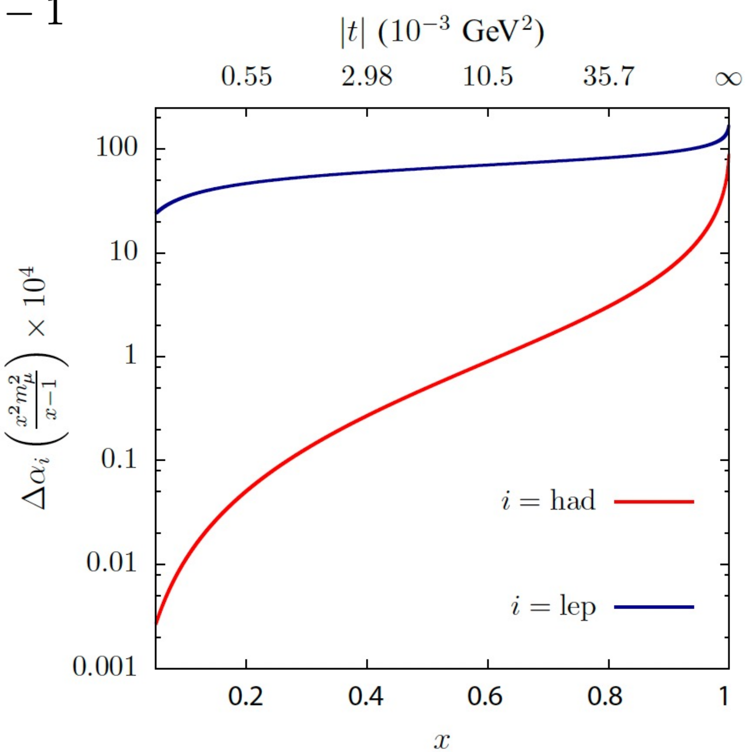

Back

Measurement of a_e ou g_e

Phys. Rev. Lett. 130 (2023) 071801

$$a_e = \frac{g_e}{2} = \frac{\omega_s - \omega_c}{\omega_c}$$

ω_s: spin frequency
ω_c: cyclotron frequency, measured in-situ

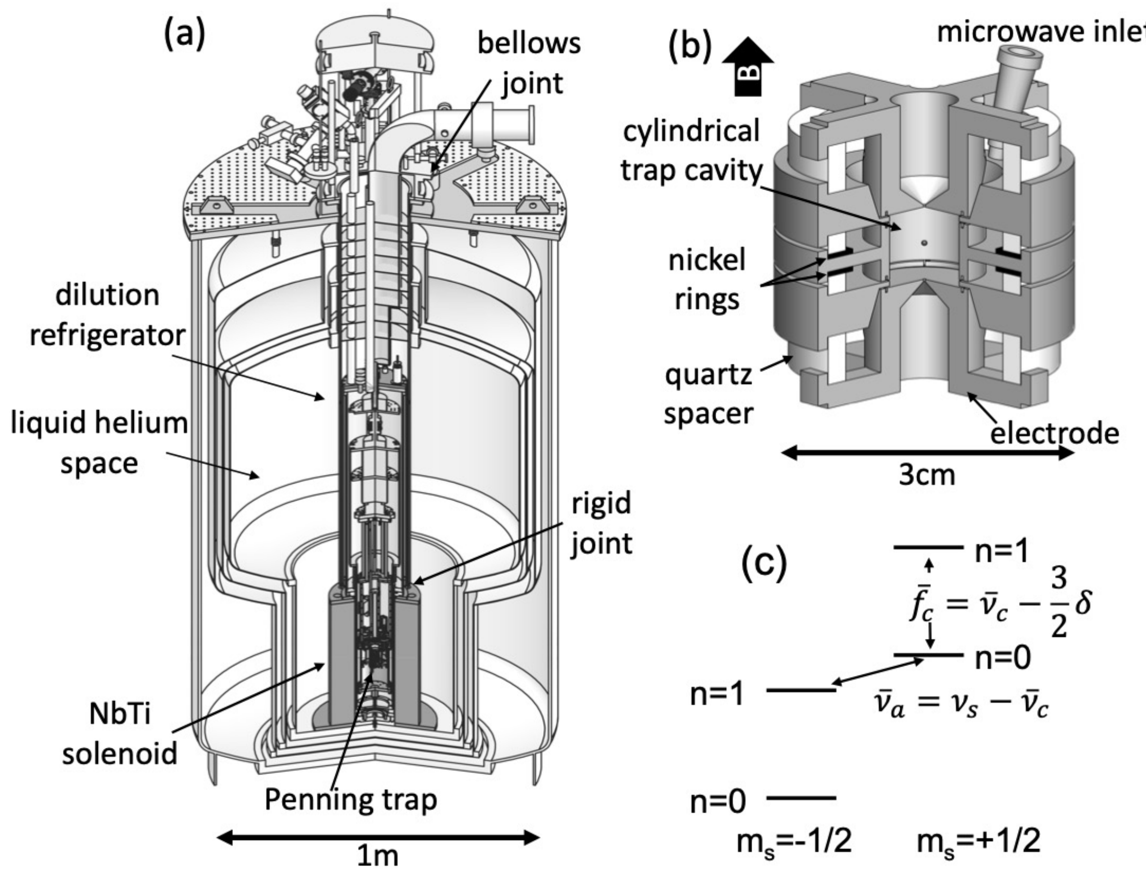

Back

Measurement of α

The measurement from atom-interferometer experiments via the recoil velocity of cesium (^{133}Cs) and rubidium (^{87}Rb) atoms X when absorbing photon:

$$\alpha(X) = \left[\frac{2R_\infty}{c}\frac{A_r(X)}{A_r(e)}\frac{h}{m_X}\right]^{1/2}$$

with R_∞=10973731.568157(12)m^{-1} [1.1ppt]: the Rydberg constant

$h/m_{Cs} = 3.002\,369\,4721(12) \times 10^{-9}\mathrm{m^2s^{-1}}$ [0.40ppb] Science 360 (2018) 191
$h/m_{Rb} = 4.591\,359\,258\,90(65) \times 10^{-9}\mathrm{m^2s^{-1}}$ [0.14ppb] Nature 588 (2020) 61

$A_r(^{133}\mathrm{Cs}) = 132.9054519585(86)$ [0.065ppb]
$A_r(^{87}\mathrm{Rb}) = 86.9091805291(65)$ [0.075ppb]
$A_r(e) = 5.485799090441(97)\times 10^{-4}$ [0.018ppb]

$$\alpha^{-1}(\mathrm{Cs}) = 137.035\,999\,045(27) \qquad [0.20\ \mathrm{ppb}],$$
$$\alpha^{-1}(\mathrm{Rb}) = 137.035\,999\,2052(97) \qquad [0.071\ \mathrm{ppb}].$$

➔ 5.6σ

Back

Two Types of $\sigma(e^+e^- \to \text{hadrons})$ Measurements

1. The scan method: e.g. CMD-2/3, SND at Novosibirsk
   - Advantages:
     - Well defined $\sqrt{s}$
     - Good energy resolution $\sim 10^{-3}\sqrt{s}$
   - Disadvantages:
     - Energy gap between two scans
     - Low luminosity at low energies
     - Limited $\sqrt{s}$ range of a given experiment

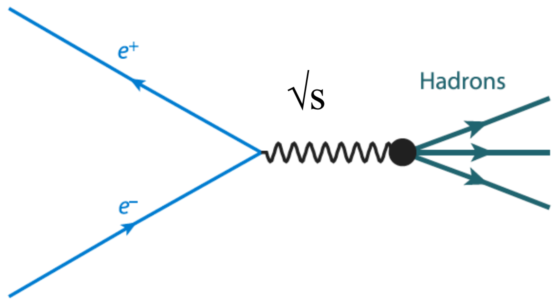

2. The ISR approach: e.g. BABAR, BES, CLEO-c, KLOE
   - Advantages:
     - Continuous cross section measurement over a broad energy range down to threshold
     - Large acceptance for hadrons if ISR detected at large angle
     - $\sigma(e^+e^- \to \text{hadrons})$ may be measured over $\sigma(e^+e^- \to \mu^+\mu^-)$ thus reducing some syst uncertainties
   - Disadvantages:
     - Require high luminosity to compensate higher order in α (that's why the $\sqrt{s}$ is chosen at a resonance)

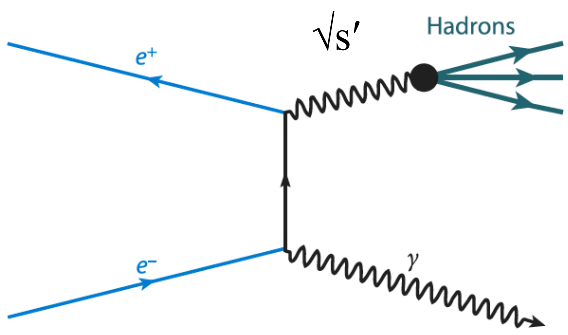

$s' = (1-x)/s$

$x = 2E_\gamma/\sqrt{s}$

Measurements of 2π Channel: CMD-2/3, SND

CMD-2 (2006)

- Energy 0.35-0.52 GeV [JETP Lett. 84:413-417, 2006 (link)]
- Energy 0.6-1.0 GeV [Phys. Lett. B 648: 28-38, 2007 (link)]

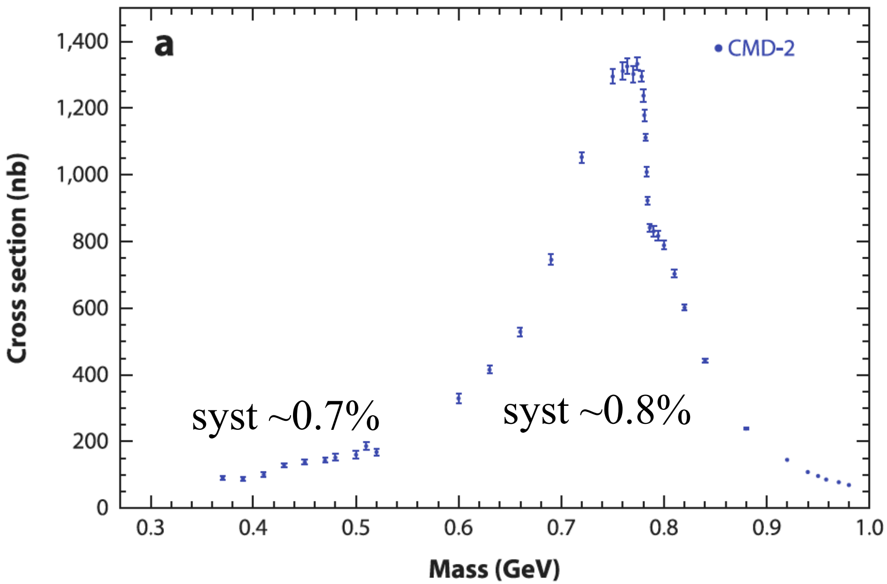

Figures a, b from M. Davier, Ann. Rev. Nucl. Part. Sci. 63 (2013) 407 (link)

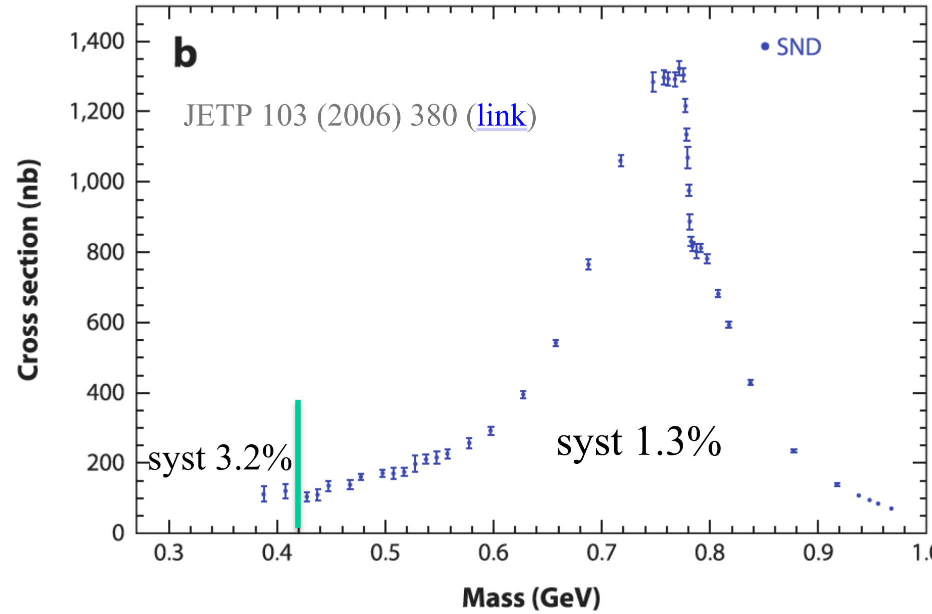

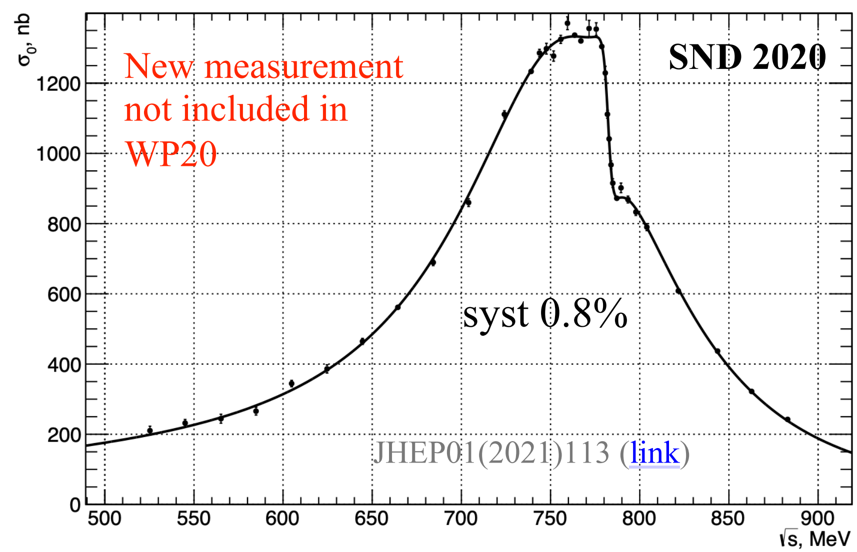

Measurements of 2π Channel: KLOE 08,10,12

$\sqrt{s}$=1.02 GeV ⇒ Soft ISR photons

Figure 3 from WP20

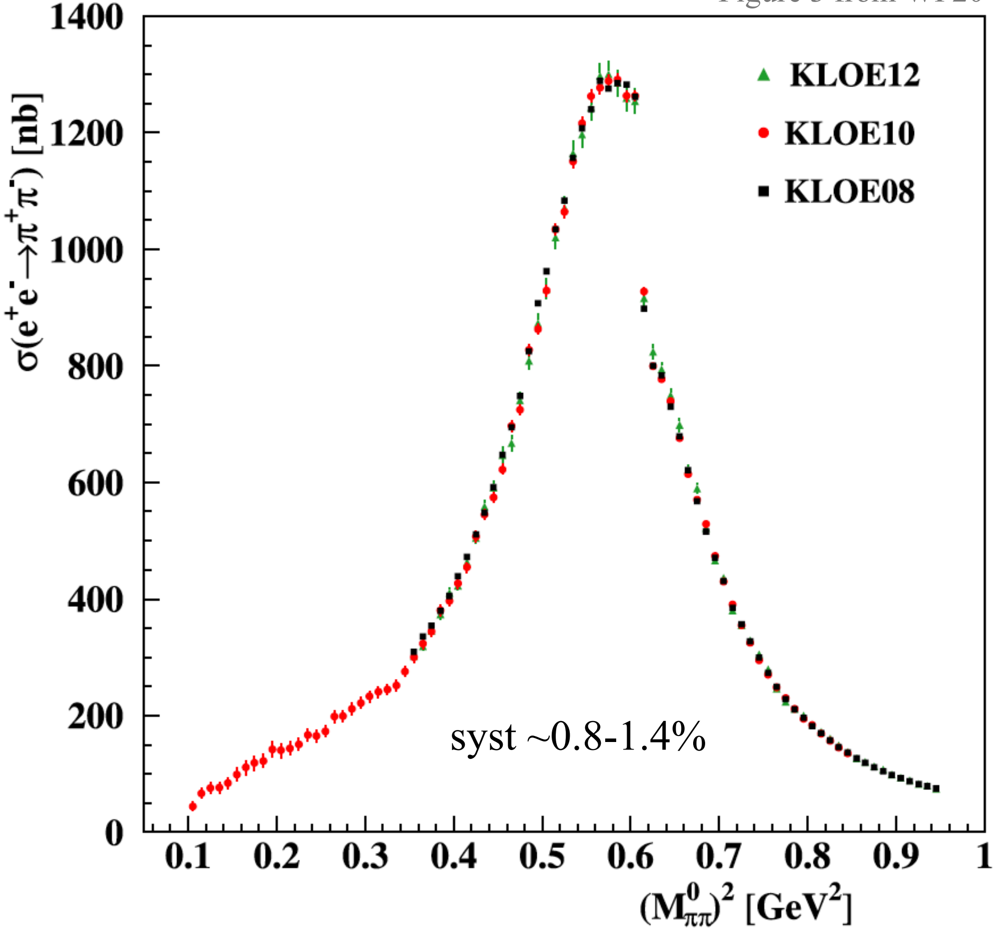

- KLOE12: photon at small angle and undetected, radiator function from measured $\mu^+\mu^-(\gamma)$ events
- KLOE10: photon at large angle and detected, radiator function from NLO QED
- KLOE08: photon at small angle and undetected, radiator function from NLO QED

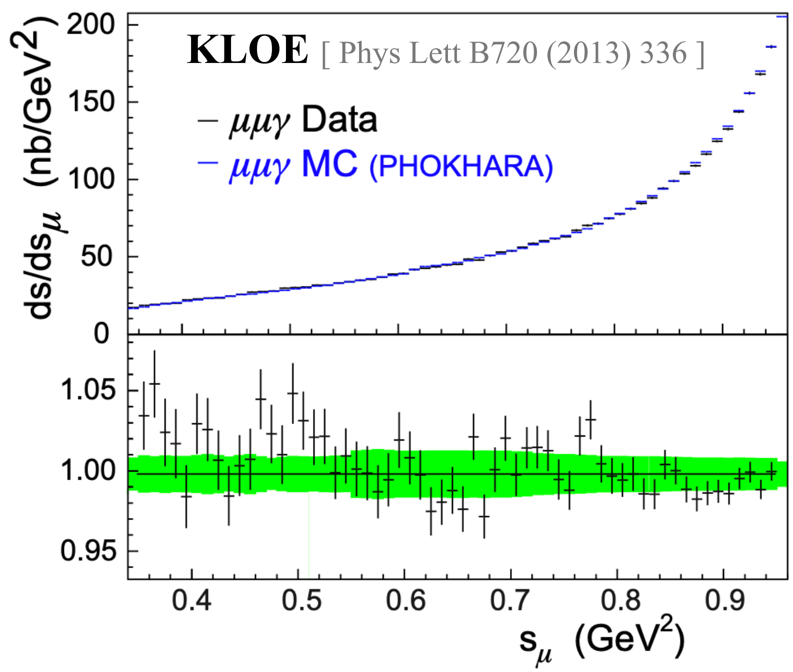

Measurements of 2π Channel: BABAR 09

$\sqrt{s}$=10.58 GeV ⇒ Hard ISR photons

Figure 3 from WP20

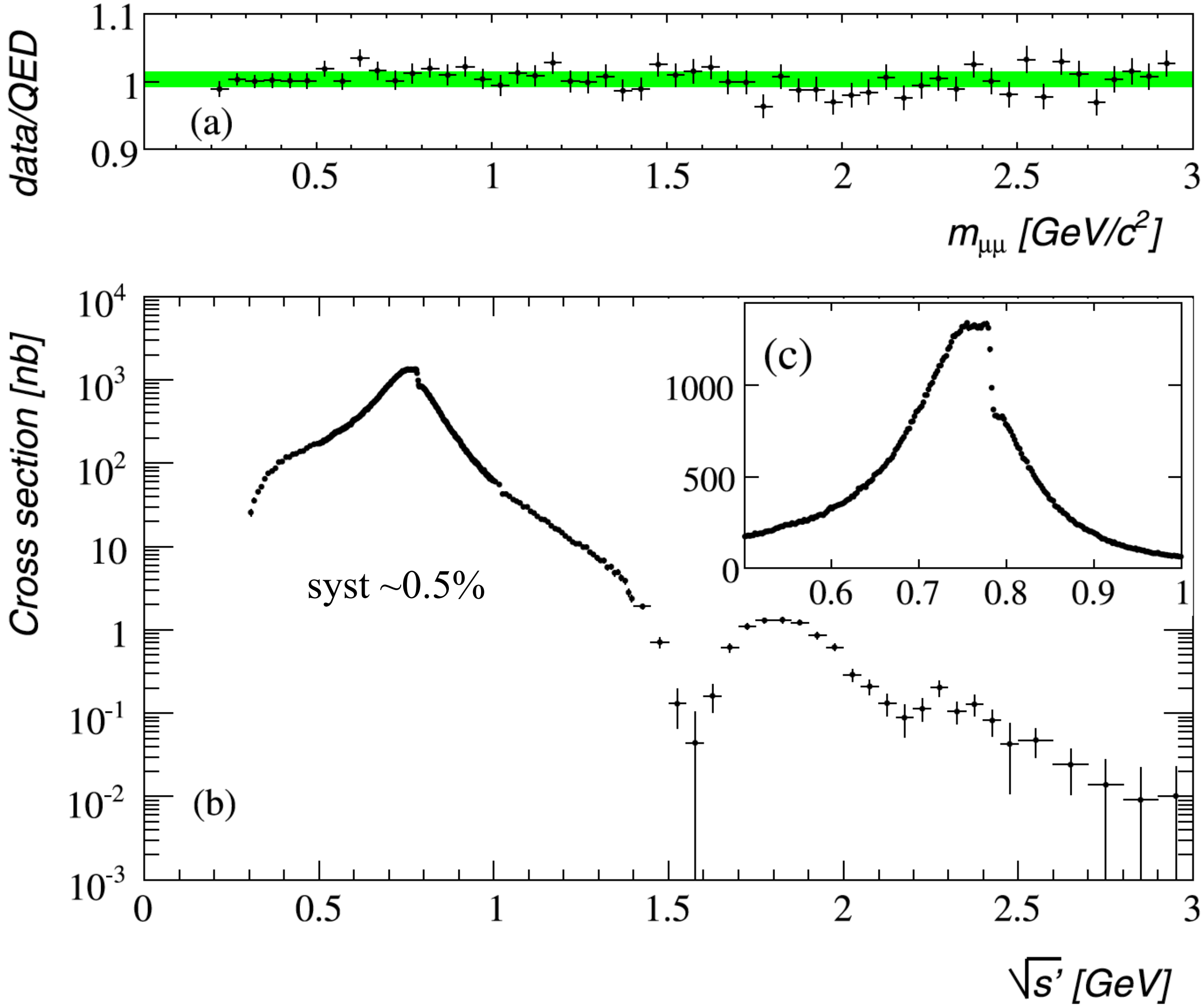

BABAR measurement covers a huge mass range from threshold to 3 GeV!

In BABAR, the ISR photon is detected at large angle

Both pion and muon pairs are measured and the ratio $\pi\pi(\gamma)/\mu\mu(\gamma)$ directly provides the $\pi\pi(\gamma)$ cross section

Measurements of 2π Channel: BESIII, CLEO-c

Original publication: Phys. Lett. B 753, 629 (2016)
Erratum: Phys. Lett. B 812, 135982 (2021) for updating the stat covariance matrix

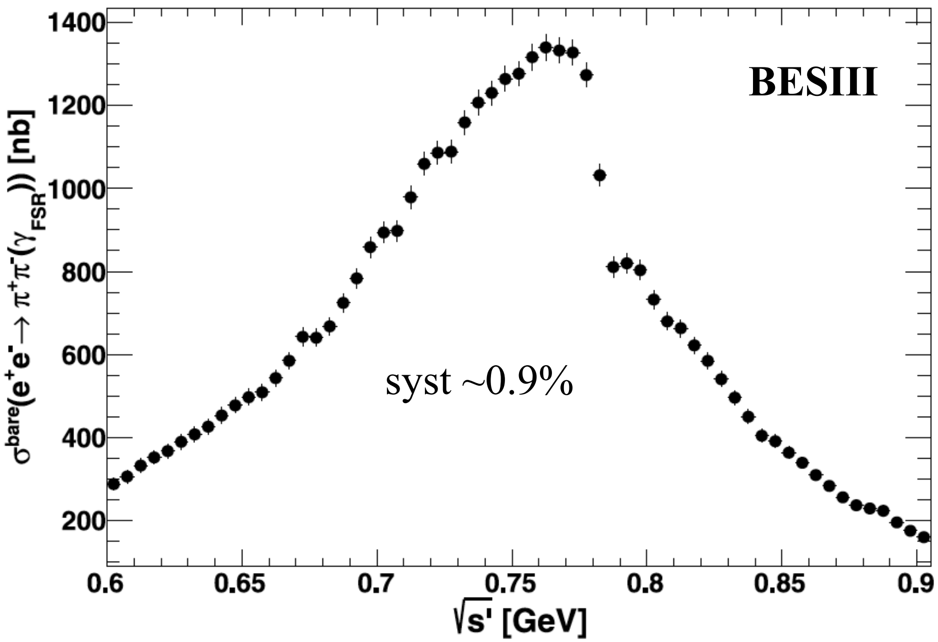

Phys. Rev. D 97, 032012 (2018)

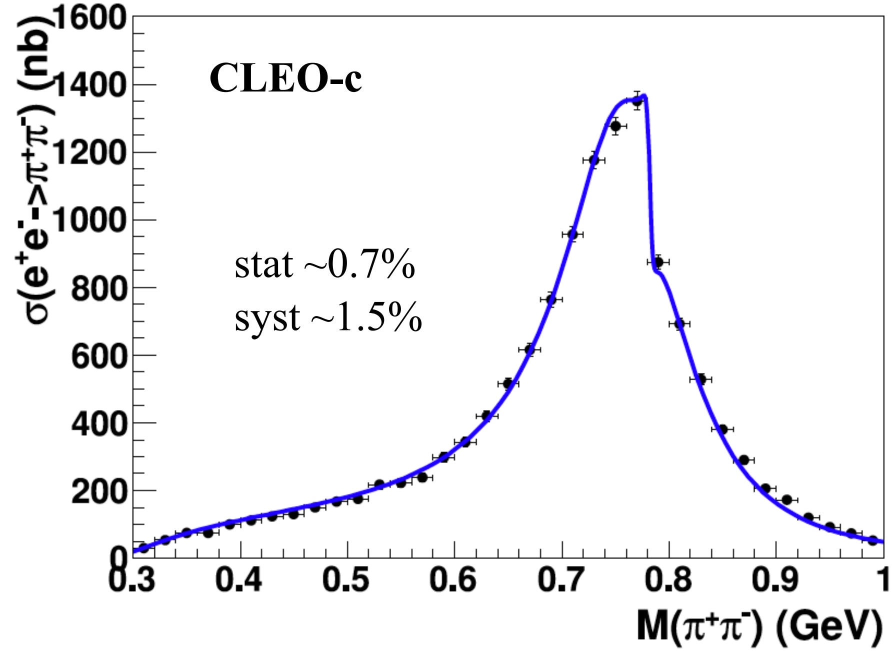

Combined 2π vs Individual Measurements

Figures from DHMZ, EPJC80 (2020) 241

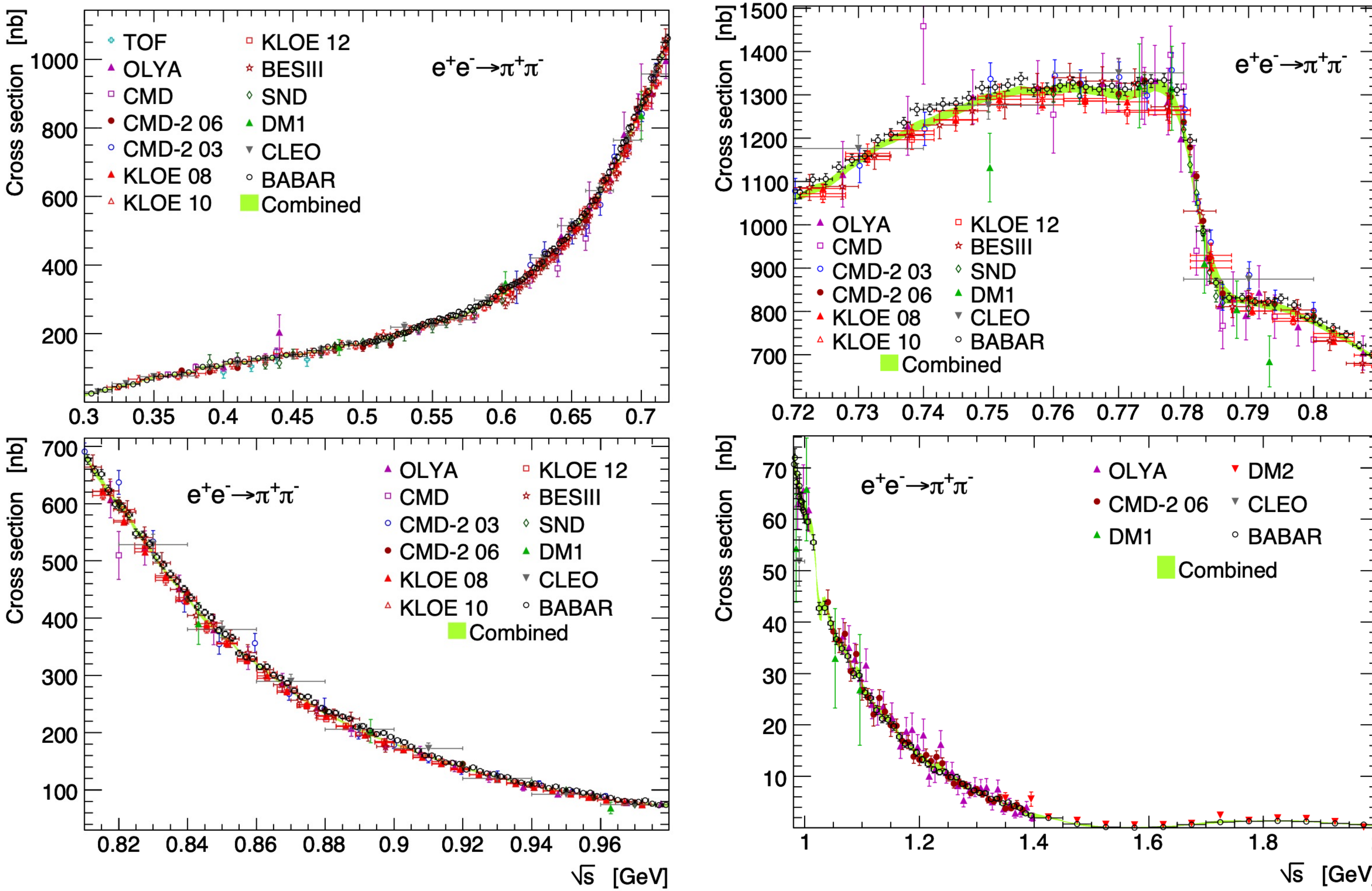

Combined 2π vs Individual Measurements

Figures from DHMZ, EPJC80 (2020) 241

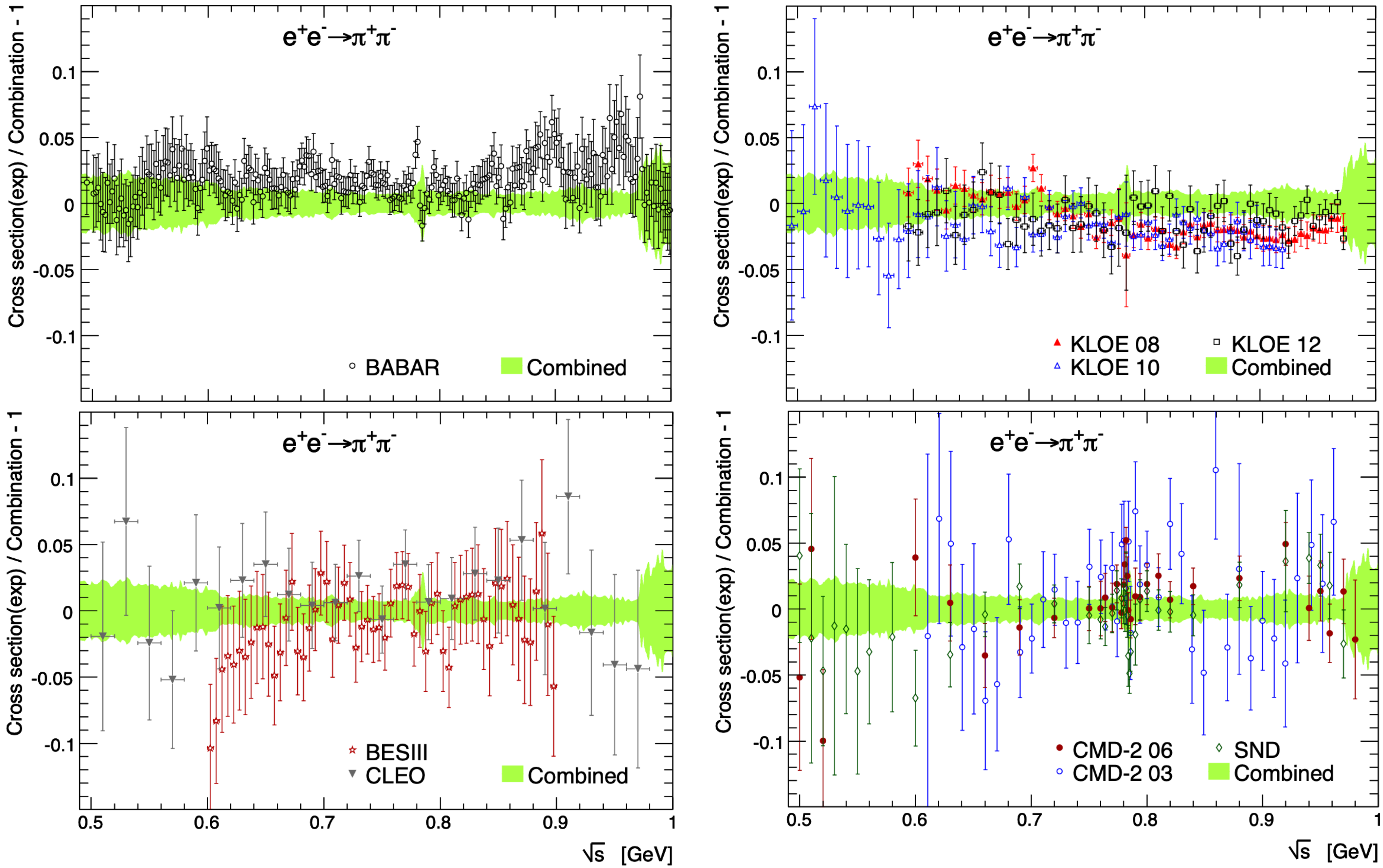

Fit at Low Energy Based on Analyticity and Unitarity

Pion form factor F_π^0 extracted from $\pi^+\pi^-$ bare cross sections as in [1810.00007]

$$|F_\pi^0|^2 = |G(s) \times J(s)|^2$$

$$G(s) = 1 + \alpha_V s + \frac{\kappa s}{m_\omega^2 - s - i m_\omega \Gamma_\omega}$$

$$J(s) = e^{1-\frac{\delta_1(s_0)}{\pi}} \left(1 - \frac{s}{s_0}\right)^{\left[1-\frac{\delta_1(s_0)}{\pi}\right]\frac{s_0}{s}} \left(1 - \frac{s}{s_0}\right)^{-1} e^{\frac{s}{\pi}\int_{4m_\pi^2}^{s_0} dt \frac{\delta_1(t)}{t(t-s)}}$$

$$\cot \delta_1(s) = \frac{\sqrt{s}}{2k^3}\left(m_\rho^2 - s\right)\left[\frac{2m_\pi^3}{m_\rho^2\sqrt{s}} + B_0 + B_1\omega(s)\right]$$

$$k = \frac{\sqrt{s - 4m_\pi^2}}{2}$$

$$\omega(s) = \frac{\sqrt{s} - \sqrt{s_0 - s}}{\sqrt{s} + \sqrt{s_0 - s}}$$

$$\sqrt{s_0} = 1.05 \text{ GeV}$$

$G(s)$ from [1611.09359]
$J(s)$ from [hep-ph/0106025, 0402285]
$\cot\delta_1(s)$ from [1102.2183]

Six free parameters to fit:
α_V, κ, m_ω, m_ρ, B_0, B_1
(Γ_ω fixed to PDG value)

Other Channels e.g. Those Measured by BABAR

There are many exclusive channels (~ 40 processes) contributing to HVP

Here are some example measurements from BABAR

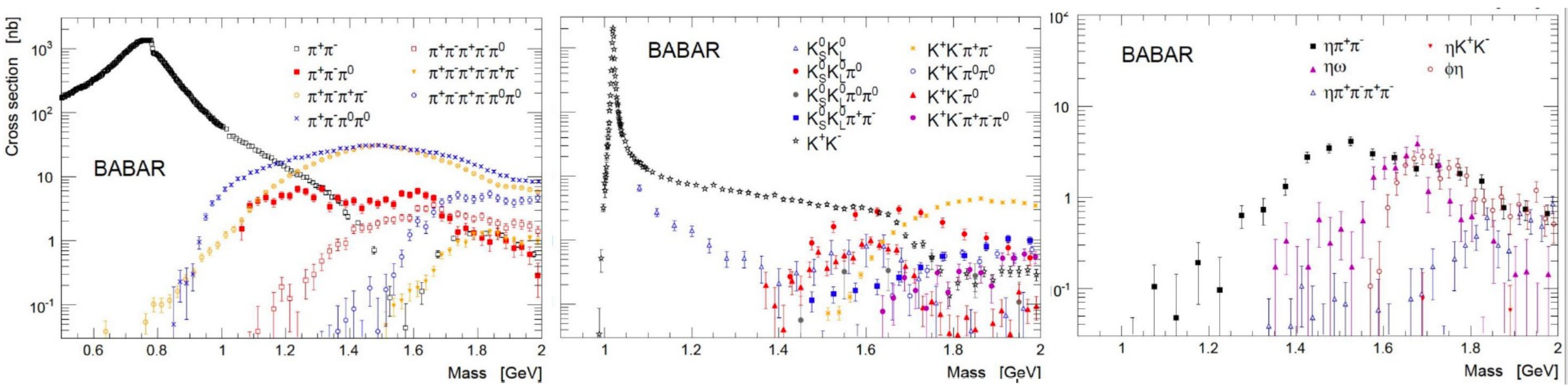

KKbar+π's Channels [DHMZ, Eur. Phys. J. C77, 827 (2017)]

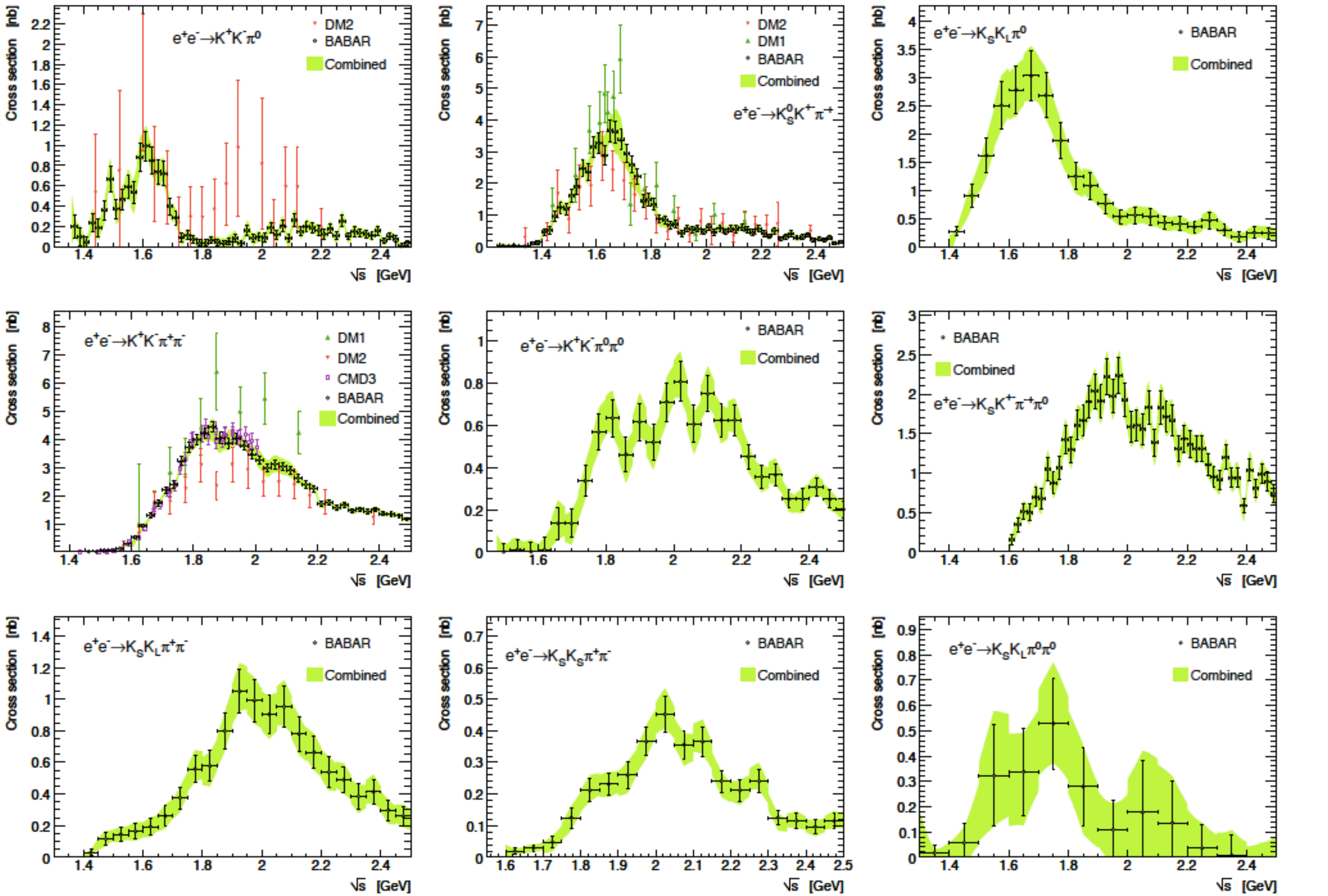

An Alternative Way Used to Evaluate HVP

Proposed by Alemany-Davier-Hoecker, EPJC 2 (1998) 123

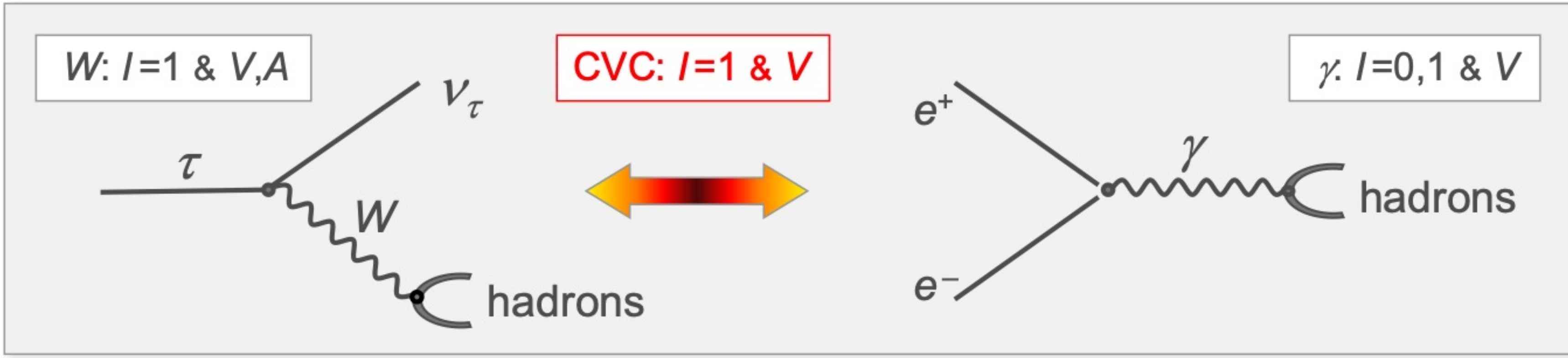

Hadronic physics factorises in Spectral Functions:
Isospin symmetry connects I=1 e^+e^- cross section to vector τ spectral functions

Fundamental ingredient relating long distance (resonances) to short distance description (QCD)

$$\boxed{\sigma^{(I=1)}\left[e^+e^- \to \pi^+\pi^-\right] = \frac{4\pi\alpha^2}{s}\upsilon\left[\tau^- \to \pi^-\pi^0\nu_\tau\right]}$$

$$\upsilon\left[\tau^- \to \pi^-\pi^0\nu_\tau\right] \propto \frac{BR\left[\tau^- \to \pi^-\pi^0\nu_\tau\right]}{BR\left[\tau^- \to e^-\bar{\nu}_e\nu_\tau\right]} \frac{1}{N_{\pi\pi^0}}\frac{dN_{\pi\pi^0}}{ds} \frac{m_\tau^2}{\left(1-s/m_\tau^2\right)^2\left(1+s/m_\tau^2\right)}$$

Branching fractions | Mass spectrum | Kinematic factors (PS)

Known Isospin Breaking Corrections

Davier et al., EPJC66 (2010) 127

$$v_{1,X^-}(s) = \frac{m_\tau^2}{6|V_{ud}|^2}\frac{\mathcal{B}_{X^-}}{\mathcal{B}_e}\frac{1}{N_X}\frac{dN_X}{ds} \times \left(1-\frac{s}{m_\tau^2}\right)^{-2}\left(1+\frac{2s}{m_\tau^2}\right)^{-1}\frac{R_{\rm IB}(s)}{S_{\rm EW}},$$

$$R_{\rm IB}(s) = \frac{{\rm FSR}(s)}{G_{\rm EM}(s)}\frac{\beta_0^3(s)}{\beta_-^3(s)}\left|\frac{F_0(s)}{F_-(s)}\right|^2.$$

Good agreement between Davier et al. and FJ for most of the isospin breaking components

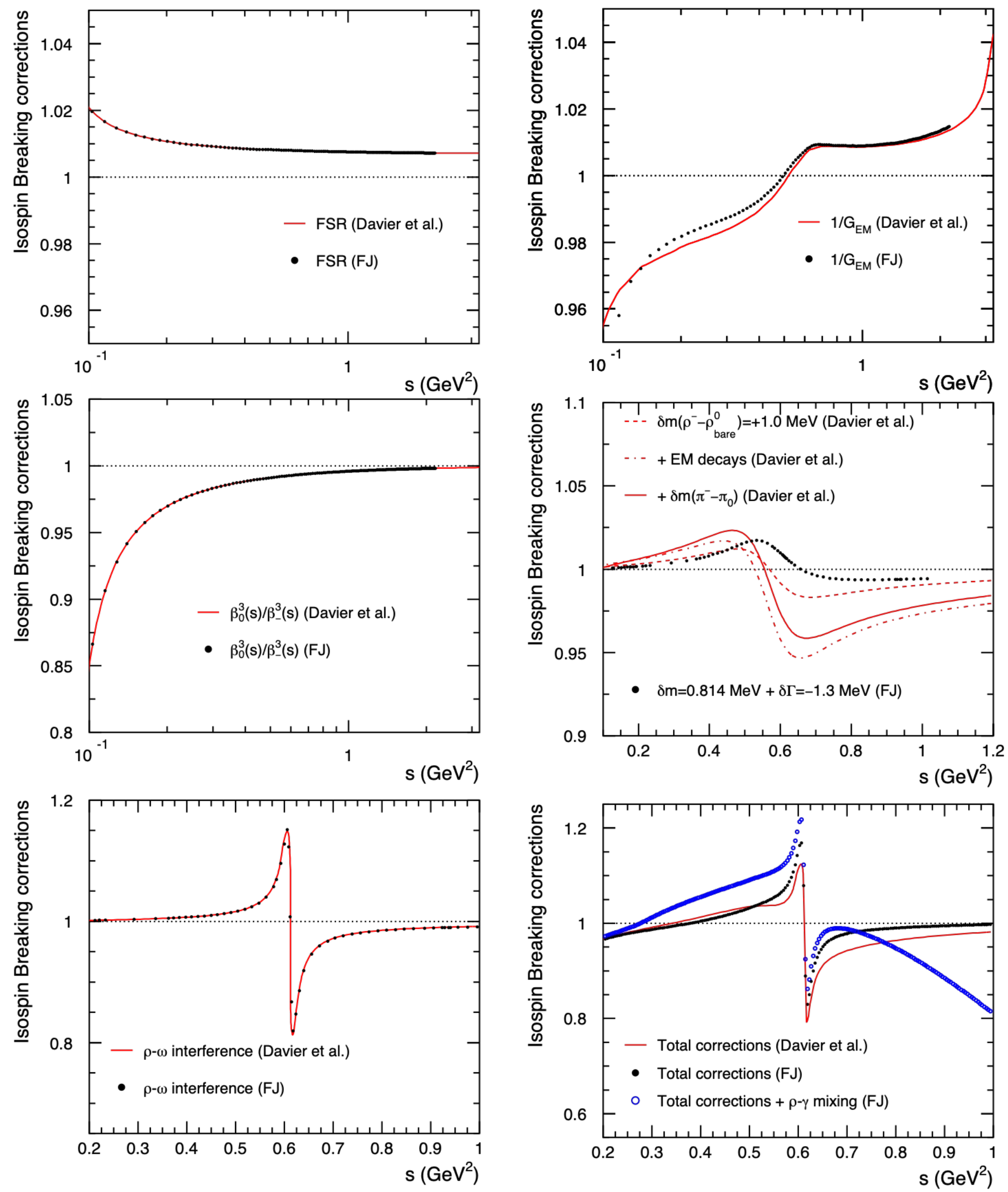

Figure 19 from WP20
Studies initiated in Davier et al., EPJC66 (2010) 127

Open Issue in 2π Channel

Take into account all known isospin breaking corrections except for the ρ–γ mixing correction

DHMYZ, EPJC66 (2010) 1

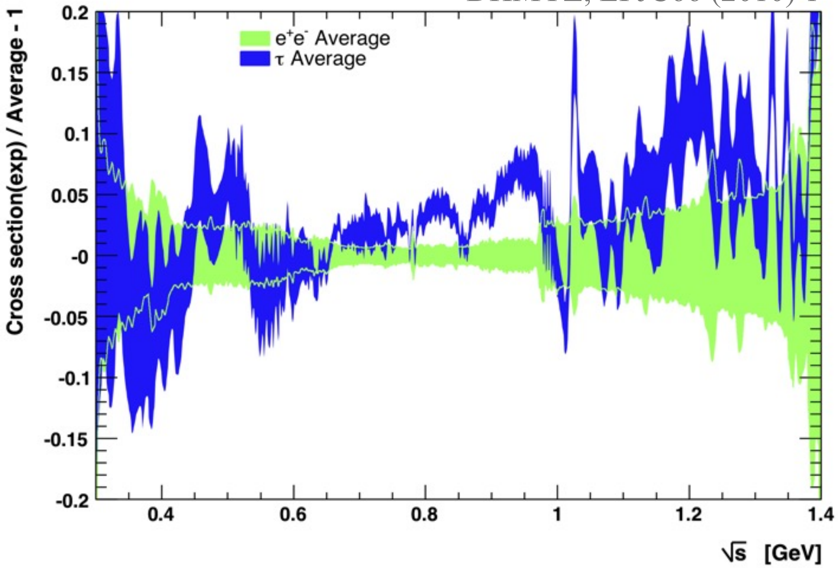

Modified version from Davier et al,, EPJC66 (2010) 127

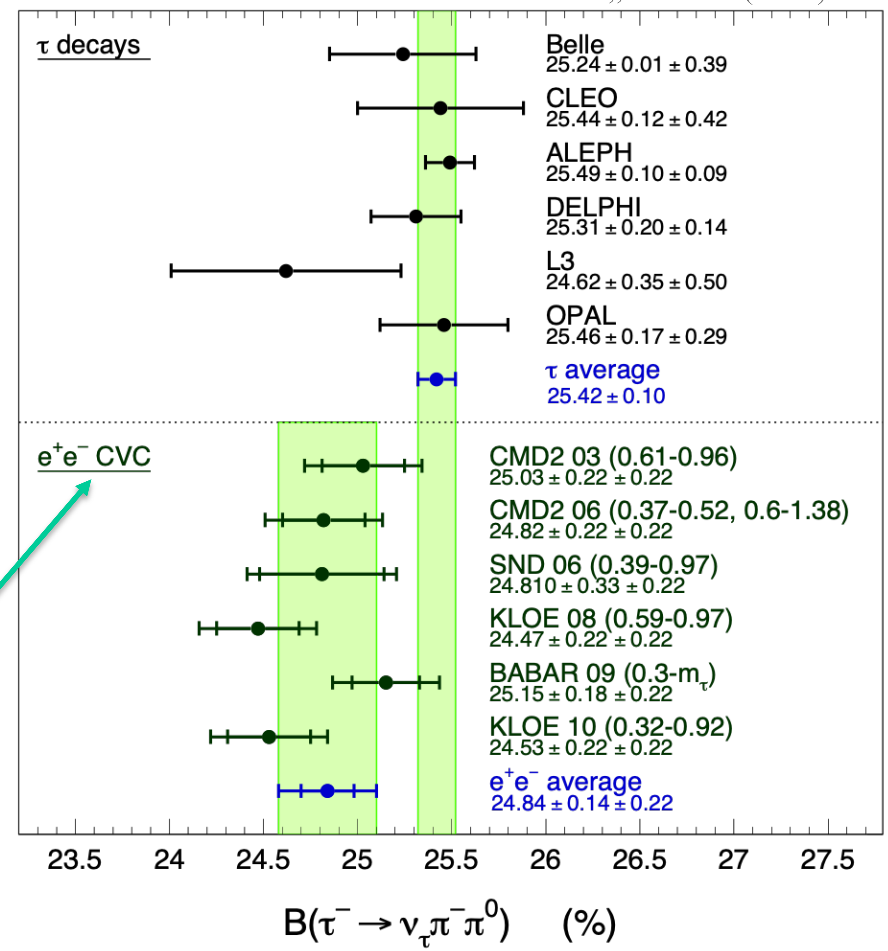

$$\boxed{\mathcal{B}_X^{\rm CVC} = \frac{3}{2}\frac{\mathcal{B}_e|V_{ud}|^2}{\pi\alpha^2 m_\tau^2}\int_{s_{\rm min}}^{m_\tau^2} ds\, s\, \sigma_{X^0}^I \left(1-\frac{s}{m_\tau^2}\right)^2\left(1+\frac{2s}{m_\tau^2}\right)}$$

Clear difference in shape and in BR between e$^+$e$^-$ and τ average

Additional EFT Based $\rho-\gamma$ Mixing Correction

Jegerlehner and Szafron proposed to use the missing $\rho-\gamma$ mixing in τ data to explain the remaining e^+e^- and τ difference

JS, EPJC71 (2011) 1632

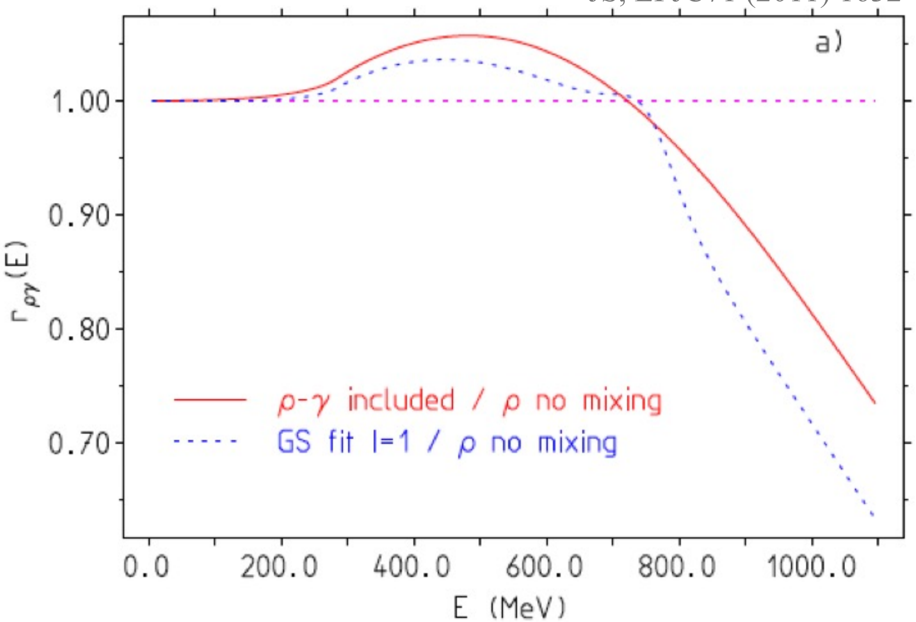

Figure 22 from WP20

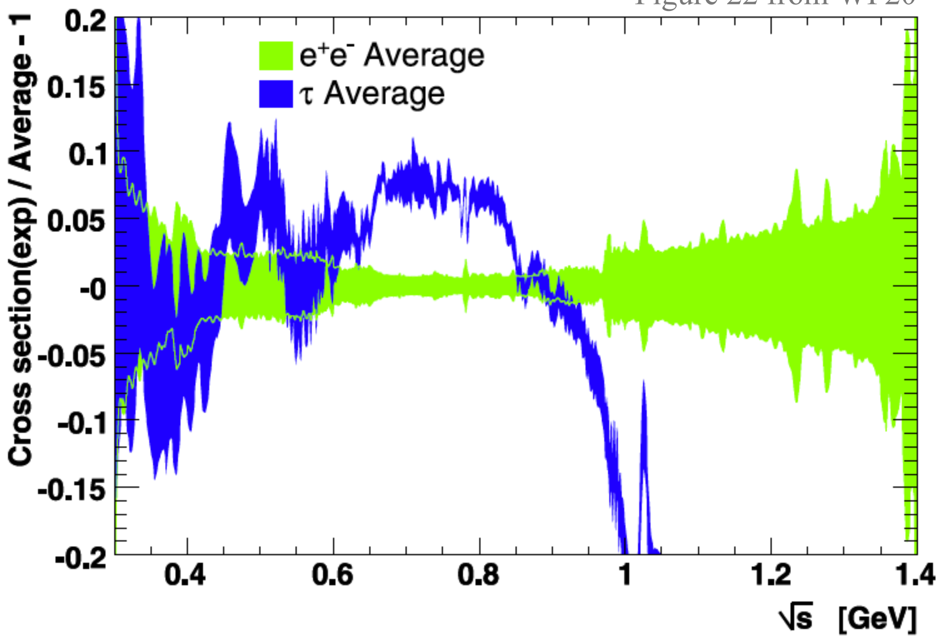

Applying the $\rho-\gamma$ mixing correction makes the e^+e^- and τ difference worse in some of the mass range

High Order HVP + HLbL Predictions

$$a_\mu^{\text{HVP, NLO}} = -9.83(7) \times 10^{-10}$$
$$a_\mu^{\text{HVP, NNLO}} = 1.24(1) \times 10^{-10}$$

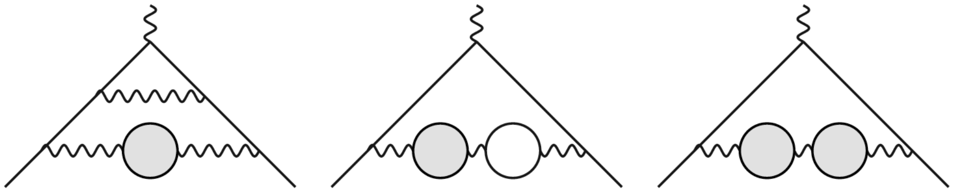

Status of hadronic light-by-light contribution

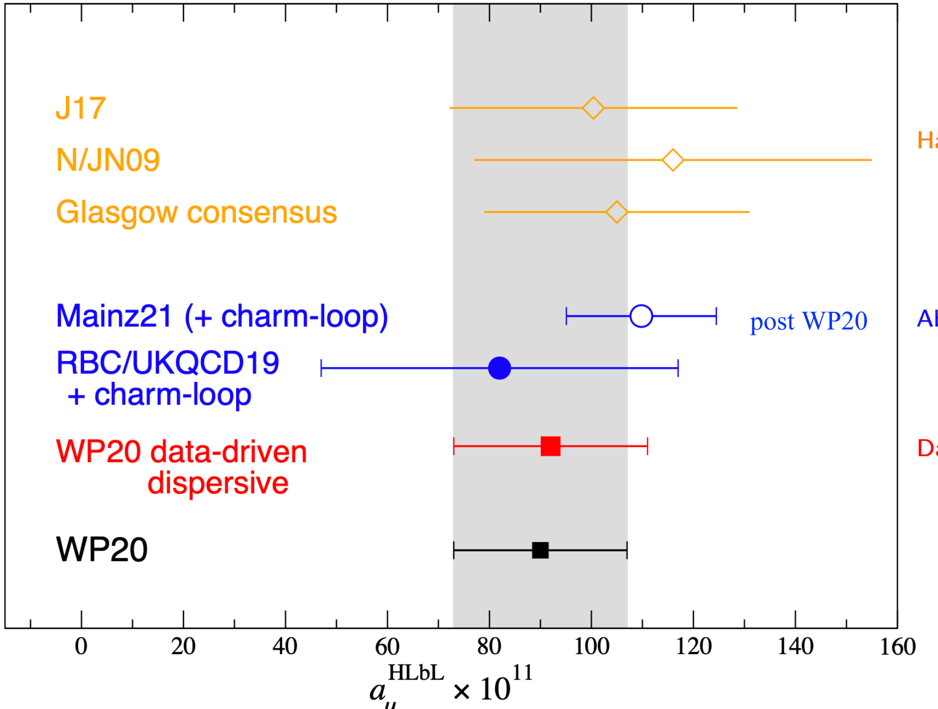

Values, graphs from WP20
Left figure from C. Lehner's CERN seminar talk

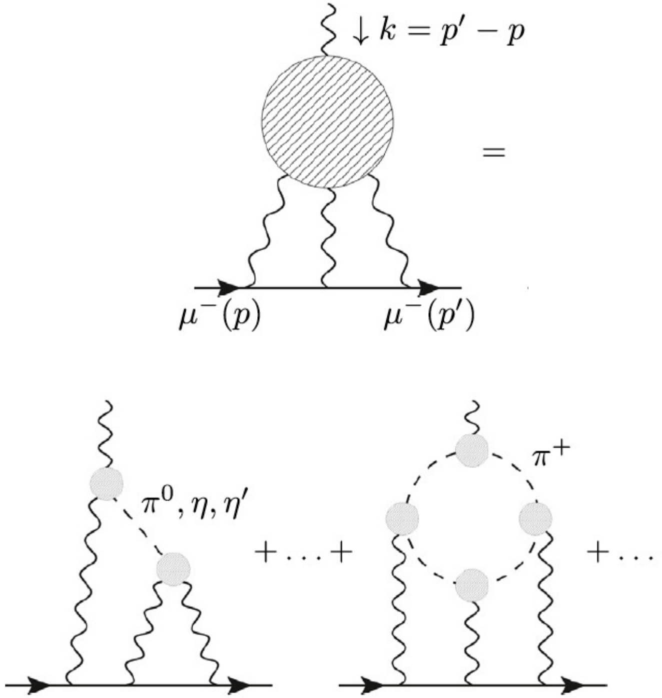

$$a_\mu^{\text{HLbL}}(\text{phenomenology + lattice QCD}) + a_\mu^{\text{HLbL, NLO}} = 92(18) \times 10^{-11}$$